MOLECULAR INTERACTIONS IN THE ADSORBED PHASE STUDIED BY THE ELECTRONIC SPECTRA: THE INTERACTION OF OXYGEN WITH ORGANIC MOLECULES.

BY

HIDEYUKI ISHIDA

February, 1972

CONTENTS

Chapter I

INTRODUCTION

Molecular oxygen is a simple compound indispensable for our daily life, for example, in the respiration and combustion. From the physico-chemical viewpoints, the interaction of molecular oxygen with organic molecules leads to a number of interesting physical and chemical phenomena. For example, oxygen dissolved in organic substances gives rise to the charge-transfer absorption bands and enhances the triplet←singlet absorption bands. Molecular oxygen also reversibly quenches both the excited singlet and triplet states of organic molecules in what appears to be a simple physical process, that is, a process in which no chemical reaction takes place. It has recently become apparent that photosentitized oxidation reactions of organic substances by oxygen involve singlet excited oxygen as an intermediate. These interesting behaviors of molecular oxygen can be ascribed to the following three characteristic properties of oxygen: (1) relatively large electron affinity, (2) paramagnetic(triplet) in the ground state, (3) having low-lying excited singlet states, $^1\Delta_g$ and $^1\Sigma_g^+$. The present work has been undertaken to make further studies

on the interaction of oxygen with organic molecules in the ground and excited states.

The microporous surface structure of some solid materials seems to have its fascinating characters for the study on intermolecular interactions. Among many spectral investigations of molecules adsorbed on the surface of solids, the changes of the electronic absorption spectra due to the physical or chemical adsorption have been of particular interest. Until now, less attention has been paid to the spectroscopic study on the molecular interactions between adsorbed molecules. The large surface area of porous materials allows adsorption of large quantities of donor and acceptor molecules in a limited volume, which facilitate the contact between donor and acceptor molecules on the surface. This helps us to measure the absorption spectra of complexes with small extinction coefficients or small equilibrium constants even in the absorption region of component molecules (hereafter we call this new technique " adsorption technique").

With this adsorption technique, we have succeeded to obtain further information on the nature of weak molecular interactions which have never been obtained by the conventional studies in solutions on account of experimental difficulties. In the present work, we have extensively examined the charge-transfer interactions between oxygen

and organic molecules in the ground and excited states through the measurement of the absorption and emission spectra by use of porous Vycor glass as an adsorbent. As the results of studying the molecular interactions on the surface, it might become possible to derive important information for the understanding of the characteristic properties of the catalytic reactions on the surface of solids. Furthermore, the study on the molecular interaction by this technique might be extended to the biological systems involving molecular oxygen such as hemoglobin and cytochrome.

In Chapter II, the charge-transfer absorption spectra arising from the interaction of oxygen with simple organic donor molecules such as olefins, aliphatic amines, ether, and aromatic hydrocarbons adsorbed on porous Vycor glass at 77°K have been examined. In most cases, the charge-transfer bands with clear maxima are newly observed, on the basis of which the electronic structures of the complexes are theoretically discussed. From the obtained spectral results, the electron affinity of oxygen and a simple expression for the energies of the charge-transfer states and the ionization potentials of the donor molecules have been derived. The oxygen-enhanced second triplet$\leftarrow$singlet absorption of benzene has been detected together with the two charge-transfer and the first triplet$\leftarrow$singlet absorption bands.

In Chapter III, the efficiencies of fluorescence quenching by oxygen have been extensively examined for a number of aromatic hydrocarbons adsorbed on porous Vycor glass plates with and without the presence of liquid oxygen at 77°K. By this technique, the intrinsic rate constants of the oxygen-enhanced radiationless transitions in the excited aromatic-oxygen pairs have been directly determined for the first time. These new observations are reasonably interpreted based on the general theory of radiationless transitions. The results of the phosphorescence quenching efficiencies for naphthalene and benzophenone under the same condition are also discussed.

In Chapter IV, the adsorption technique is extended to the well-known typical charge-transfer complexes such as iodine complexes with benzene and ether and tetracyano-ethylene complex with naphthalene. On the basis of the spectral results and those already obtained in both the gas and liquid phases, the nature of the weak charge-transfer interaction in solutions as well as the characteristic molecular interaction on the surface are discussed in terms of possible adsorbent and solvent effects on the complexes.

In Chapter V, the charge-transfer interaction of acetone with electron-donating and electron-accepting

olefins has been examined using the adsorption technique, which provides important information for the stereospecifical oxetane formation of aliphatic ketones with olefins and the fluorescence quenching of ketones by olefins. The charge-transfer states arising from the interaction of acetone with tetramethylethylene and trans-dicyanoethylene have been confirmed in the present work.

In the Appendix, the list of our papers on the molecular interactions in the adsorbed phase already published is given, together with a collection of the reprints of these papers, and some additional experimental data.

Chapter II

Charge-Transfer Interaction of Oxygen with Olefins, Aliphatic Amines and Aromatic Hydrocarbons at Low Temperature

SUMMARY

Electronic absorption spectra arising from the interaction of oxygen with simple organic donor molecules such as olefins, alphatic amines, ether, and aromatic hydrocarbons adsorbed on porous Vycor glass plates at 77°K have been extensively examined in the ultraviolet region. In most cases, the charge-transfer absorption bands with clear maxima are observed. As previously pointed out by us for the charge-transfer bands between aromatic amines and oxygen, the splitting of the charge-transfer bands due to the two degenerate electron-accepting orbitals of oxygen, is clearly observed in the cases of olefins and aliphatic amines. The electronic structures of the olefin-oxygen complex are theoretically investigated in detail by considering the interactions among the ground no-bond configuration, the locally excited configurations for the olefinic part, and two charge-transfer configurations. As the results, a reasonable explanation for the experimental results was obtained. It has been found that energies of

charge-transfer states(E_{CT}) as expressed by the well-known equation by use of the ionization potentials of the donors(I_p), $E_{CT} = I_p - C_1 + C_2/(I_p - C_1)$, where C_1 and C_2 are constants, is reasonably applicable to the olefin-oxygen system with C_1 and C_2 equal to 4.4 eV and 1.6 $(eV)^2$, respectively. From the observed charge-transfer absorption bands of methylated ethylenes with oxygen and tetracyanoethylene, the electron affinity of oxygen has been estimated to be 0.15 eV taking that of tetracyanoethylene (2.35 eV) as a standard.

In the case of benzene, two distinct charge-transfer bands have been detected in the absorption region of benzene together with the first and the second triplet←singlet absorption bands enhanced by oxygen. A weak absorption band ascribable to the simultaneous transition between oxygen and naphthalene has also been confirmed in the present work on the long wavelength side of the charge-transfer band. Spectral characteristics of the charge-transfer bands are qualitatively discussed with reference to those in the solutions by use of the concept of the contact charge-transfer interaction. The nonfluorescent behavior of the charge-transfer states is also discussed from the energy-level aspects.

INTRODUCTION

We have shown recently that the adsorption technique is of great use for the studies of weak intermolecular interactions such as the contact charge-transfer interaction of oxygen with organic molecules[1,2] and the charge-transfer interaction of aromatic hydrocarbons with amines(so-called exciplex system) in the ground state.[3] For the donor-acceptor systems in the liquid phase, which has been so far studied most frequently, either donor or acceptor must inevitably exist in great excess because of the very weak interaction in the ground state. Consequently, the absorption spectra arising from the molecular interactions are obscured by the overlap of the absorption of the component molecules.

By use of our adsorption technique, we can easily measure the absorption spectra of weakly interacting systems at various temperatures even in the absorption region of component molecules, since the adsorption of a lot of donor and acceptor molecules on the large surface of porous solids facilitates the contact between them. The porous Vycor glass, which is transparent in the region above 210 nm, shows none of the specific interactions with the adsorbates and is therefore a suitable adsorbent for our purpose. Among many spectroscopic studies on adsorbed molecules, the interactions of adsorbed molecules with the surface of adsorbents have been of particular interest(i.e., physical or chemical adsorption).[4] Until now,

insufficient attention has been paid to the spectroscopic study of the interactions between adsorbed molecules on the surface, which would provide important information for the understanding of the characteristic behaviors of the catalytic reactions on the surface of solids.

As described in the previous paper[1], we have obtained the charge-transfer absorption bands between aromatic amines and oxygen with a certain number of clear maxima, and interpreted them to represent separate charge-transfer excited states corresponding to the electron transfers from the donor to the two degenerate electron-accepting orbitals of oxygen. In order to confirm these interesting interpretations of the charge-transfer excited states and to elucidate the electronic structures of the contact charge-transfer systems, simple organic donor molecules such as olefins, aliphatic amines and ether are used in the present work. The charge-transfer absorption bands between olefins and tetracyanoethylene are also examined in the adsorbed state to estimate the electron affinity of oxygen from the observed charge-transfer bands with tetracyanoethylene as a standard. Absorption spectra arising from the interaction of oxygen with aromatic hydrocarbons such as benzene, naphthalene and anthracene, which are of interest in view of the fluorescence and phosphorescence quenching phenomena by oxygen, are also investigated in detail at 77°K.

EXPERIMENTAL

Materials.—The purifications of oxygen, naphthalene and anthracene were described in the previous paper.[1,2] Thiophene-free benzene was dried with phosphorous pentoxide and repeatedly distilled. Tri-n-propylamine and triethylamine were dried over pellets of potasium hydroxide and fractionally distilled. Triethylenediamine was purified by recrystallization from ether and by sublimation under vacuum. n-Propyl ether was dried with calcium chloride and distilled. Commercially available tetramethylethylene, trimethylethylene, 2-methyl-1-butene, pentene-2, and cyclohexene were purified by distillation. The preparation of tetrakis-(dimethylamino)-ethylene(TMAE), and 1,1';3,3'-tetramethyl-$\Delta^{2,2'}$-bi(imidazolidene),(TMBI), were described elsewhere.[5] Being very unstable in the presence of oxygen, both TMAE and TMBI were preserved under vacuum. Tetracyanoethylene (TCNE) was recrystallized, followed by sublimation under vacuum.

The porous Vycor glass(PVG) of Corning Glass Works was supplied in the form of plate.Small pieces of the PVG plates were firsrly washed with ethanol and after washing with water treated with 46 % hydrofluoric acid for 30 sec, followed by extraction with water for deveral days. After drying, the glass plates were treated in air at 400°C for two days. In this way, transparent colorless glass plates were obtained.

Procedure.—The PVG plate(40x10x0.8mm) pretreated in the above mentioned way was placed in a thin quartz cell(1.5mm),

and evacuated at 400°C for 5-8 hr, and the vapor of organic molecules which was previously degassed was exposed to the PVG at room temperature.[1] The amount of adsorbed organic molecule was determined from the volume change of liquid in a capillary tube. In the case of naphthalene and anthracene, a known amount of the crystalline material was adsorbed. After the adsorption, the glass was cooled down to 77°K and purified oxygen gas(∿20mmHg) was introduced into the system at 77°K. The amount of adsorbed oxygen was measured with an ordinary mercury manometer. In the case of TCNE complexes, firstly TCNE vapor and then the olefin vapor were exposed to the PVG at room temperature.

The absorption spectra of the PVG-adsorbates were measured at 77°K before and after the introduction of oxygen with a Shimadzu Multi-Purpose recording spectrophotometer, Model 50L. The emission spectra were measured with an Aminco-Bowman spectrophotofluorometer.

In our present study, oxygen was always adsorbed in a large excess so that most of the adsorbed organic donor molecules are in the form of the complexes with oxygen. We have tentatively estimated the molar extinction coefficients of the charge-transfer bands and triplet←singlet absorption bands based on the concentrations of donors in the bulk of the PVG, which are determined from both the volume of the PVG plate and the amounts of adsorbed organic donors. The thickness of the PVG plate, taken as the path length, is 0.08 cm. It was

confirmed using benzene, iodine and chrysene that the molar extinction coefficients of the adsorbed molecules determined by the present method, are in good agreement with the known values. Wong and Allen[6] have recently determined the G-values of radical production from organic molecules adsorbed on PVG plates under γ-ray irradiations in the similar way.

RESULTS

Charge-Transfer Absorption Spectra with Olefins.——When oxygen was adsorbed on the olefin-PVG adsorbates at 77°K, absorption spectra with clear maxima were observed as shown in Fig.1 and 2, where the absorption before the adsorption of oxygen is subtracted. With increasing the sample temperature, the intensity of the observed absorption band reversibly decreased owing to the desorption of oxygen. This confirms that the observed absorption bands are caused by the charge-transfer interaction, not by the reaction products.

The observed charge-transfer absorption spectra for methylated ethylenes are reasonably interpreted as the superposition of two bands as shown in the case of tetramethylethylene in Fig. 1(1). It was also found that the band at the lower energy side is always stronger than the other band at the higher energy side and the energy difference between the two bands ranges in the region from 2.5 to 3.0 kK for the

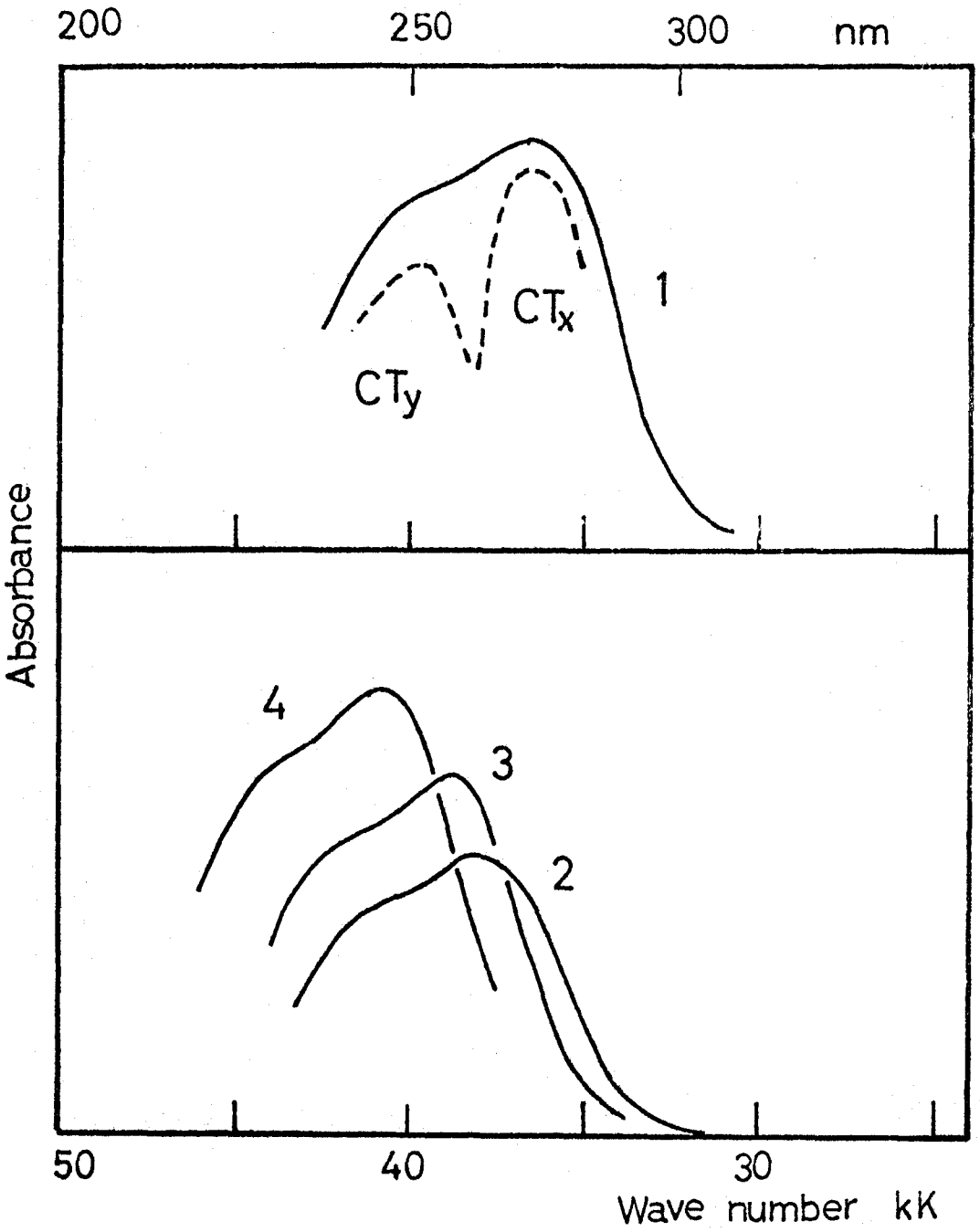

Fig.1. Charge-transfer absorption spectra between oxygen and methylated ethylenes adsorbed on porous Vycor glass(PVG) at 77°K: (1) tetramethylethylene, (2) trimethylethylene, (3) cyclohexene, (4) pentene-2.

methylated ethylenes regardless of the donors. The similar splitting of the first charge-transfer band has been observed for aromatic amines as described in the previous paper.[1] The tentatively determined molar extinction coefficient of the charge-transfer band was about 100 $M^{-1}cm^{-1}$ for tetramethylethylene. The absorption bands due to the triplet←singlet transitions as observed for ethylene under high oxygen pressures,[7] have not been detected clearly for the methylated ethylenes. Itoh and Mulliken[8] recently measured the absorption spectra of methylated ethylenes such as tetramethylethylene and trimethylethylene with oxygen under high pressures in the gas phase. They also observed strong absorption bands attributable to the contact charge-transfer transitions from the ethylenes to oxygen, which in our results correspond to the absorption tails of the charge-transfer bands in the longer wavelength region. We attempted to detect the fluorescence spectra by exciting the observed charge-transfer bands. However, no detectable emission was obtained for the used olefins.

In the case of TMAE and TMBI, which show chemiluminescence as a result of the reaction with oxygen at higher temperatures,[9] we could easily detect the charge-transfer bands with oxygen by our present method at 77°K as shown in Fig.2. When the samples were warmed up from 77°K, yellow-green chemiluminescence was also observed with the simultaneous disappearance of the charge-transfer bands. The reactive character of TMAE and TMBI

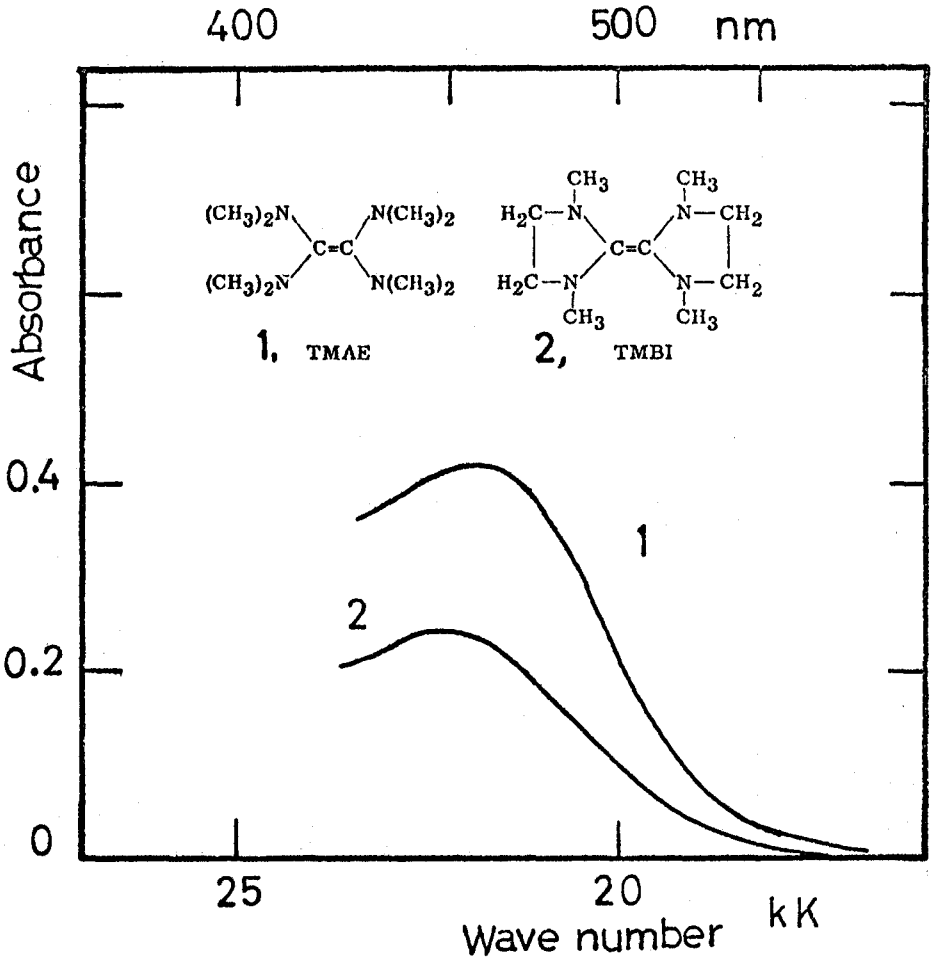

Fig.2. Charge-transfer absorption spectra between oxygen and tetraaminoethylenes adsorbed on PVG plates at 77°K.

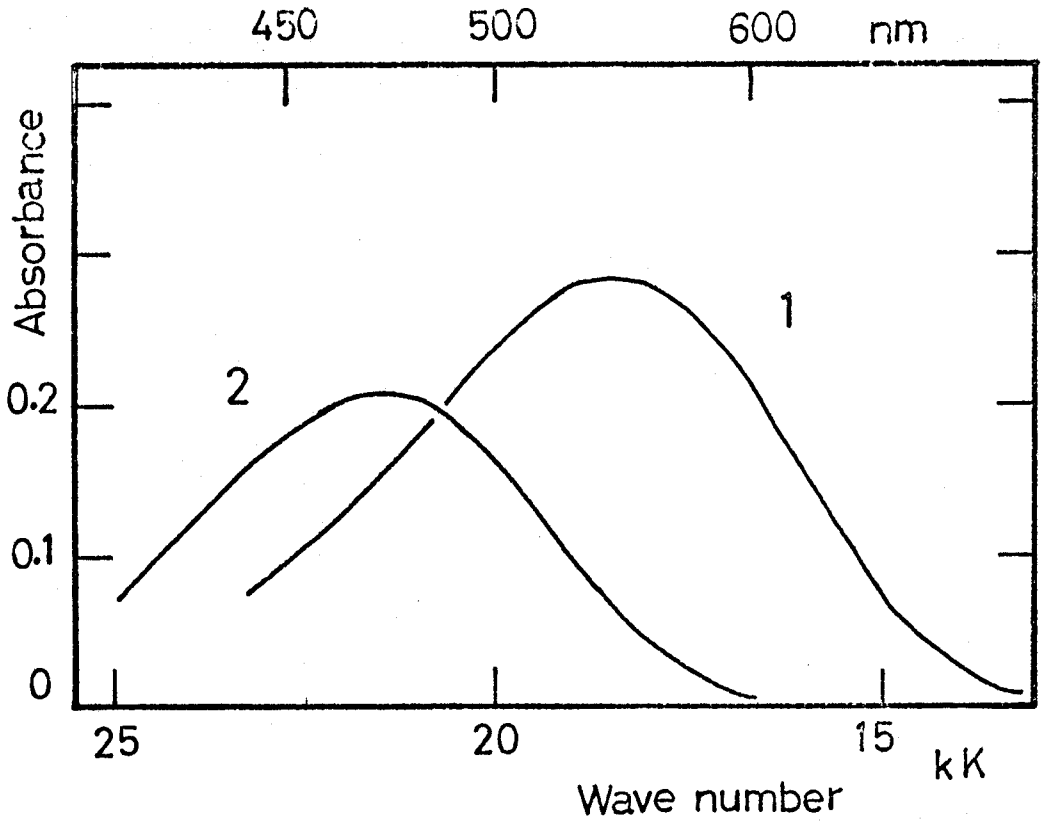

Fig.3. Charge-transfer absorption spectra of the TCNE complexes of methylated ethylenes adsorbed on PVG plates at 77°K: (1) tetramethylethylene, (2) trimethylethylene.

toward the ground-state oxygen molecule[9] seems to be due to the low energy levels of the charge-transfer states, as predicted from the extremely low ionization potentials of TMAE and TMBI.[5]

In order to estimate the electron affinity of oxygen from the clearly obtained charge-transfer bands between oxygen and olefins, the absorption spectra of the TCNE complexes of tetramethylethlene and trimethylethylene adsorbed on the PVG plates were measured at 77°K, that is, under the same condition as the oxygen complexes. When the vapor of olefins was exposed to the TCNE-PVG adsorbate, symmetrical broad absorption bands were observed in the visible region. With decreasing the temperature, the intensities of these bands increased reversibly and the bands showed a slight red shift, which seems to be due to the increased charge-transfer interaction at low temperature. The absorption spectra of the TCNE complexes at 77°K are shown in Fig.3. When the vapor of triethylamine was exposed to the TCNE-PVG adsorbate, the characteristic absorption of TCNE anion radical was observed instead of the expected charge-transfer band.

Charge-Transfer Absorption Spectra with Aliphatic Amines and Ether.— When aliphatic amines such as triethylamine, tri-n-propylamine and triethylenediamine, and n-propyl ether were used as donors, absorption bands ascribable to the charge-transfer absorption bands from the amines or ether to oxygen

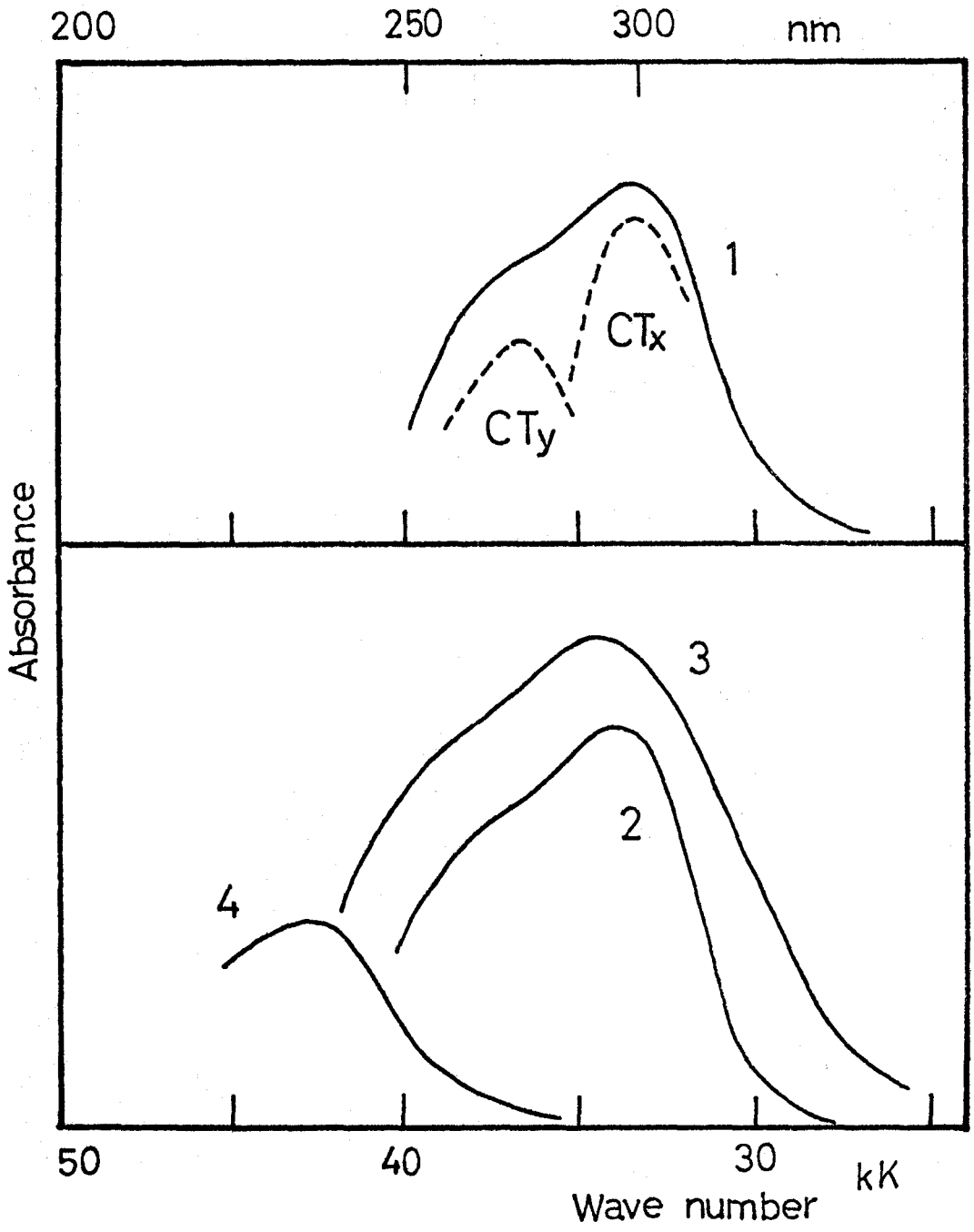

Fig.4. Charge-transfer absorption spectra arising from the interaction of oxygen with aliphatic amines and ether adsorbed on PVG plates at 77°K: (1) triethylamine, (2) tri-n-propylamine, (3) triethylenediamine, (4) n-propyl ether.

were also detected at 77°K as shown in Fig.4. In the studies on the contact charge-transfer absorption spectra of the amines carried out so far in the solutions,[10] the band maxima have been obscured by the strong absorption of the amines themselves. In the present system, the charge-transfer absorption bands with clear maxima have been detected. As found out in the case of olefins, the observed charge-transfer absorption seems to consist of two bands(see 1 in Fig.4). It was also found that the band at the lower energy side is considerably stronger than that at the higher energy side and the energy difference between the two bands is also in the range from 2.5 to 3.0 kK, almost the same as those of olefins. The molar extinction coefficient of the charge-transfer band was about 180 $M^{-1}cm^{-1}$ for triethylamine. In these cases also, no charge-transfer fluorescence could be detected at 77°K.

Absorption Spectra Arising from the Interaction of Oxygen with Aromatic Hydrocarbons.—Though the charge-transfer and triplet←singlet absorption bands of naphthalene were already examined in the previous work,[1] the absorption spectrum at shorter wavelengths was obscured by the absorption and light scattering due to the porous glass used in the form of a tube. By use of the PVG plates, it has become possible to measure the absorption spectra arising from the interaction with oxygen into the shorter wavelength region. The results for the case

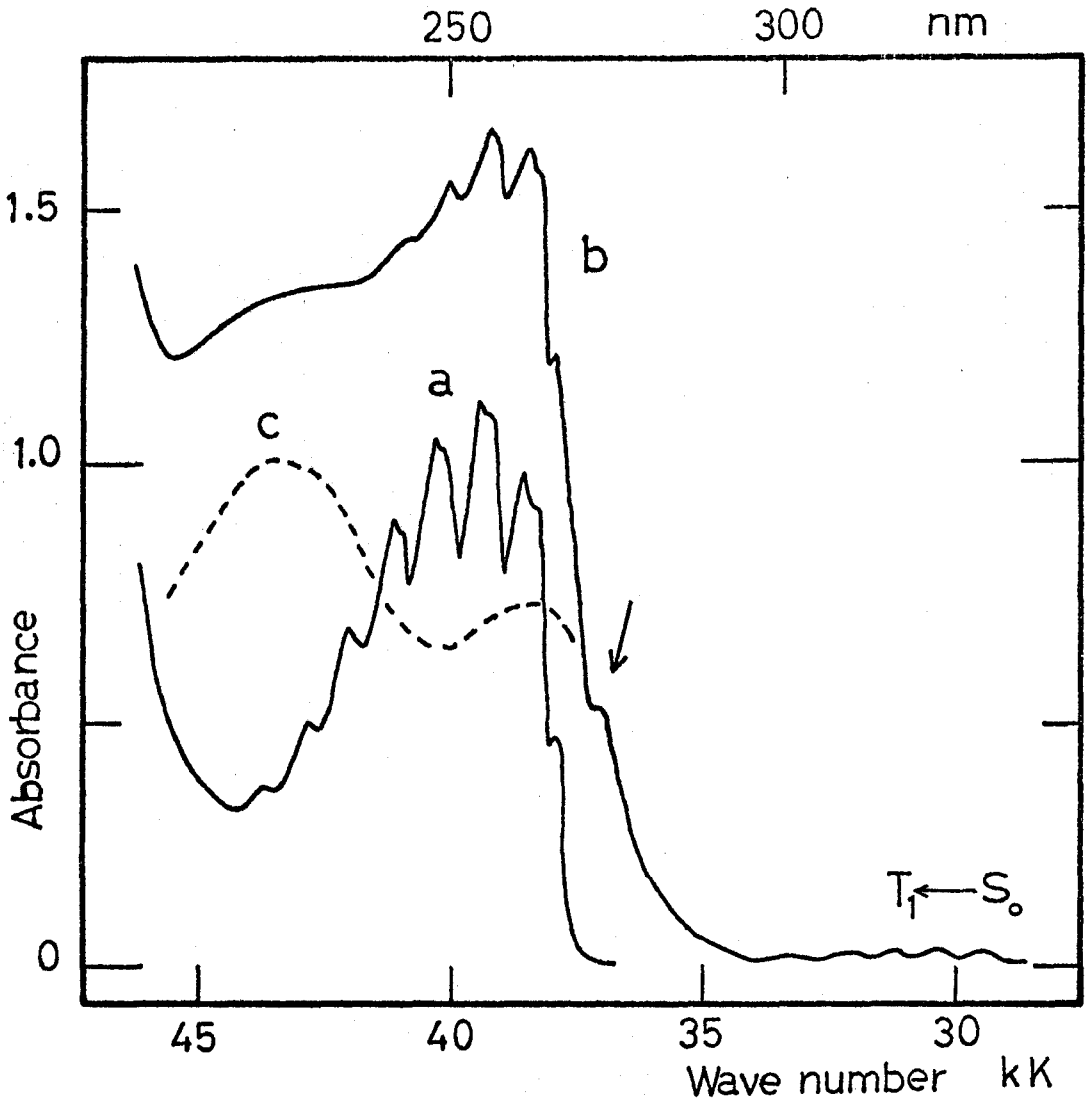

Fig.5. Absorption spectra arising from the interaction between benzene and oxygen adsorbed on PVG plate at 77°K: (a) benzene alone, (b) after the adsorption of oxygen, (c) a curve obtained by subtracting a from b.

of benzene and naphthalene at 77°K are shown in Fig.5 and 6, respectively.

In the case of benzene, remarkable changes in the absorption were observed by the adsorption of oxygen at 77°K.[11] The observed weak first triplet←singlet($^3B_{1u} \leftarrow {}^1A_{1g}$) absorption bands at the longer wavelengths are in good agreement with those detected for pure benzene liquid and oxygen under high pressures.[12] By subtracting the absorption spectrum of benzene alone from that of benzene-oxygen system, the absorption attributable to the charge-transfer interaction with oxygen can be obtained (see curve c in Fig.5). As seen from the spectrum, there exist two charge-transfer bands with maxima at 265 and 230 nm. The energy difference between the two bands is found to be 5.7 kK. Furthermore, a weak absorption band, which is however relatively strong compared to the first triplet←singlet absorption bands, was observed only in the presence of oxygen at 270 nm on the longer wavelength side of the first charge-transfer band as shown by an arrow in Fig.5.

Colson and Bernstein[13] have examined the absorption spectrum of a benzene-oxygen mixture deposited on a quartz window cooled to 4.2°K by a spectrographic method and observed a weak oxygen-enhanced band at 273 nm. They have concluded that this band, relatively stronger than the first triplet←singlet band, is due to the second triplet←singlet($^3E_{1u} \leftarrow {}^1A_{1g}$) transition. The possibility of the simultaneous transition

between benzene and oxygen, $[^3B_{1u}\,^1\Delta_g] \leftarrow [^1A_{1g}\,^3\Sigma_g^-]$, where $^1\Delta_g$ and $^3\Sigma_g^-$ indicate the singlet excited state and ground state of oxygen, respectively, was eliminated. The 270 nm band observed in our present case is at least 600 cm^{-1} lower than the predicted position of the simultaneous transition. Pariser-Parr theory[14] also predicts the second triplet state of benzene($^3E_{1u}$) to lie between the first excited singlet($^1B_{2u}$) and lowest triplet state($^3B_{1u}$). It seems quite reasonable to conclude from these results that the weak band at 270 nm is due to the second triplet←singlet transition of benzene and the band due to the simultaneous transition is obscured by the relatively strong charge-transfer band and absorption of benzene itself.

In the case of naphthalene, the absorption bands due to first triplet←singlet($^3B_{2u} \leftarrow {}^1A_{1g}$) transition, which are also in good agreement with those obtained by Evans,[12] were observed at the longer wavelengths. The absorption band which appears to have the maximum at about 320 nm can be assigned to the charge-transfer band. A shoulder, which is relatively weak compared to the first triplet←singlet absorption bands as shown by an arrow in Fig.6, was found at about 345 nm on the long wavelength side of the charge-transfer band. Robinson and Hanson[15] have examined the absorption spectrum of crystalline naphthalene at 4.2°K and found the second triplet←singlet($^3B_{3u} \leftarrow {}^1A_g$) absorption band at ca. 320 nm

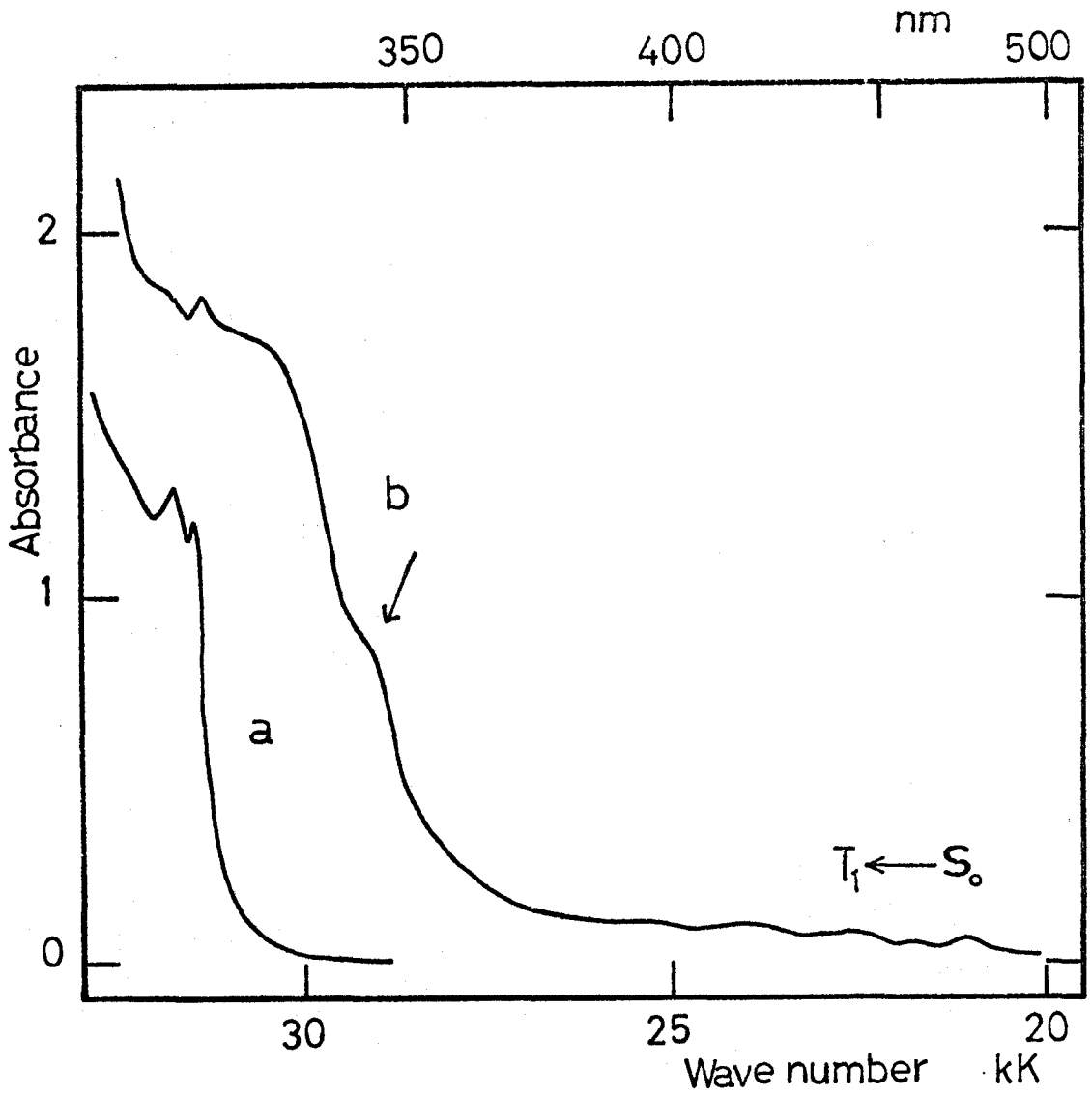

Fig.6. Absorption spectra arising from the interaction between naphthalene and oxygen adsorbed on PVG plate at 77°K: (a) naphthalene alone, (b) after the adsorption of oxygen.

which is by a factor of 10∿100 stronger than the bands due to the first triplet←singlet transition. The electron impact spectrum of naphthalene vapor[16] also predicts the second triplet state of free naphthalene to lie at nearly the same energy as the first excited singlet state. In the present system, the absorption band ascribable to the second triplet←singlet transition seems to be obscured by the charge-transfer band and absorption of naphthalene itself. The weak shoulder observed in the present system agrees energetically well with that detected by Hoijtink et al.[17] in the solution with oxygen under high pressures, though from their experiments no information could be obtained concerning the charge-transfer state. Therefore, our results support their assignment that the pronounced shoulder at 345 nm is due to the simultaneous transition between naphthalene and oxygen, $[^3B_{2u}\,{}^1\Delta_g \leftarrow {}^1A_g\,{}^3\Sigma_g^-]$.

In the case of anthracene, a weak charge-transfer absorption band monotonically increasing from ca. 440 nm toward the shorter wavelength was observed on the longer wavelength side of the first absorption band of anthracene.

DISCUSSION

Relationship between the Ionization Potentials of Organic Molecules and the Energies of the Charge-Transfer States.—— It is of interest that each of the charge-transfer spectra

with simple organic donors such as olefins and aliphatic amines consists of two bands with nearly constant energy differences regardless of the donors. This seems to support strongly our previous interpretation that the splitting of the first charge-transfer bands between aromatic amines and oxygen is due to the originally degenerate electron-accepting orbitals of oxygen.[1] On this basis, the relatively strong band at the longer wavelengths is denoted by CT_x and the other by CT_y as done in the previous paper. The accurate ionization potentials of olefins, amines and aromatic hydrocarbons are well known as summarized in Table 1 together with the band maxima of the CT_x bands. The energies of the CT_x bands and the first charge-transfer bands for benzene and naphthalene are plotted versus the ionization potentials of the organic donors in Fig.7. For reference, a few previous results for aromatic amines are shown together.

It was concluded from spectroscopic results that in the solutions there exists no specific interaction between organic molecules and oxygen, in other words, that the association constants K are nearly zero in the ground state.[10,18] We have suggested that the attractive interactions of adsorbent with adsorbed molecules might favorable for the weak interaction between oxygen and organic molecules and might enhance the tendency for them to take more fixed geometrical configurations than in the solutions. In addition, a stronger interaction is

Table 1

Maxima of the Charge-Transfer Absorption Bands and the Ionization Potentials of Organic Molecules.

	Donor molecule	I_p (eV)	E_{CT} (nm)	(CT_x) (eV)
1	n-Propyl ether	9.28[a]	235	5.28
2	Pentene-2		246	5.04
3	Cyclohexene	8.95[a]	255	4.86
4	2-Methyl-1-butene		260	4.77
5	Trimethylethylene	8.68[a]	260	4.77
6	Tetramethylethylene	8.30[a]	273	4.53
7	Triethylamine	7.50[b]	296	4.19
8	Tri-n-propylamine	7.23[b]	294	4.22
9	Triethylenediamine	7.2[c]	290	4.28
10	TMBI	5.41[d]	450	2.76
11	TMAE	5.36[d]	455	2.73
12	Benzene	9.25[a]	265	4.68
13	Naphthalene	8.13[a]	320	3.87
14	Anthracene	7.38[a]		

a) F.I.Vilesov, USP.Fiz.Nauk, 81, 669(1963).

b) K.Watanabe and J.R.Mottle, J.Chem.Phys., 26, 1773(1957).

c) Ref. 30. d) Ref. 5.

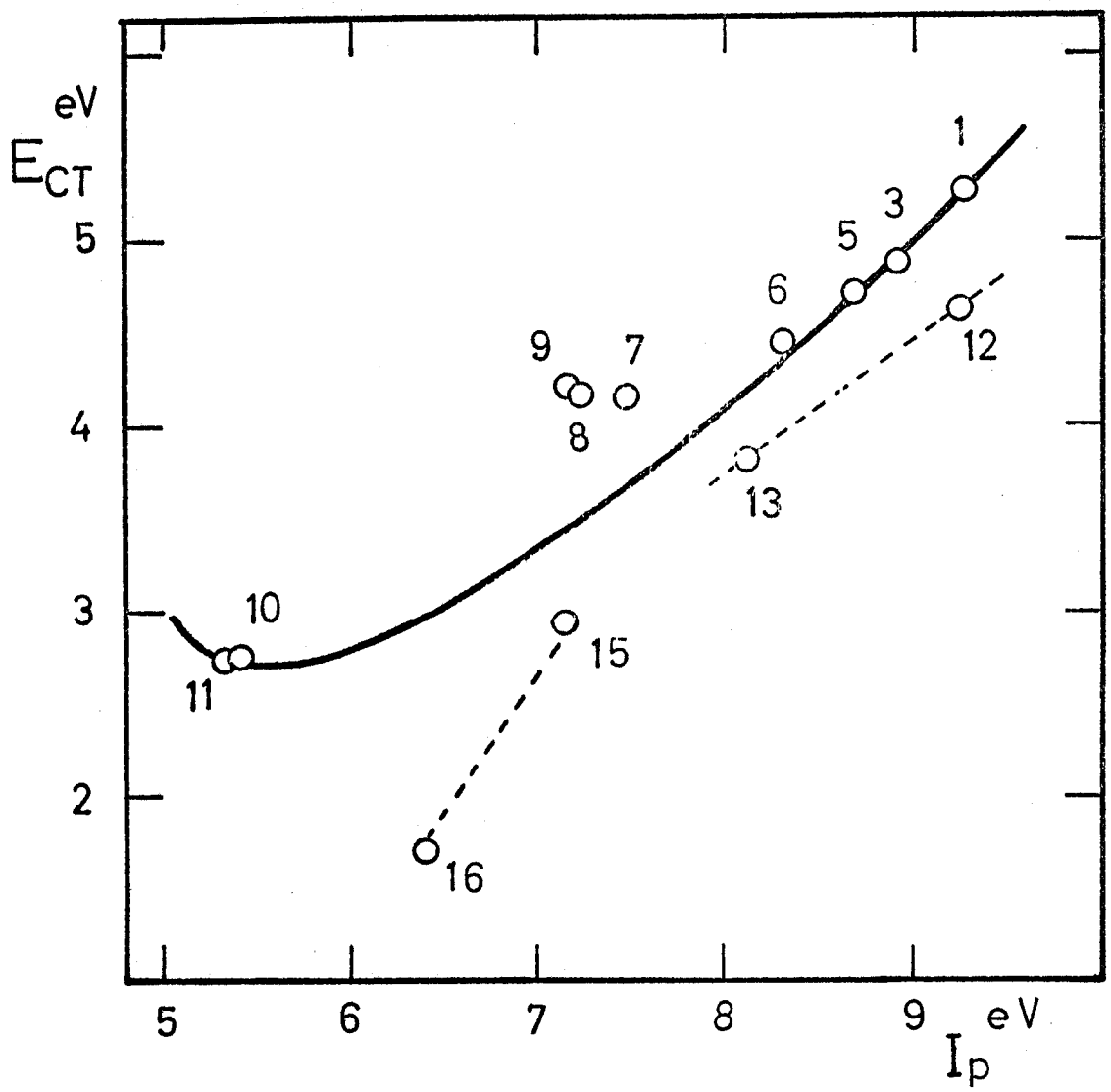

Fig.7. Relationship between the energies(E_{CT}) of the charge-transfer states and the ionization potentials (I_p) of organic donors. The numbers for the donors are identical with those given in Table 1, except for the aromatic amines: (15) N,N-dimethylaniline, (16) N,N-dimethyl-p-phenylenediamine(see ref.1). The solid curve shows the equation (1) with C_1 and C_2 equal to 4.4 eV and 1.6 $(eV)^2$, respectively.

expected in the present system because of the measurement at low temperature.

As evident from Fig.7, the relationship between the ionization potentials and the charge-transfer bands can't be represented by a single curve, that is to say, the aliphatic amines, which are expected to interact strongly with oxygen, do not fit in the curve applied to olefins and ether. It is also found that the charge-transfer states for the aromatic donors lie at relatively lower energies than predicted from the ionization potentials compared to those of others. As can be seen from the structural formulae of TMAE and TMBI in Fig.2, the steric hindrance of TMAE is expected to be less favorable for the charge-transfer interaction with oxygen compared to TMBI. On the contrary, the positions of the observed charge-transfer bands for TMAE and TMBI with almost identical ionization potentials are nearly equal to each other as predicted from the general charge-transfer theory. This indicates that TMAE or TMBI and oxygen have geometrical configurations probably with less steric hindrance, for example, those with oxygen above the carbon-carbon double bond.

When the second-order perturbation theory is applied to the charge-transfer interaction, the energy of the charge-transfer transition, E_{CT}, is given by the equation[19]

$$E_{CT} = I_p - C_1 + C_2/(I_p - C_1) \qquad (1)$$

where I_p represents the ionization potential of the donor and

and C_1 and C_2 are approximately constant for a series of similar donors with the same acceptor. C_1 is approximately the sum of the Coulombic attraction energy and the electron affinity of the acceptor, and C_2 reflects the charge-transfer interaction, that is, the interaction between the dative(ionic) and no-bond configurations. The solid curve in Fig.7 is obtained from the equation(1) with C_1 and C_2 equal to 4.4 eV and 1.6 $(eV)^2$, respectively. It is clear from the curve that the expression (1) gives good agreement with the experimental results for the olefins and ether. It is the first time that such a clear reliable relation has been obtained for the charge-transfer bands involving oxygen as an acceptor. It is of interest to compare the C_2 value with those for iodine and TCNE complexes in the solutions. For the iodine complexes of olefins, ether and alcohols, C_2 is 3.4 $(eV)^2$ at room temperature.[20] The C_2 value determined for the relatively weak TCNE complexes of methylated benzenes is 1.25∿1.30 $(eV)^2$ in the solutions at room temperature.[21] From these results, it can be seen that the charge-transfer interaction of oxygen with the olefins and ether in the present system at 77°K is comparable with that between TCNE and methylated benzenes in the solutions at room temperature and considerably weak compared to that of the iodine complexes. These results seem to encourage us in attempting to determine the electron affinity of oxygen by using the charge-transfer bands of oxygen and TCNE complexes with olefins.

Electronic Structures of the Charge-Transfer States.— As pointed out in the preceding section, the charge-transfer interaction of oxygen with olefins or amines in the ground state can't be neglected in the present system. The appearance of the charge-transfer bands with clear maxima also seems to suggest the formation of the complexes having the relatively strong binding and fixed geometrical configurations. For simplicity, we will discuss in detail the electronic states arising in the olefin(D) and oxygen 1:1 pair in order to clarify the interpretation of the intensities and structures of the observed charge-transfer bands.

For the methylated ethylene as a donor, the following three orbitals are taken into account[22]: the 2pπ bonding molecular orbital(ϕ_1), the 2pπ antibonding molecular orbital(ϕ_2) and the 3sσ bonding-type Rydberg orbital(ϕ_R). We shall use two real molecular orbitals of oxygen(π_x and π_y) as the electron accepting orbitals, each of which are originally occupied by one unpaired electron. These two orbitals are schematically illustrated in Fig.8 together with the assumed geometrical configuration between the olefin and oxygen. As the electron-accepting orbitals of oxygen are 2pπ antibonding molecular orbitals, the probable configuration with oxygen-oxygen double bond just above the carbon-carbon double bond is unfavorable for the ground-state stabilization due to the charge-transfer interaction because of the negligible overlap

between the ϕ_1 and π_x or π_y orbitals. For simplicity, we here tentatively assume the geometrical configuration giving rise to a considerable overlap between the ϕ_1 and π_y orbitals as shown in Fig.8. In the stereospecific 1,2-addition of singlet excited oxygen to diethoxyethylene, an oxygen complex with a similar geometrical configuration has been proposed as an intermediate by Bartlett and Schaap.[23]

Strictly speaking, the excited states of oxygen, for example, $^3\Sigma_u^- \leftarrow\!- {}^3\Sigma_g^-$ transition in the vacuum ultraviolet region, must be taken into account. For simplicity, however, only the excited states of the donor part are taken into account here. It is well known that the olefin has two typical excited states due to $V \leftarrow\!- N(\phi_2 \leftarrow\!- \phi_1)$ and $R \leftarrow\!- N(\phi_R \leftarrow\!- \phi_1)$ transitions.[24] The wave functions for the electronic configurations of the olefin and triplet-state oxygen pair, which are either symmetric or antisymmetric with respect to the center of symmetry, are given by Slator determinants.[10]

antisymmetric

$\Psi_G = |\phi_1 \bar{\phi}_1 \pi_x \pi_y|$ Ground no-bond configuration

$\Psi_R = 1/\sqrt{2}\{|\phi_1 \bar{\phi}_R \pi_x \pi_y| - |\bar{\phi}_1 \phi_R \pi_x \pi_y|\}$ Rydberg(R) configuration

$\Psi_{CT_y} = |\phi_1 \pi_x \pi_y \bar{\pi}_y|$ Charge-transfer(CT_y) configuration

symmetric

$\Psi_{CT_x} = |\phi_1 \pi_x \bar{\pi}_x \pi_y|$ Charge-transfer(CT_x) configuration

$\Psi_V = 1/\sqrt{2}\{|\phi_1 \bar{\phi}_2 \pi_x \pi_y| - |\bar{\phi}_1 \phi_2 \pi_x \pi_y|\}$ 'V' configuration

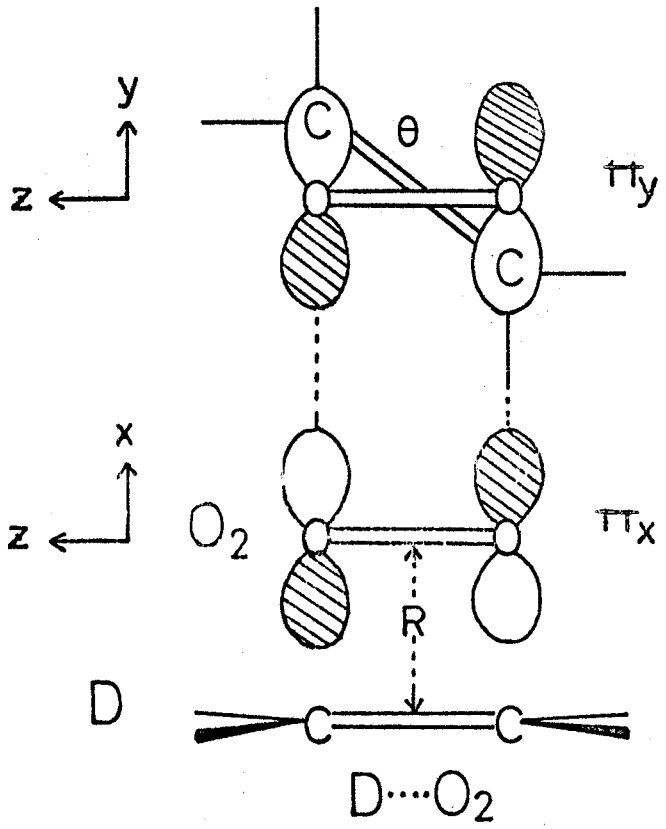

Fig.8. Schematic representations of the geometrical configuration of the oxygen complex with an olefin and the two electron-accepting orbitals of oxygen. Shaded and unshaded volumes in the orbitals indicate negative and positive region, respectively.

As the bond lengths of the carbon-carbon and oxygen-oxygen double bonds are 1.34 and 1.21 Å, respectively, the line linking the carbon and oxygen atoms becomes just perpendicular to the oxygen-oxygen double bond, if we take the angle θ shown in Fig.8 to be 27°. As pointed out in the previous paper,[1] the two charge-transfer configurations split in energy from each other with E_{CT_y} higher than E_{CT_x} owing to the difference in the electrostatic interaction between D^+ and O_2^-. At the intermolecular distance(R) of 3 Å, which is probable from the van der Waals radii, the splitting is about 1.5 kK($E_{CT_y} - E_{CT_x} = 1.5$ kK) as shown in Fig.9, where the levels of the charge-transfer configurations are estimated for the case of tetramethylethylene from the ionization potential(8.30 eV), the energies of the electrostatic interaction[1] and the electron affinity of oxygen(0.15 eV).[25] The energy of the 'V' configuration was taken from the edge of the absorption spectrum of tetramethylethylene in the low-temperature matrix.[26] The R←N absorption band is observed only in the vapor phase at longer wavelength than the V←N absorption band.[27] However, the Rydberg absorption band generally shows a large blue shift in a condensed medium(solution or low-temperature matrix) because the large-size Rydberg orbital would be strongly perturbed by closely neighboring molecules.[26] Hence, the energy of the R configuration should be taken appreciably above that of the 'V' configuration also in the present system.

By application of the second-order perturbation theory, the CT_x configuration will be stabilized by the interaction with the 'V' configuration, because they belong to the same symmetry, by an amount $\beta_{xv}^2/\Delta E_{xv}$, where $\beta_{xv} = \langle \Psi_{CT_x} | H | \Psi_V \rangle$ and $\Delta E_{xv} = E_V - E_{CT_x}$. As the matrix element, β_{xv}, is represented approximately by the core reasonance integral between the ϕ_2 and π_x orbitals, we can evaluate the matrix element semiempirically $\beta_{xv} = -KS(\pi_x\phi_2)$, where $S(\pi_x\phi_2)=\langle \pi_x\phi_2 \rangle$ and K is taken to be constant as experimental parameters.[28] For the present Slator-type orbitals, K can be set equal to $-30\sim35$.[28,29] The overlap integral was calculated for the assumed geometrical configuration ($\theta = 27°$ and $R = 3$ Å in Fig.8) from Mulliken's table.[30] Thus, the stabilization of the CT_x configuration due to the interaction with the 'V' configuration is calculated to be about 900 cm^{-1}, leading to the additional splitting of the two charge-transfer states. As the result of the interaction of the CT_y configuration with the ground configuration, the ground state is stabilized by about 100 cm^{-1}. It was found that the interaction of the CT_y configuration with the R configuration is negligible due to the negligible overlap between ϕ_R and π_y orbitals. The energy level diagram after the configuration interaction is also shown in Fig.9. The resulting energy difference between the CT_y and CT_x states becomes about 2.5 kK which is in good agreement with the observed values, $2.5\sim3.0$ kK. The intensity of the CT_x band can be borrowed almost from

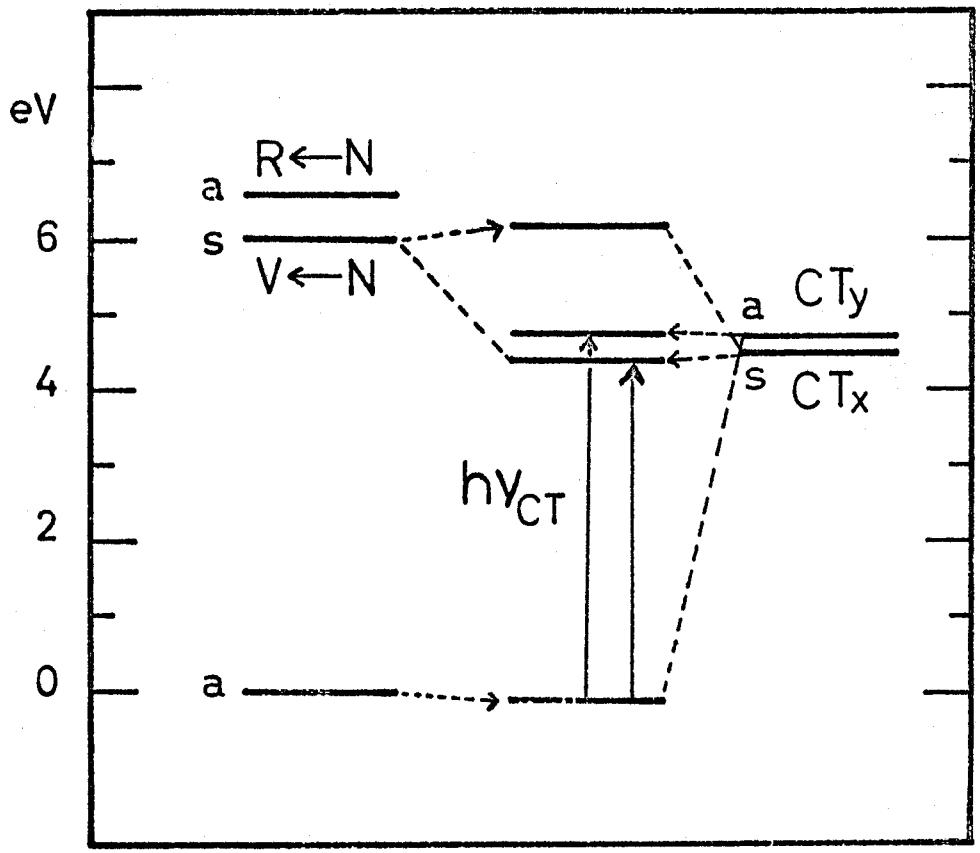

Fig.9. Energy level diagram of the various electronic configurations and states for tetramethylethylene-oxygen complex with the assumed geometry indicated in Fig.8. The letters s(symmetric) and a(antisymmetric) represent the symmetry properties with respect to the center of symmetry(C_2). The vertical arrows show the two charge-transfer transitions.

the strong V←N transition of the olefin, which also seems to be consistent with the experimental fact that the CT_x band is relatively stronger compared to the CT_y band.

Similar treatments are possible for the aliphatic amine complexes. For example, triethylamine has a strong absorption band at about 200 nm due to 3p←n Rydberg transition(of nitrogen atom).[31] In this case, the CT_x configuration can strongly interact with the ground no-bond and the Rydberg configurations under the most probable geometrical configuration of the complex,[1] giving rise to more intense charge-transfer band compared to those of olefins.

In the case of benzene, we have found two distinct charge-transfer bands with a large energy difference of 5.7 kK. As the donor molecular orbitals of benzene is spread over the benzene ring and are much larger in size than those of olefins and amines, the splitting of the charge-transfer band due to the two degenerate orbitals of oxygen is expected to be small from our theoretical viewpoint mentioned above. It seems, therefore, reasonable that the observed two charge-transfer bands correspond to the two charge-transfer states resulting from the two degenerate donor orbitals of benzene. Generally speaking, several charge-transfer states can be expected to exist in the cases of aromatic donors by the presence of many closely lying donor orbitals and the interactions with the several locally-excited states of the donors should be considered.

Consequently, the first charge-transfer bands for the case of aromatic donors will be much stabilized compared to those of olefins and amines. As Fig.7 shows, our observation seems to give an experimental evidence for this expectation.

In Table 2 the apparent molar extinction coefficients of the charge-transfer and triplet←singlet absorption bands for aromatic hydrocarbons and triethylamine are summarized together with the values obtained from the measurements of the liquid donors containing oxygen. As evident from Table 2, the intensity of the charge-transfer band decreases with increasing the size of the aromatic hydrocarbon. In the complexes between oxygen and the hydrocarbons, we can expect that the overlap between the donor and acceptor orbitals will generally decrease with increasing the size of the hydrocarbon, since the donor orbitals are presumably spread over the whole aromatic ring. Similar behavior of the intensities of the charge-transfer bands has been found for the iodine complexes of aromatic hydrocarbons.[32]

It is also of interest that the charge-transfer bands in the liquids are always stronger than those in the present system, where relatively strong interactions are expected as shown in the cases of olefins and amines. As the oxygen molecules in the solution are considered to be weakly interacting with the surrounding solvent donor molecules with random orientations, there would exist special orientations which give less stable complexes and more intense charge-transfer bands, that is,

Table 2

Molar Extinction Coefficients of the Charge-Transfer and Triplet←—Singlet Absorption Bands

Donor molecule	ε_{CT} ($M^{-1}cm^{-1}$)	ε_{S-T} ($M^{-1}cm^{-1}$)
Benzene	90 [250][a] at 265nm	1.8 [1.0][a] at 337nm
Naphthalene	50 at 320nm	0.4 at 475nm
Anthracene	20 at 385 nm	
Triethylamine	170 [550][a] at 296nm	

a) Molar extinction coefficients based on the concentrations of dissolved oxygen in the liquids. For benzene; see ref.18 and D.F.Evans, Proc.Roy.Soc., A255, 55(1960). For triethylamine; a result obtained in the present work by assuming the solubility of oxygen in triethylamine equal to that in aniline(see ref.10).

the orientations favorable for the interaction of the charge-transfer states with the donor excited states but not with the ground state. On the other hand, the organic donor molecules and oxygen adsorbed on the PVG plates at 77°K are considered to be interacting strongly in the ground state with fixed geometrical configurations which are favorable for the interaction of the charge-transfer states with the ground state but not with the donor excited states, leading to the formation of the stable complexes giving weaker charge-transfer bands. It has also been found that the charge-transfer band between iodine and benzene adsorbed on the PVG plate is extremely weak compared to that obtained in the liquid phase.[33] Generally speaking, the relative behavior of the intensity of the charge-transfer band and the stability in the weak complex wuold depend on the difference in energy between the most stable configuration and the configuration giving the most intense charge-transfer band under various conditions.[34]

Electron Affinity of Oxygen Determined from the Charge-Transfer Bands.—By using the observed charge-transfer bands of methylated ethylenes with oxygen and TCNE, let us estimate the electron affinity of oxygen with that of TCNE as a standard. If we assume the electrostatic terms and other terms due to the charge-transfer interaction(that is, the second term in the equation 1) to be constant for both the oxygen and

TCNE complexes, the following equation is approximately given;

$$E_{CT}(O_2) - E_{CT}(TCNE) = E_A(TCNE) - E_A(O_2) \qquad (2)$$

where $E_A(O_2)$ and $E_A(TCNE)$ indicate the electron affinities of oxygen and TCNE, respectively, and $E_{CT}(O_2)$ and $E_{CT}(TCNE)$ are the energies of the charge-transfer bands of oxygen(CT_x) and TCNE complexes, respectively. The electron affinity of TCNE has been estimated to be 2.30 eV[35] or 2.55 eV[36] from the energies of the charge-transfer states in the gas phase, and 2.56 eV from the half-wave reduction potential.[35] By use of the charge-transfer bands of TCNE and benzoquinone complexes with various donors in the solutions, the value of 2.31~2.37 eV has been determined for TCNE with the absolute value of benzoquinone(1.40 eV) as a standard.[35] From these results, the electron affinity of TCNE seems to be in the range from 2.30 to 2.50 eV. Therefore, we tentatively use the value of 2.35 eV as the electron affinity of TCNE for the present purpose.

As summarized in Table 3, 0.15 eV has been obtained as the electron affinity of oxygen by using the equation(2). Jortner and Sokolov[37] have also estimated the electron affinity of oxygen(0.74 eV) from the charge-transfer bands of the oxygen and iodine complexes of benzene and alcohol in the solutions. However, as they chose the energies of the charge-transfer states arbitarily from the continuous absorption bands with oxygen, the estimated value seems to be less reliable than the present value based on the distinct charge-transfer

Table 3

Determination of the Electron Affinity of Oxygen from the Charge-Transfer Bands

Donor molecule	$E_{CT}(O_2)$ (eV)	$E_{CT}(O_2)$ (eV)	$E_A^*(O_2)$ (eV)
Tetramethylethylene	4.525	2.290	0.115
Trimethylethylene	4.769	2.610	0.191
		average	0.15

*E_A(TCNE) = 2.35eV

bands with clear maxima. It is worth noting that the obtained value is in good agreement with the value(0.15 eV) which has been determined from the threshold energy in the photodetachment of O_2^- and supported in terms of molecular orbital theory by Mulliken.[25] Relatively large values are reported as the electron affinity of oxygen by various other methods: 0.95 eV by lattice energies;[38] ≥0.7 eV[39] and ≥0.58 eV[40] by electron attachment.

As described in the previous section, the C_1 value of 4.4 eV has been obtained for the oxygen complexes of olefins in the equation(1), where C_1 can be approximated by the sum of the electrostatic term and the electron affinity of oxygen. The electrostatic energy calculated for the geometrical configuration assumed for the complex between an olefin and oxygen is 4.3 eV. Therefore, the electron affinity of oxygen obtained can well satisfy the relation of C_1. Though there exist some ambiguities in the present procedure, the obtained value(o.15 eV) seems to be highly probable as the vertical electron affinity of oxygen.

Nonfluorescent Behavior of the Charge-Transfer States.— We could not detect the fluorescence corresponding to the charge-transfer absorption bands for olefins and aliphatic amines. Previously, we have reported the charge-transfer fluorescence for the aromatic amines-oxygen complexes, where the first charge-transfer states lie sufficiently below the

lowest triplet states of donor molecules.[1] The energies of the lowest triplet states of methylated ethylenes have recently been determined by use of the external heavy atom effect or oxygen enhancement.[8,27] Figure 10 shows the possible potential energy curves of the electronic states of tetramethylethylene as a function of the angle of twist about the double bond.[26] The presently detected charge-transfer state between oxygen and tetramethylethylene lies fairly above the lowest triplet (T←N) state of the donor. Under such a condition, the lowest triplet state of the donor seems to play an important role in the quenching of the charge-transfer fluorescence, since the charge-transfer state has the same spin multiplicity as the electronic state(triplet) formed between the triplet ground-state oxygen and the excited triplet-state donor.[10] The angular dependence of the energy of the charge-transfer state seems to be determined mostly by the angular dependence of the energy of the ethylene cation, which is opposite to that of the excited states of the ethylene according to the theoretical computations[41] as shown in Fig.10.

When the oxygen-olefin pair is excited in the charge-transfer band, a rapid radiationless transition might occur to the low-lying triplet state of olefin, leading to the quenching of the charge-transfer fluorescence and in some cases to the subsequent isomerization of olefin. As can be evaluated from the small molar extinction coefficients($\sim 100 M^{-1} cm^{-1}$) of the

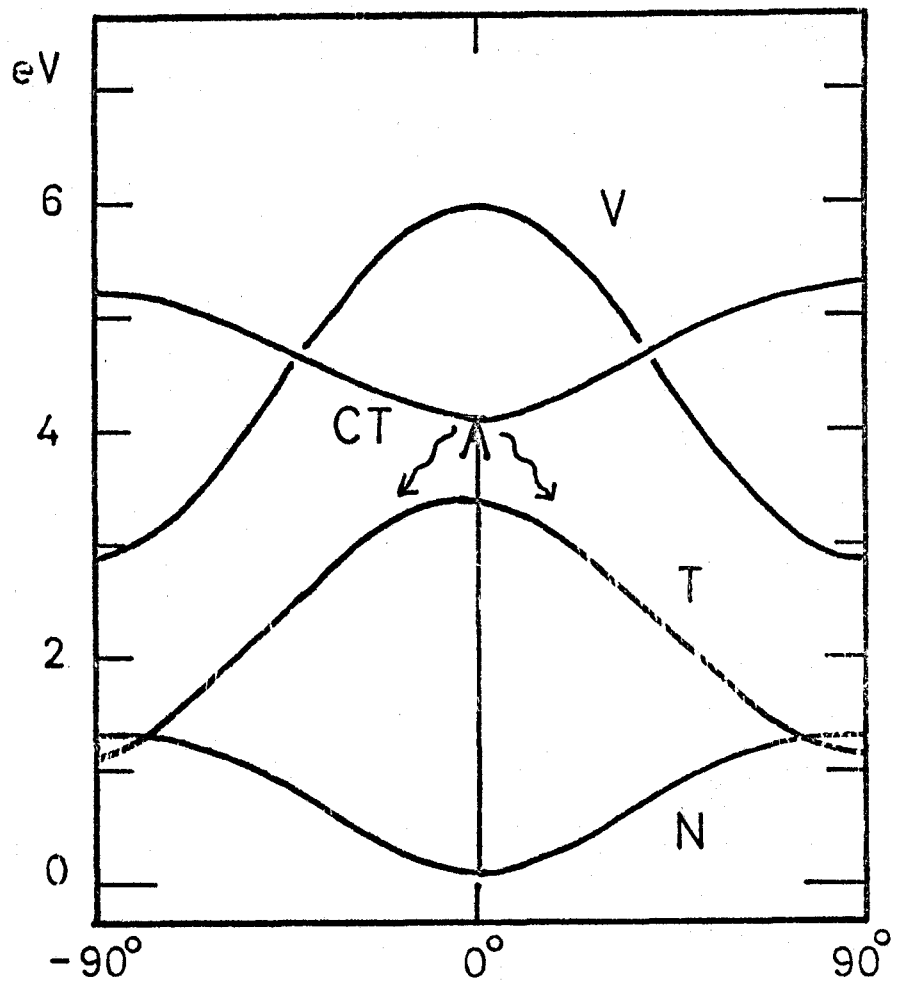

Fig.10. Schematic potential energy curves of the electronic states of tetramethylethylene and the charge-transfer state of the oxygen complex as a function of the angle of twist about the double bond. The vertical arrow represents the lowest charge-transfer transition.

charge-transfer bands observed for the olefins at 77°K, the radiative process from the charge-transfer state seems to be extremely slow compared to the above radiationless process. In practice, in the case of aromatic amines having the first charge-transfer states below the lowest triplet states of donor amines, we could detect the weak charge-transfer fluorescence having relatively long lifetime only at 77°K.[1] On the other hand, in the case of aromatic hydrocarbons having the first charge-transfer states above the lowest triplet states, no charge-transfer fluorescence has been detected.

In the case of aliphatic amines, though the accurate energies of the triplet states are not known at the present time, our observations of no any charge-transfer fluorescence seem to indicate the presence of the lowest triplet states of the aliphatic amines below the observed charge-transfer states. Our expectation is highly probable according to a recent experimental result that even the lowest triplet state of water is surprisingly low, ~4 eV above the ground state, from both the low-energy electron impact spectroscopy in the gas phase[42] and the thermoluminescence of ice using electron-reflection spectroscopy.[43] The other possible explanation is that the charge-transfer state, where the aliphatic amine seems to have an electronic structure almost similar to the cation, is less stable to the reactions such as dissociation. However, in the case of tertiary amines as electron donors and aromatic hydrocarbons as electron acceptors, charge-transfer flourescence has recently been observed in the solutions.[44]

REFERENCES

1) H.Ishida, H.Takahashi, H.Sato and H.Tsubomura, J.Am.Chem.Soc., 92, 275(1970); part I of a series.

2) H.Ishida, H.Takahashi and H.Tsubomura, Bull.Chem.Soc.Japan, 43, 3130(1970); part II of a series.

3) H.Ishida and H.Tsubomura, Chem.Phys.Letters, 9, 296(1971).

4) See, for example, C.H.Nicholls and P.A.Leermakers, in "Advance in Photochemistry", vol.8, W.A.Noyes, G.S.Hammond, and J.N.Pitts, Wiley-Interscience, New York, 1971,p-315.

5) Y.Nakato, M.Ozaki, A.Egawa and H.Tsubomura, Chem.Phys.Letters, 9, 615(1971).

6) P.W.Wong and A.O.Allen, J.Phys.Chem., 74, 774(1970).

7) D.F.Evans, J.Chem.Soc., 1735(1960).

8) M.Itoh and R.S.Mulliken, J.Phys.Chem., 73, 4332(1969).

9) N.Wiberg, Angew. Chem., 7, 766(1968).

10) H.Tsubomura and R.S.Mulliken, J.Am.Chem.Soc., 82, 5966(1960).

11) In the absorption spectrum of adsorbed benzene at 77°K (a in Fig.5), there appear vibrational bands on the long wavelength side from the main bands(A° series) with distance of 160 cm^{-1}. This vibrational progression, which is different from that detected by Ham in a glass containing ccl_4 at 77°K [J.S.Ham, J.Chem.Phys., 21, 756(1953)], can be reasonably attributable to the A^1 series: H.Sponer and E.Teller, Rev. Mod.Phys., 13, 76(1941).

12) D.F.Evans, J.Chem.Soc., 1351(1957).

13) S.D.Colson and E.R.Bernstein, J.Chem.Phys., 43, 2661(1965); 45, 3873(1966).

14) R.Pariser and R.G.Parr, ibid., 21, 466;767(1953).

15) D.M.Hanson and G.W.Robinson, ibid., 43, 4174(1965).

16) J.B.Birks, L.G.Christophorou and R.H.Huebner, Nature, 217, 809(1968).

17) C.Dijikgraaf, R.Sitters and G.J.Hoijtink, Mol.Phys., 5, 643(1962).

18) E.C.Lim and V.L.Kowalski, J.Chem.Phys., 36, 1729(1962).

19) R.S.Mulliken and W.B.Person, Ann.Rev.Phys.Chem., 13,107(1962).

20) S.H.Hastings, J.L.Franklin, J.C.Schiller and F.A.Matsen, J.Am.Chem.Phys., 75, 2900(1953).

21) M.Kroll, ibid., 90, 1097(1968).

22) H.Hosoya and S.Nagakura, Bull.Chem.Soc.Japan, 37, 249(1964).

23) P.D.Bartlett and A.P.Schaap, J.Am.Chem.Soc., 92, 3226(1970).

24) A.J.Merer and R.S.Mulliken, Chem.Rev., 69, 639(1969).

25) R.S.Mulliken, Phys.Rev., 115, 1225(1959); D.S.Burch, S.J.Smith and L.M.Branscomb, ibid., 112, 171(1958).

26) W.J.Potts,Jr., J.Chem.Phys., 23, 65(1955).

27) F.H.Watson and S.P.McGlynn, Theoret.Chim.Acta, 21,309(1971).

28) S.Iwata, J.Tanaka and S.Nagakura, J.Am.Chem.Soc., 89,2813(1967).

29) J.L.Lippert, M.W.Hanna and P.J.Trotter, ibid., 91,4035(1969).

30) R.S.Mulliken, C.A.Rieke, D.Orloff and H.Orloff, J.Chem.Phys., 17, 1248(1949).

31) A.M.Halpern, J.L.Roebber and K.Weiss, ibid., 49, 1348(1968).

32) R.Bhattacharya and S.Basu, Trans.Faraday Soc., 54,1286(1958).

33) H.Ishida and H.Tsubomura, to be published; see Chapter III.

34) J.N.Murrell, J.Am.Chem.Soc., 81, 5037(1959).

35) H.Akamatsu et al., "Tables of the Electron Affinities of Organic Molecules", to be published.

36) J.Aihara, M.Tsuda and H.Inokuchi, Bull.Chem.Soc.Japan, 43, 2439(1970).

37) J.Jortner and U.Sokolov, Nature, 190, 1003(1961).

38) H.O.Pritchard, Chem.Rev., 52, 529(1953).

39) J.A.P.Stockdale, R.N.Compton, G.S.Hurst and P.W.Reinhart, J.Chem.Phys., 50, 2176(1969).

40) R.K.Curran, ibid., 35, 1849(1961).

41) U.Kalder and I.Shavitt, ibid., 48,191(1968).

42) S.Trajmar, W.Williams and A.Kuppermann, ibid., 54,2274(1971).

43) D.Lewis and W.H.Hamill, ibid., 51, 456(1969).

44) M.G.Kuzmin and L.N.Guseva, Chem.Phys.Letters, 3, 71(1969).

Chapter III

Radiationless Transitions in the Excited Aromatics-Oxygen Systems at Low Temperature

SUMMARY

The efficiencies of fluorescence quenching by oxygen have been extensively examined for a number of aromatic hydrocarbons adsorbed on porous Vycor glass plates immersed in liquid oxygen at 77°K. Surprisingly, the fluorescence spectra of aromatic hydrocarbons are detected in most cases even in the presence of liquid oxygen. It has been found that the oxygen-enhanced radiationless transitions in the excited aromatic-oxygen pairs are so fast as to compete with the fluorescence decays under the present condition, and the intrinsic rate constants for the former depend to a large extent on the nature of the electronic states inherent in each aromatic hydrocarbon. By assuming the oxygen-enhanced intersystem crossing, these new interesting observations are reasonably interpreted in terms of Franck-Condon factors, the location of the second triplet states, and the symmetries of the related electronic states based on the general theory of radiationless transitions. Surprisingly, a relatively strong phosphorescence of benzophenone has been observed even in the

presence of liquid oxygen. The results of the phosphorescence quenching efficiencies for benzophenone and naphthalene by oxygen are also discussed in comparison with those of fluorescence quenching efficiencies.

INTRODUCTION

It is well known that molecular oxygen quenches the excited singlet and triplet states of aromatic molecules almost at a diffusion-controlled rate in the solutions[1-3]. Recent theoretical[4] and experimental[5,6] results of the oxygen quenching of triplet-state molecules have established that the quenching is due dominantly to the energy transfer process to singlet excited oxygen. Ottolenghi and co-workers[7] recently showed by use of a pulsed nitrogen laser that the conversion to the triplet state is the major path for the fluorescence quenching of aromatic hydrocarbons by oxygen(i.e., enhanced intersystem crossing process), analogous to the typical charge-transfer quenching of the fluorescence of aromatic hydrocarbons by diethylaniline[7].

As can be seen from the experimental observations of the diffusion-controlled quenching by oxygen in the solutions, the absolute rate of quenching must be higher than 10^{10} sec^{-1}, the reciprocal of the possible lifetime of a collision complex between an excited aromatic molecules and oxygen in the solutions.[4,7]

Kearns et al.[4] theoretically predicted an absolute quenching rate of $10^{11} \sim 10^{12}$ sec^{-1} for the oxygen quenching of the excited triplet state. Because of the experimental restriction mentioned above, it has ever been impossible to derive any reliable intrinsic quenching rate experimentally for a $D^*...O_2$ pair, where D* denotes an excited aromatic molecule. The purpose of the present work is to obtain the intrinsic quenching rate constants for several aromatic donor molecules, which is considered to be of great importance for understanding the mechanism and nature of the enhanced intermolecular radiationless transitions as well as the nature of the effective quenching interaction.

In a previous paper[8], we investigated the oxygen quenching of the fluorescence and phosphorescence of adsorbed aromatic hydrocarbons. There, we remarked an interesting phenomena that the fluorescence and short-lived phosphorescence are observed even from naphthalene adsorbed on porous glass immersed in liquid oxygen at 77°K. Under such a condition where the adsorbed aromatic hydrocarbon molecules are surrounded by oxygen molecules, it is possible to examine the intrinsic quenching rate of the $D^*...O_2$ pair. In the present work, we have extensively studied on the fluorescence quenching efficiencies of several aromatic hydrocarbons-porous Vycor glass plate adsorbates immersed in liquid oxygen at 77°K. The phosphorescence quenching efficiencies are also discussed for benzophenone and naphthalene in

comparison with those of fluorescence quenching under the same condition.

EXPERIMENTAL

Materials.——Oxygen, naphthalene and anthracene were purified in the same way as described in previous papers[8,9]. The purification of benzene was described in the preceding Chapter.[10] Pyrene, perylene and chrysene were chromatographed on activated alumina and silica gel, and recrystallized from benzene, followed by sublimation under vacuum. Tetracene and 2-methylanthracene were recrystallized from benzene and sublimed under vacuum. Specially prepared 9,10-diphenylanthracene of Nakarai Chemicals was used without further purification. Benzophenone was purified by recrystallization from ethanol and by sublimation under vacuum. The porous Vycor glass(PVG) plates of Corning Works were pretreated in the same way as described in the preceding Chapter.

Procedure.——Benzene and naphthalene were adsorbed on the pretreated PVG plates(40x10x0.8mm) from the vapor phase.[9,10] Other aromatic hydrocarbons were adsorbed from the n-hexane solutions and dried in a thin(1.5mm) quartz cell by evacuation at 100°C for 5~10 hr. Firstly, the fluorescence spectrum and decay time of the aromatic-PVG adsorbate was recorded at 77°K with the absence of liquid oxygen, and then purified oxygen gas was condensed into the quartz cell containing the PVG cooled

down to 77°K. The fluorescence spectrum of the aromatic-PVG adsorbate immersed in liquid oxygen was subsequently recorded under the same conditions at 77°K. In the case of benzophenone, the phosphorescence spectra and decay times were examined in the same way.

A Shimadzu Bausch-Lomb Monochromator with a dispersion of 7.4nm/mm was used to obtain the monochromatic exciting light from a 500W high pressure mercury lamp. Nalumi 1 meter Grating Spectrograph RM-23-I equipped with an RCA 1p-28 photomultiplier was used for recording the fluorescence spectra. The fluorescence decay times of adsorbed aromatic hydrocarbons were measured using the exciting light pulse of a coaxial UV-N_2 laser(337nm).[11] A Q-switched Ruby laser was used for the measurement of the phosphorescence decay times of benzophenone without and with the presence of liquid oxygen.[11] Absorption spectra were measured with a Shimadzu Multi-Purpose Spectrophotometer, Model 50L.

RESULTS AND DISCUSSION

Absorption and Fluorescence Spectra of Adsorbed Aromatic Hydrocarbons.——The concentrations of adsorbed aromatic hydrocarbons were set in the range from $1x10^{-7}$ to $1x10^{-6}$ mole/gram of PVG, where no luminescence and absorption bands characteristic of the aggregates or microcrystals of aromatic hydrocarbons could not be detected. At higher sample concentrations,

new bands ascribable to excimer fluorescence were observed besides monomer fluorescence for several aromatic hydrocarbons as described in the previous paper.[8] The absorption and fluorescence spectra of adsorbed anthracene at two sample concentrations are shown in Fig.1. At the lower concentration, the absorption and fluorescence spectra are in good agreement with those in the solutions, while remarkable spectral changes are observed at the higher concentrations.

The observed excimer fluorescence of anthracene is nearly in agreement with that observed in the photolytic dissociation of dianthracene in a low-temperature matrix,[12] where the sandwich dimer of anthracene giving rise to the excimer fluorescence is formed by the photolysis. The intensity ratio of the excimer band to the monomer band increases with increasing the concentration and depend on the exciting wavelength. From these results, the absorption spectrum at the higher concentration(b in Fig.1) is reasonably interpreted as the superposition of the absorption bands of the monomer and sandwich dimer easily formed at the higher concentration possibly due to the attractive interaction of adsorbed aromatic hydrocarbon with the surface of PVG. For the present purpose, the samples with lower concentrations are used as described above.

The absorption spectrum of aromatic hydrocarbon-PVG adsorbate does not appreciably change in the intensity, but

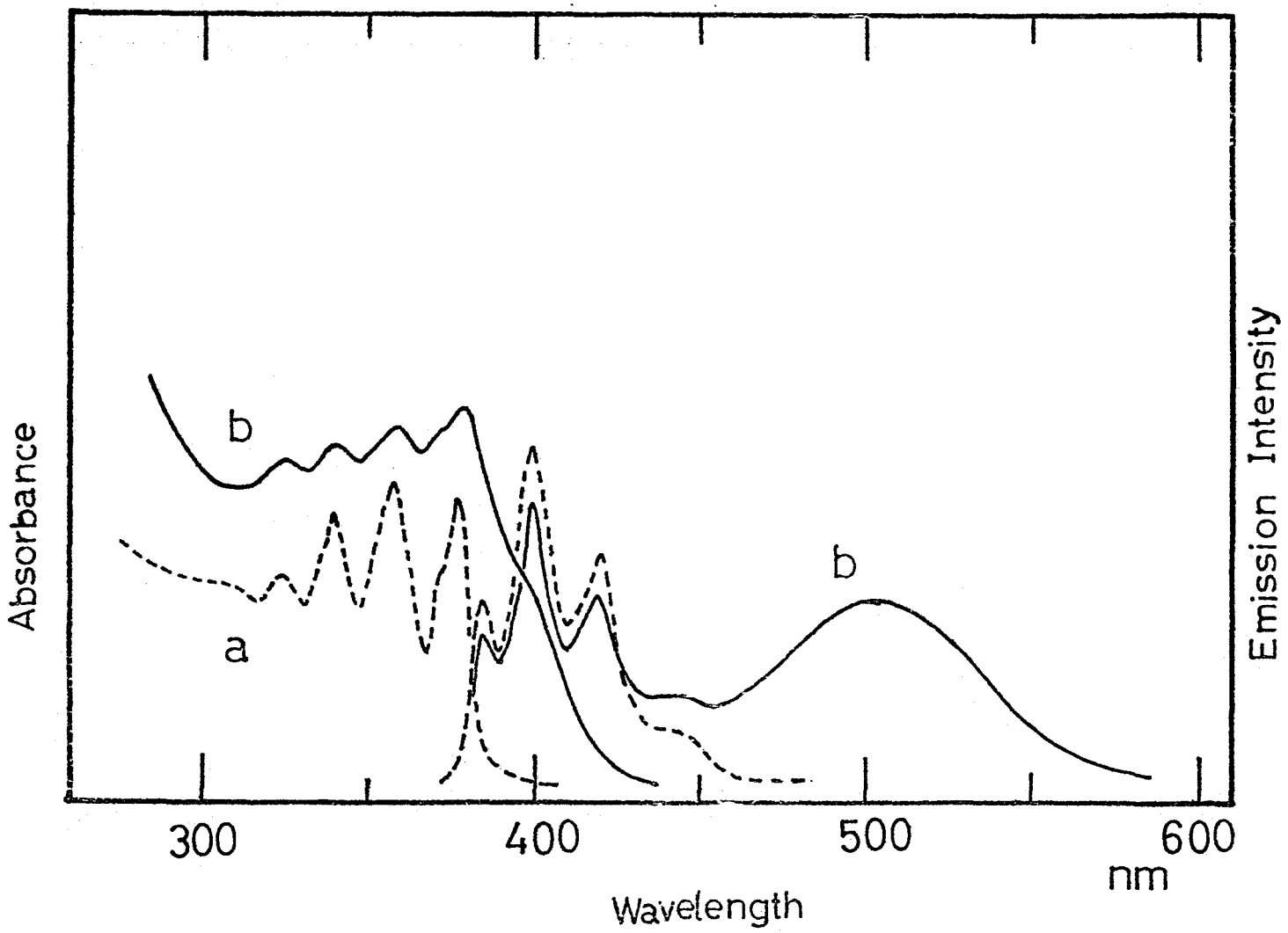

Fig.1. Absorption and fluorescence spectra of anthracene adsorbed on porous Vycor glass(PVG) plates at 77°K: (a) 2×10^{-7} mole/g, (b) 5×10^{-6} mole/g. Excitation wavelength: 340 nm.

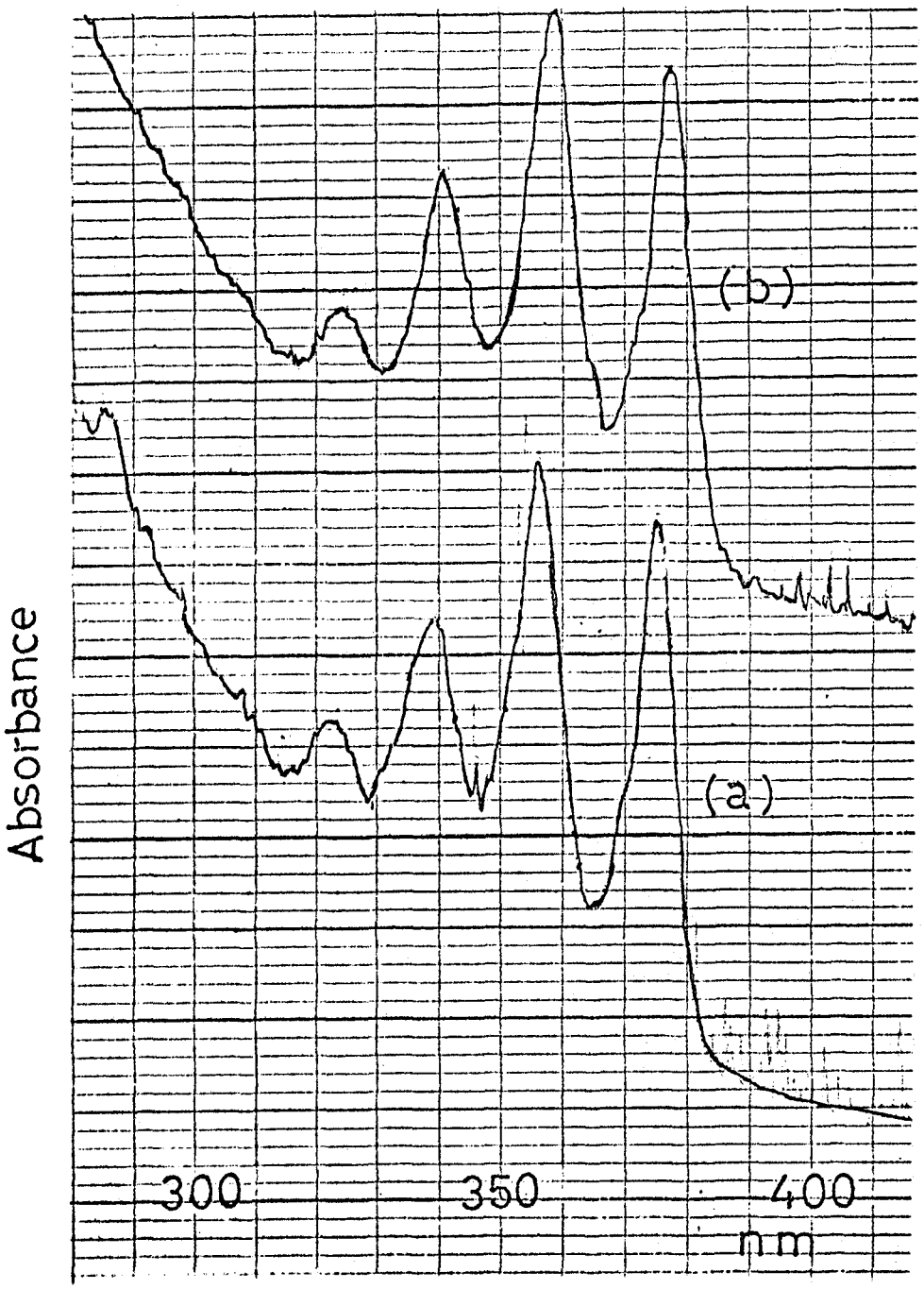

Fig.2. Absorption spectra of anthracene adsorbed on PVG plate: (a) without and (b) with the presence of liquid oxygen at 77°K.

shows only a slight red shift by the contact with liquid oxygen as shown in Fig.2 for the case of anthracene. The charge-transfer bands arising from the interaction between the aromatics and oxygen were negligible because of the low sample concentrations and the weakness of the charge-transfer bands.[10] The energies of the first excited singlet states(S_1) were determined for several aromatic hydrocarbons from the absorption spectra observed in the presence of liquid oxygen as summarized in Table 1, which are also in good agreement with those obtained in the solutions. As described previously, the triplet←—singlet($T_1 \leftarrow S_o$) absorption spectra of aromatic hydrocarbons and the charge-transfer absorption bands are observed clearly at much higher concentrations in the presence of excess oxygen or liquid oxygen at 77°K.[9,10] The energies of the lowest triplet states(T_1) for benzene and naphthalene were determined from the observed $T_1 \leftarrow S_o$ absorption bands, which are in good agreement with those in the solutions. Therefore, the T_1 energies for other compounds were taken from literature as summarized in Table 1. The onset energies of the observed first charge-transfer bands are also listed together with the ionization potentials of aromatic hydrocarbons. The values of the fluorescence lifetimes measured in the absence of oxygen at 77°K are also summarized in Table 1.

Table 1. Fluorescence Quenching Efficiencies of Aromatic Hydrocarbons by Oxygen

Aromatic	$I_f(O_2)/I_f$	$k_{fn}(O_2)$ (sec^{-1})	S_1[a] (cm^{-1})	T_1[b] $[L_a]$ (cm^{-1})	$\Delta E(S_1-T_1)$ (cm^{-1})	$\Delta E(S_1-T_2)$ (cm^{-1})	I_p[c] (eV)	τ_f[d] (ns)	E_{CT_1}[e] (cm^{-1})
Benzene	≤0.0001	$\geq 3.4\times10^{11}$	38100$[L_b]$	29400	8700	1000[e,f,g]	9.245	29	36000
Naphthalene	0.15	5.2×10^{7}	31800$[L_b]$	21300	10500	∿0[e,g,h]	8.12	110	28500
Anthracene	0.046	1.6×10^{9}	26400$[L_a]$	14850	11550	300[i]	7.38	13	22500
2-Methyl-anthracene	0.023	3.9×10^{9}	26100$[L_a]$	14560	11540	∿300[i]		11	
9,10-Diphenyl-anthracene	0.028	2.2×10^{9}	24500$[L_a]$	14290	10210	<0[i]		16	
Tetracene	0.14	3.0×10^{8}	21100$[L_a]$	10300	10800	≤0[j]	6.88	21	
Chrysene	0.49	2.3×10^{7}	27000$[L_b]$	19800	7200	≤0[k]	7.80	44	
Pyrene	≤0.0001	$\geq 3.6\times10^{10}$	26600$[L_b]$	16800	9800	(>0[l])	7.55	280	
Perylene	0.0011	8.3×10^{10}	22900$[L_a]$	12600	10300		7.03	12	

a) Data from the absorption spectra of adsorbed aromatic hydrocarbons in the presence of oxygen at 77°K. The electronic states are represented by a Platt notation in brackets(see ref. 27). b) Data from ref.3; P.S.Engel and B.M.Monroe, in "Advances in Photochemistry", vol.8, W.A.Noyes, G.S.Hammond and J.N.Pitts, Wiley-Interscience, 1971,p-297. c) Ref. 33. d) Data measured for the present system in the absence of oxygen at 77°K except for benzene(ref. b). e) Ref. 10. f) Ref. 17. g) Ref. 19. h) Ref. 18. i) Ref.20 and 21. j) Ref.22. k) Ref. 22 and 24. l) Ref. 25 and 26.

Fluorescence Quenching Efficiencies of Several Aromatic Hydrocarbons in Liquid Oxygen.—When liquid oxygen was introduced into the cell containing the aromatic-PVG adsorbates, remarkable differences in the fluorescence quenching efficiency was observed for the several aromatic hydrocarbons examined. The fluorescence spectra without and with the presence of liquid oxygen are shown in Fig.3-6 for anthracene, 9,10-diphenyl-anthracene, pyrene, and perylene, respectively. From the results of the absorption spectra in liquid oxygen, we can expect that the rate constants for radiative transitions(k_f) from the excited singlet-state aromatic hydrocarbons are almost the same under both conditions. The low-lying electronic states of the typical aromatic donor-O_2 pair, [D...O_2], are schematically represented in Fig.7.[13]

If we assume that the effective quenching interaction occurs not in the higher or non-relaxed excited singlet state but only in the relaxed lowest fluorescent state,S_1, the following equation can be obtained for the oxygen quenching:

$$I_f(O_2)/I_f = \tau_f(O_2)/\tau_f = 1/[1 + \tau_f k_{fn}(O_2)] \qquad (1)$$

$$\tau_f = 1/(k_f + k_{fn}), \quad \tau_f(O_2) = 1/[k_f + k_{fn} + k_{fn}(O_2)]$$

where $I_f(O_2)$ and I_f are the fluorescence intensities with and without the presence of liquid oxygen, respectively, $\tau_f(O_2)$ and τ_f are the corresponding fluorescence lifetimes, and

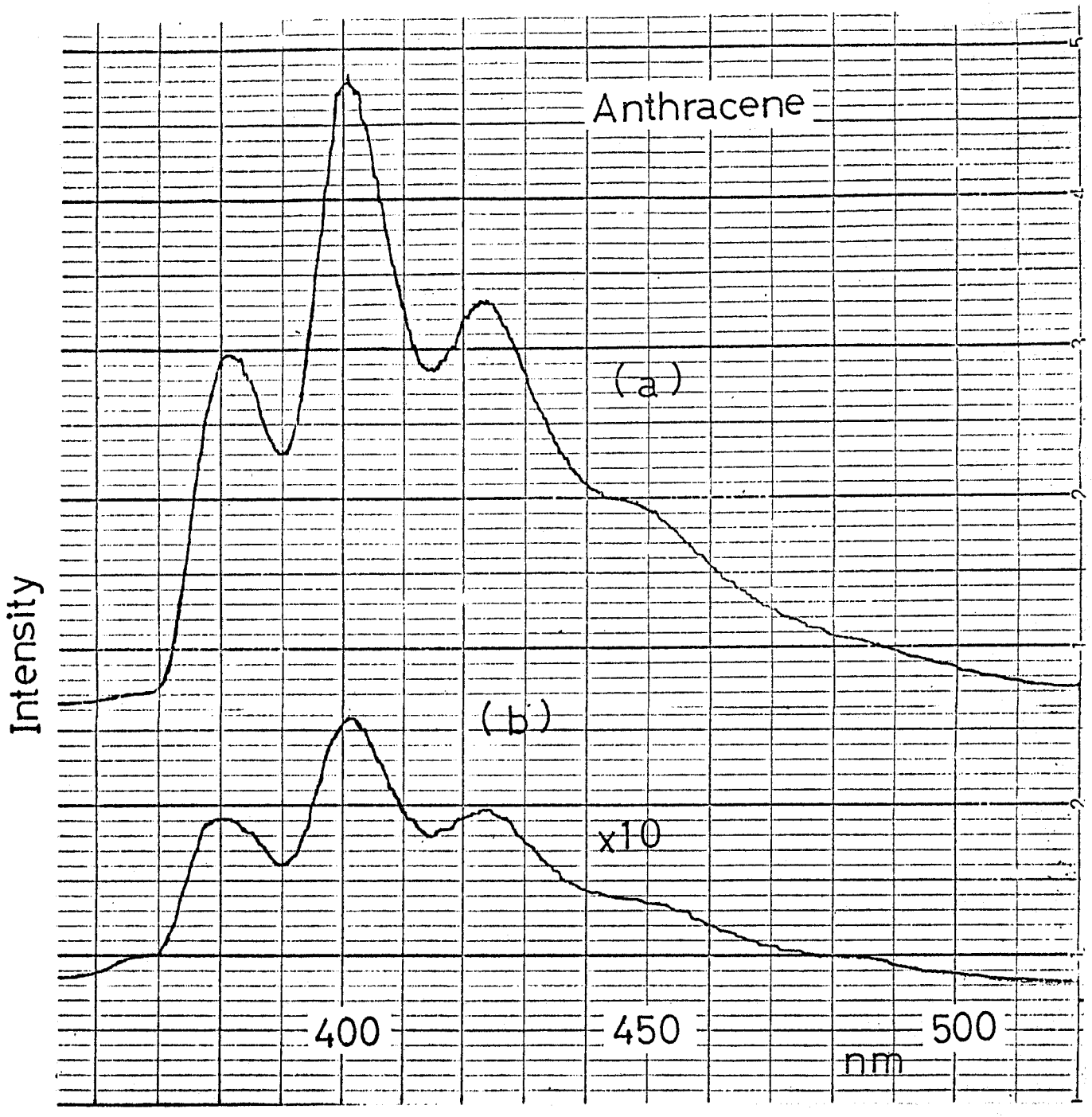

Fig.3. Fluorescence spectra of anthracene adsorbed on PVG plate: (a) without and (b) with the presence of liquid oxygen at 77°K.

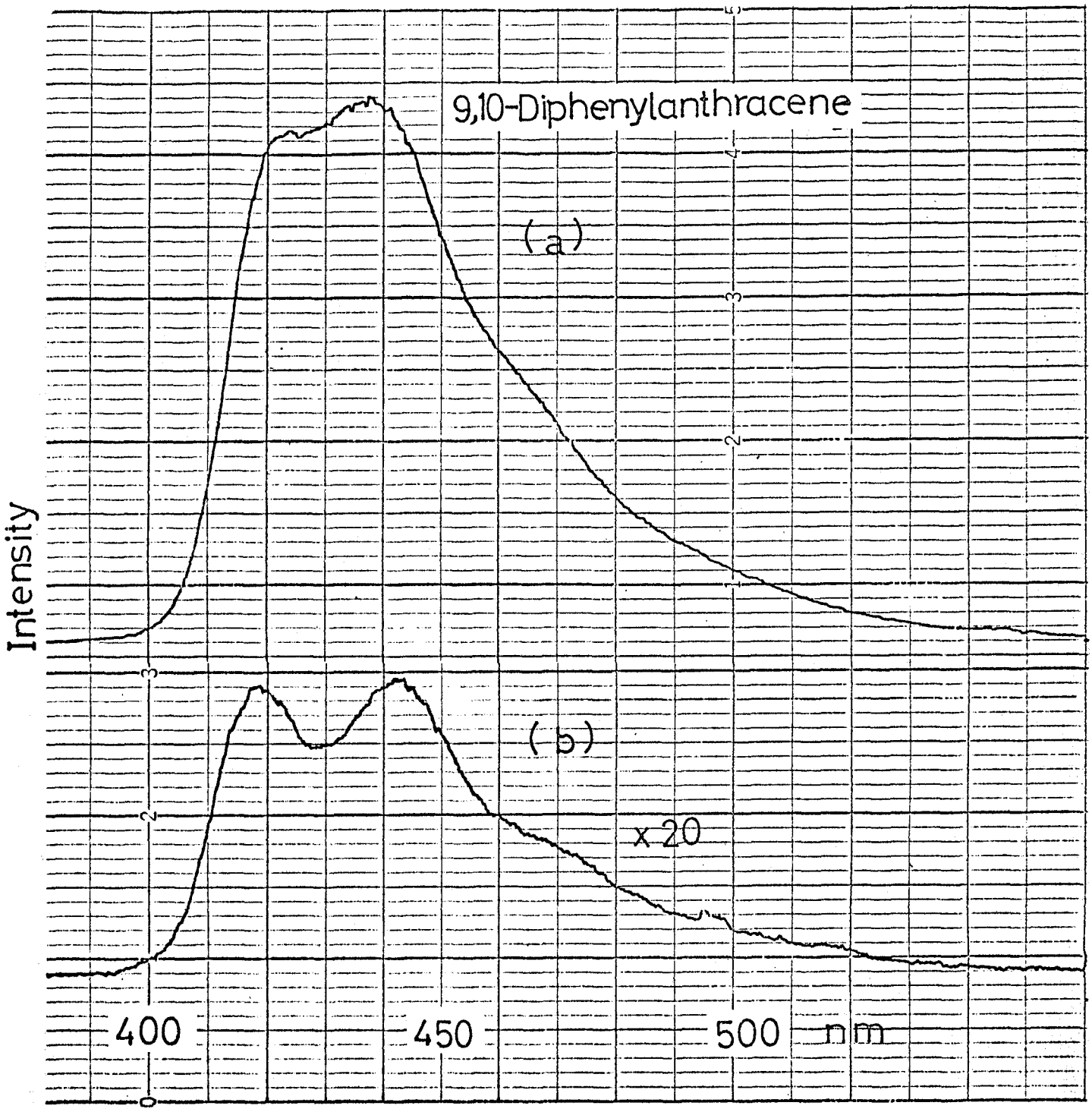

Fig.4. Fluorescence spectra of 9,10-diphenylanthracene adsorbed on PVG plate: (a) without and (b) with the presence of liquid oxygen at 77°K.

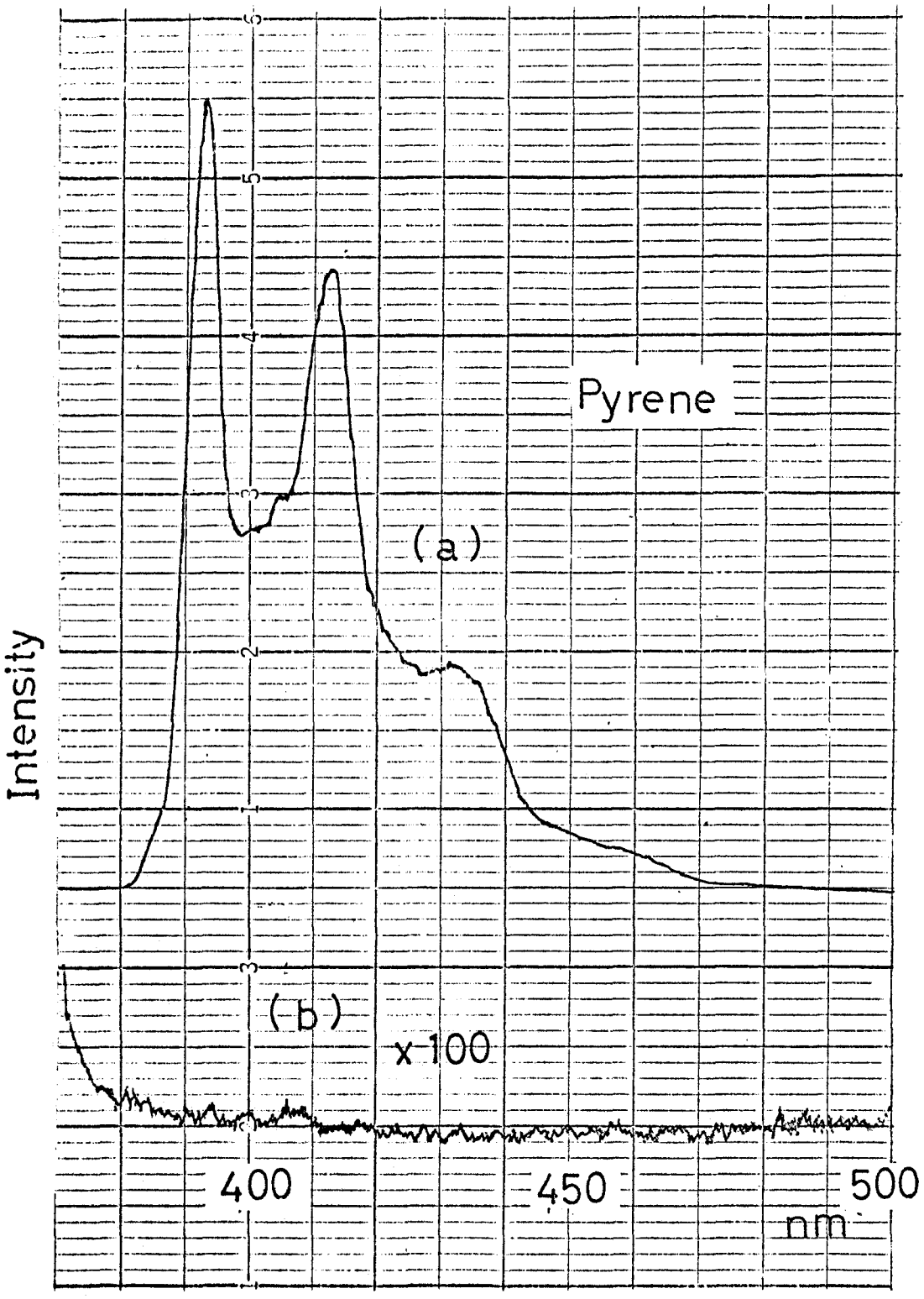

Fig.5. Fluorescence spectra of pyrene adsorbed on PVG plate: (a) without and (b) with the presence of liquid oxygen at 77°K.

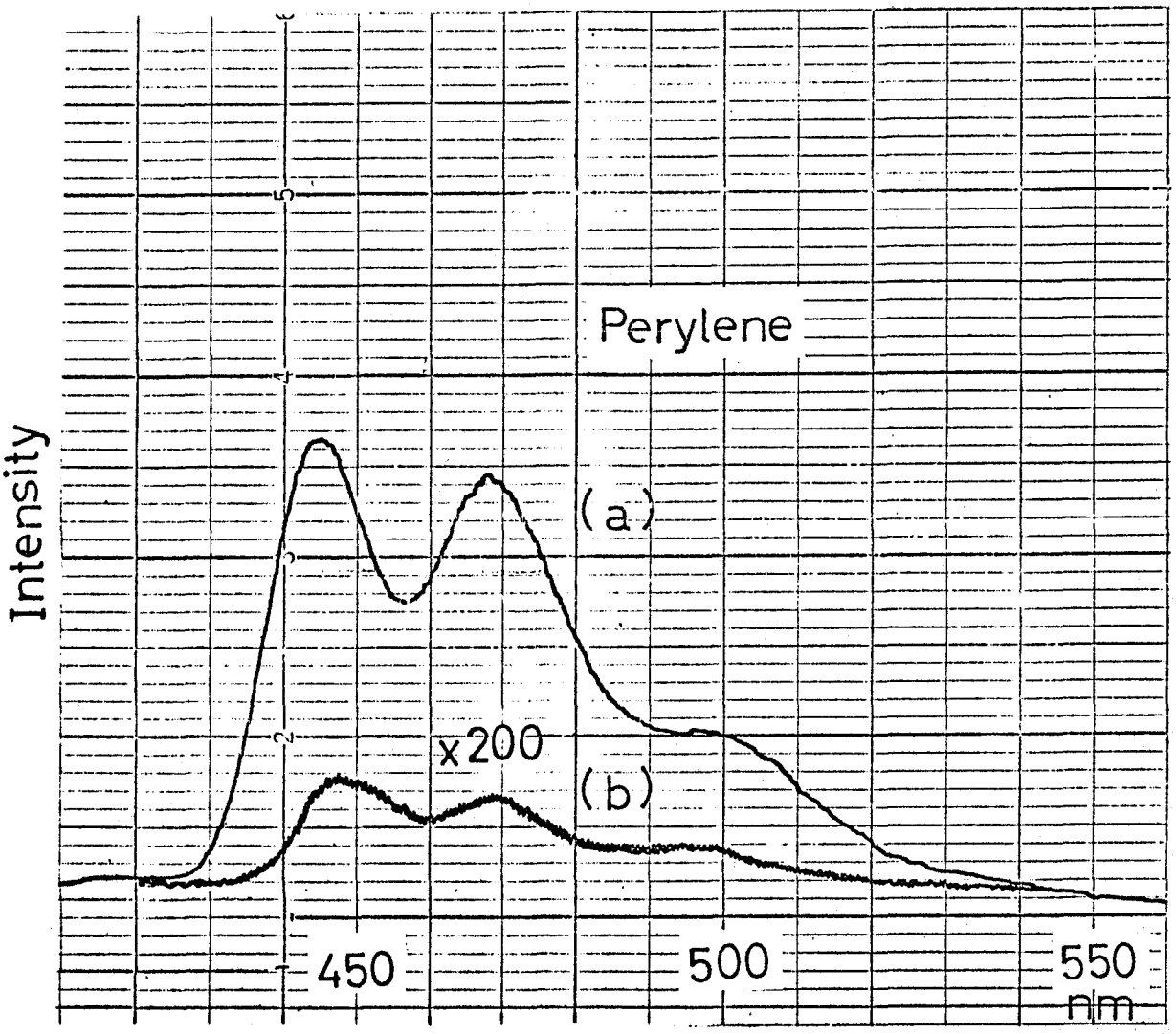

Fig.6. Fluorescence spectra of perylene adsorbed on PVG plate: (a) without and (b) with the presence of liquid oxygen at 77°K.

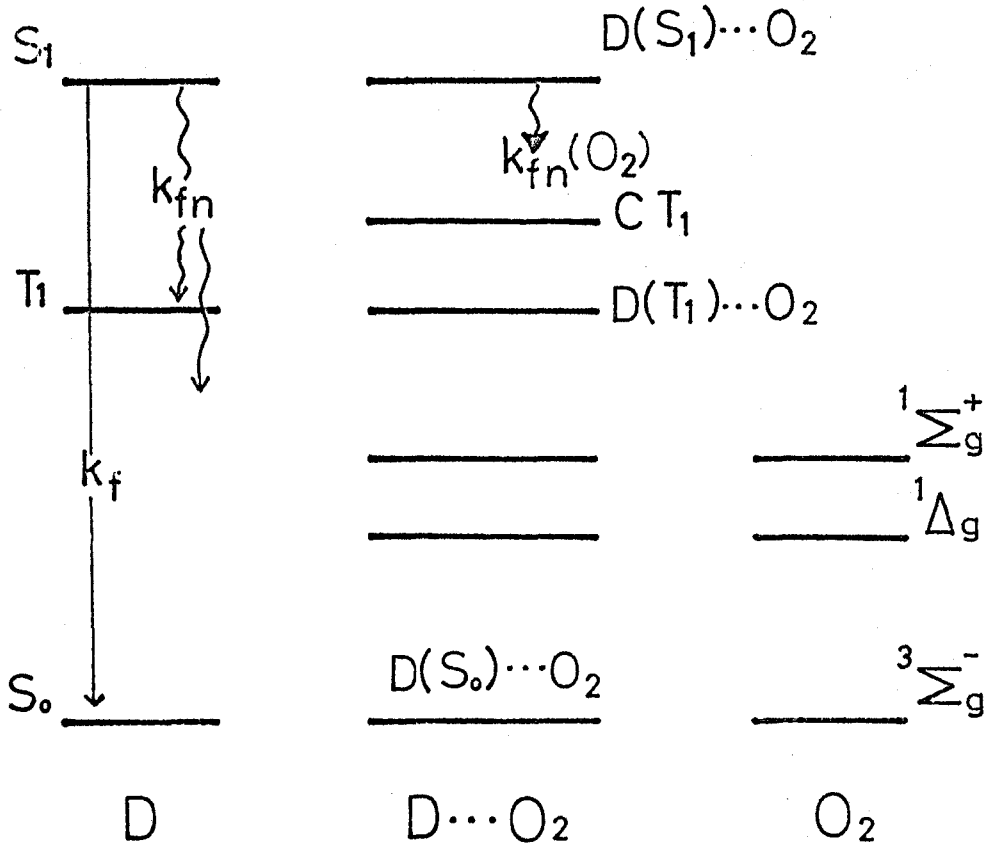

Fig.7. The low-lying electronic states of a 1:1 pair [D...O_2] between an aromatic molecule D and O_2. $K_{fn}(O_2)$ indicates the rate constant of the oxygen-enhanced radiationless transition from $D(S_1)$.

$k_{fn}(O_2)$ is the rate constant for the oxygen-enhanced radiationless transition from S_1 in the presence of oxygen (from $D(S_1)...O_2$ in Fig.7). The fluorescence decay curve was measured for chrysene in the presence of liquid oxygen at 77°K as shown in Fig.8. The decay curve was found to be completely exponential and the lifetime, $\tau_f(O_2)$, was 22ns. It is seen from Table 1 that $I_f(O_2)/I_f$ value of 0.49 is in very good agreement with $\tau_f(O_2)/\tau_f$ value of 0.50 in the case of chrysene. These results indicate the validity of the postulate that all the adsorbed aromatic molecules are interacting with oxygen in the excited fluorescent state, S_1, in the presence of liquid oxygen.

We can calculate $k_{fn}(O_2)$ values from the equation (1) based on the measured τ_f and $I_f(O_2)/I_f$ values for nine aromatic hydrocarbons as summarized in Table 1. The $k_{fn}(O_2)$ values for these molecules vary to a large extent from $\sim 10^7 sec^{-1}$ to $\sim 10^{11} sec^{-1}$, which are so large as to compete with the fluorescence decays despite the low temperature of 77°K. The $k_{fn}(O_2)$ values derived from the present work can be regarded as the intrinsic quenching rates in the $D(S_1)...O_2$ pairs suppressed by the low-temperature surrounding medium and, therefore, reflect the nature of the electronic states inherent in each aromatic hydrocarbon. On the other hand, the fluorescence quenching by oxygen in solutions is most reasonably seen to be diffusion-controlled process ($\sim 10^{10} M^{-1} sec^{-1}$).[3,14]

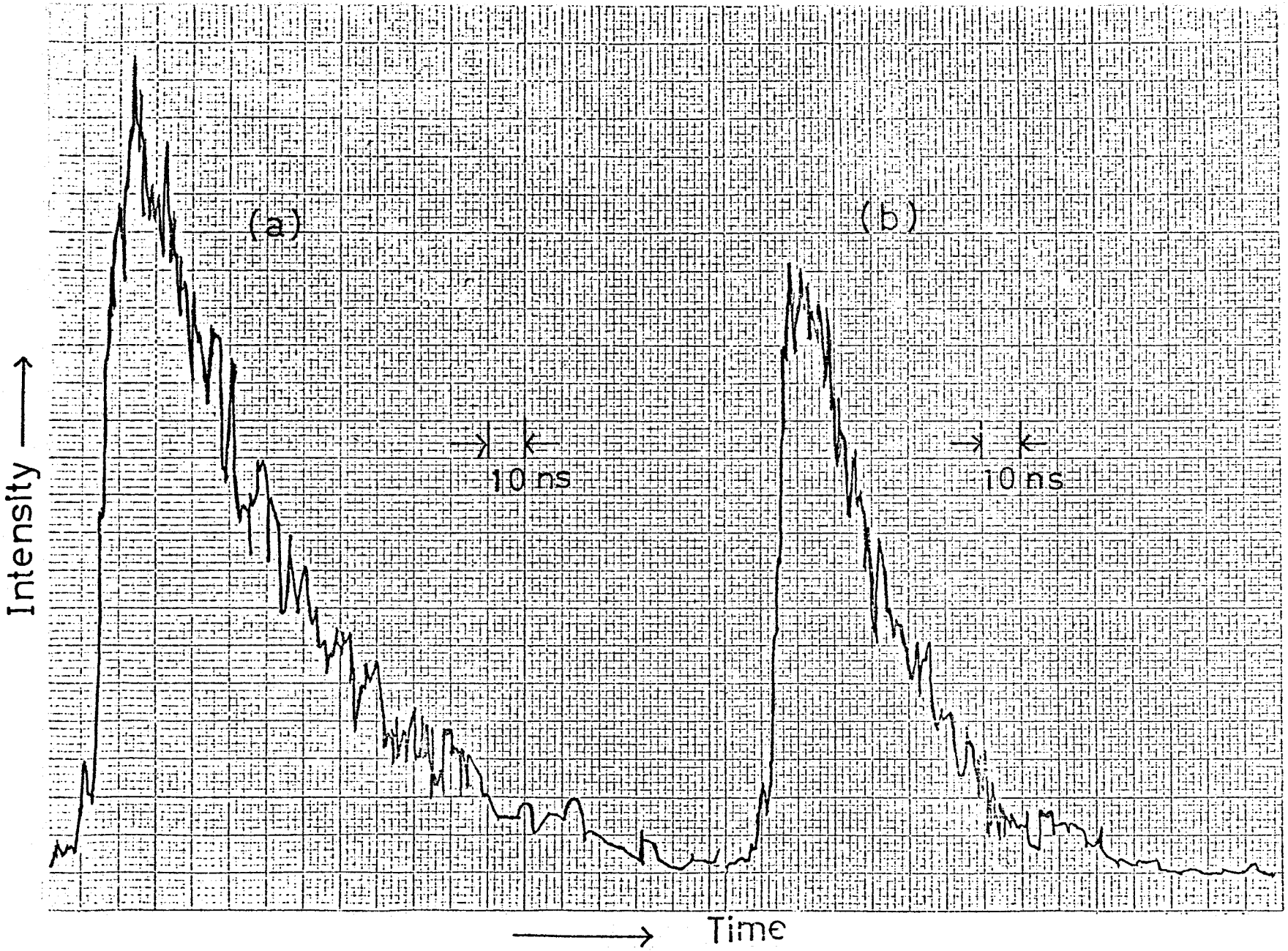

Fig.8. Fluorescence decay curves of chrysene adsorbed on PVG plate: (a) without and (b) with the presence of liquid oxygen at 77°K; excited with an N_2 laser(337 nm).

Mechanism and Classification of the Oxygen-Enhanced Radiationless Transitions from Singlet Excited Aromatic Hydrocarbons in the Presence of Oxygen.—— The energy levels of the low-lying excited singlet and triplet states, and the ionization potentials of aromatics as well as the $k_{fn}(O_2)$ values are diagramatically shown in Fig.9. As described in the preceding Chapter, we observed the first charge-transfer absorption bands with oxygen between S_1 and T_1 for benzene, naphthalene and anthracene(see Table 1).[10] As can be seen from Table 1 and Fig.7, the first charge-transfer states between aromatic hydrocarbons and oxygen, which are expected to show almost a linear dependence on the ionization potentials, will lie between S_1 and T_1 for all the other aromatic hydrocarbons. From the experimental facts of no any reliable dependence of the $k_{fn}(O_2)$ values on the charge-transfer states or the ionization potentials, the radiationless transition to the charge-transfer state (a)

$$D(S_1)\ldots O_2 \longrightarrow CT(D^+O_2^-) \qquad (a)$$

does not seem to be a dominant quenching process. The indifferent behavior of the $k_{fn}(O_2)$ values against the energy level of S_1 also indicate that the oxygen-induced internal conversion process(b)

$$D(S_1)\ldots O_2 \longrightarrow D(S_o)\ldots O_2 \qquad (b)$$

is not operative in the oxygen-enhanced quenching process.

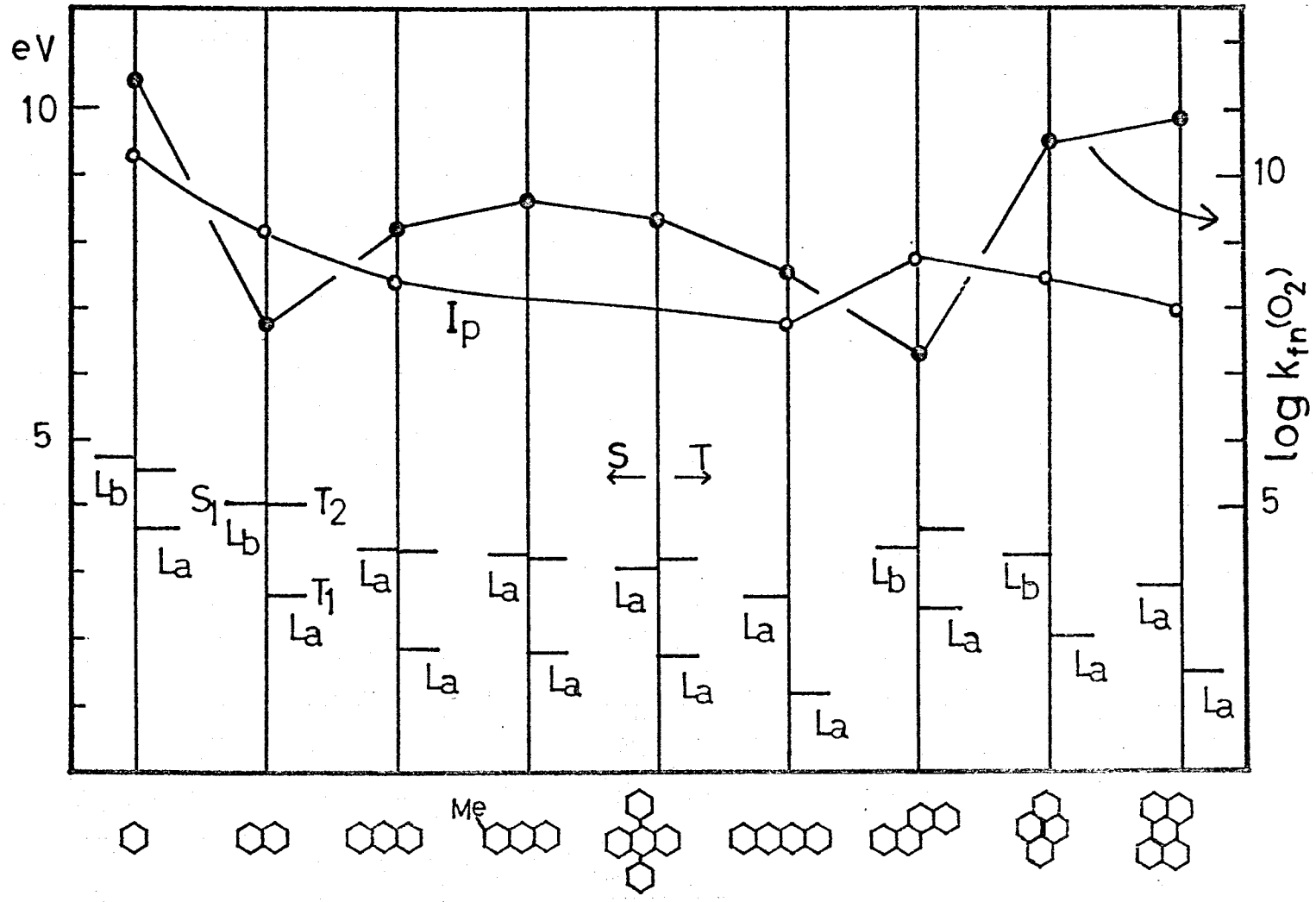

Fig.9. A schematic representation of the energy levels and the ionization potentials of aromatic hydrocarbons, and the rate constants $k_{fn}(O_2)$ of the oxygen-enhanced radiationless transitions in the $D(S_1)...O_2$ pairs.

Since the process (b) is expected to depend mainly on the Franck-Condon factors,[4,15,16] the $k_{fn}(O_2)$ values should increase with decreasing S_1 energy because of the increasing Franck-Condon factor.

We can also exclude the possible energy transfer process(c)

$$D(S_1)\ldots O_2 \longrightarrow D(T_1)\ldots O_2^*(\ ^1\Delta_g \text{ or } ^1\Sigma_g^+) \quad (c)$$

in the oxygen-enhanced quenching from the experimental observation that the $k_{fn}(O_2)$ value of naphthalene with S_1-T_1 energy gap of 10500cm^{-1} is nearly comparable to that for chrysene, in which the S_1-T_1 energy gap falls below 7900cm^{-1}, the energy required to produce excited singlet-state oxygen($^1\Delta_g$) in the quenching. Though Parmenter and Rau[3] have also excluded the quenching process(c) from the diffusion controlled quenching rate constants for several aromatic hydrocarbons in the solutions, our results provide more reliable experimental evidence for the conclusion. Taking into account the relative location of the second triplet states T_2 compared to S_1 and the symmetries of S_1 and T_1 along with the general theory of radiationless transitions[16] as will be shown below, it is found that the oxygen-enhanced intersystem crossing process(d)

$$D(S_1)\ldots O_2 \longrightarrow D(T_{1 \text{ or } 2})\ldots O_2 \quad (d)$$

appears to be mainly operative in the oxygen-enhanced quenching process of $D(S_1)\ldots O_2$.

Reliable data on the energies of the second triplet states T_2 of aromatic hydrocarbons are insufficient at the present

stage as seen from Table 1. T_2 of benzene was determined from the $T_2 \leftarrow S_o$ absorption band enhanced by oxygen in the present system,[10] which is in good agreement with that determined by Colson and Bernstein[17] from the oxygen-perturbed solid benzene at 4.2°K. In the case of naphthalene, the $T_2 \leftarrow S_o$ absorption band was not detected in the region between $S_1 \leftarrow S_o$ and $T_1 \leftarrow S_o$ bands.[10] According to the absorption spectrum of crystalline naphthalene at 4.2°K[18] and the electron impact spectrum of naphthalene vapor,[19] the second triplet state of naphthalene seems to lie at about the same energy as S_1. The second triplet states of anthracene and 2-methylanthracene were determined by the $T_2 \leftarrow T_1$ absorption spectra by Kellogg[20] and by Bennet and McCartin.[21] Taking into account the theoretical results by Kearns[22] and the experimental result of anthracene, the second triplet state of tetracene also seems to lie above S_1 or nearly at the same energy as S_1. The second triplet state of 9,10-diphenylanthracene is said to lie above S_1 from the very high fluorescence quantum yield even at room temperature,[21] since the intersystem crossing to T_2 is considered to be precluded by the large activation energy. In the case of chrysene having the lowest S_1-T_1 energy gap, the second triplet state is expected at about the same energy as S_1 or above S_1 from the result of $T_n \leftarrow T_1$ absorption[23] and the theoretical calculation by Pariser.[24] Ham and Ruedenberg[25] have theoretically predicted the T_2 energy level of pyrene to be sufficiently below S_1 ($2600 cm^{-1}$). This

result seems to be consistent with the results of the temperature dependence of the fluorescence quantum yield of pyrene in the solutions.[23,26]

In the Born-Oppenheimer approximation we can express the complete wavefunctions Ψ of the states as a product of two functions ψ and χ such that $\Psi = \chi\psi$, where ψ is a function of all electronic coordinates and depends parametrically on the nuclear coordinates, and χ depends only on the nuclear coordinates. From the general theory of radiationless transitions, the rate constant for the radiationless process(d) can be expressed as follows.[4,16]

$$k_{fn}(O_2) = (2\pi/\hbar)\rho\beta^2 F_{if} \qquad (2)$$

In this expression, β is the electronic matrix element for the initial Ψ_i and final Ψ_f states, ρ is the density of the final state quasidegenerate with the initial state, and F_{if} is the Franck-Condon factor for the transition to the directly coupled final state.

As the indirect mixing of the initial, $D(S_1)\ldots O_2$, and final, $D(T)\ldots O_2$, states via the charge-transfer state with oxygen appears to be more important in enhancing the radiationless transition than direct mixing(exchange interaction)[13], β is given as follows,[4]

$$\beta = \langle\psi_f|H|\psi_{CT}\rangle\langle\psi_{CT}|H|\psi_i\rangle/(E_i - E_{CT}) \qquad (3)$$

where H is the total Hamiltonian, ψ_i and ψ_f indicate the electronic wavefunctions of the initial and final states, respectively, ψ_{CT}

indicates the charge-transfer state, and $E_i - E_{CT}$ equal the energy difference between the corresponding states. F_{if} is given by

$$F_{if} = \sum_n |\langle \chi_f^n | \chi_i \rangle|^2 \qquad (4)$$

where n runs over all vibrational levels of the final state.

As indicated by Tsubomura and Mulliken,[13] the triplet state formed between $^3D(T)$ and $^3O_2$, $^3\psi_f$, mixes strongly with $^3\psi_{CT}$, which in turn mixes with the triplet state formed between $^1D(S_1)$ and $^3O_2$, $^3\psi_i$. It is worth noting that the electronic matrix elements $\beta(3)$ are considerably larger than the intramolecular direct S-T mixing matrix elements of free aromatic molecules through the spin-orbit interaction.[27] This seems to offer a reasonable explanation for the experimental fact that the fluorescence quenching of aromatics by oxygen is a very fast process.

According to a notation by Platt,[28] the lowest triplet states T_1 of the nine aromatic hydrocarbons are all represented by ^3L_a. The S_1 states are represented by ^1L_b for benzene, naphthalene, chrysene and pyrene, and by ^1L_a for the others as shown in Fig.9. The second triplet states T_2 are believed to be ^3B_b.[19,24,25] L_a corresponds to the B_{2u} electronic state of the aromatic hydrocarbons belonging to the D_{2h} point group, and both L_b and B_b to B_{1u}.[28,29] The possible symmetry correlation diagram of the excited states D* in the $D...O_2$ pair with C_{2v} or C_s symmetry is shown in Fig.10, although the actual geometrical configurations will not be so simple.

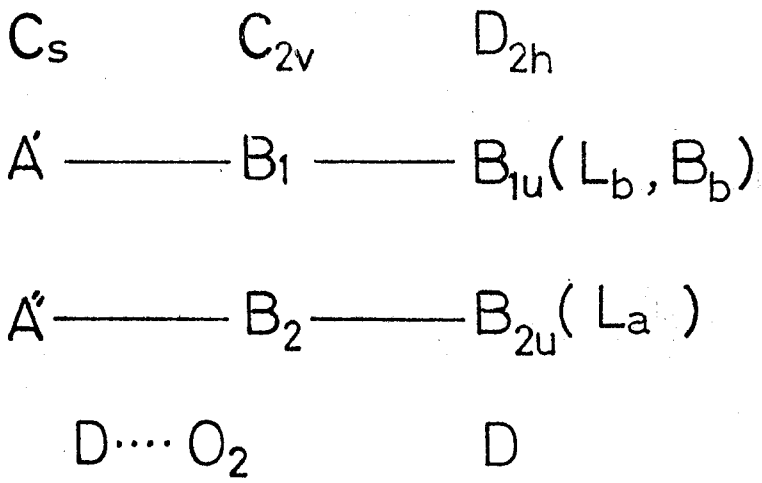

Fig.10. A possible symmetry correlation diagram of the excited electronic states of aromatic hydrocarbon D belonging to D_{2h} point group in the D...O_2 pair with C_{2v} or C_s symmetry.

The oxygen-enhanced radiationless transition process(d) is possibly classified into following three cases for the aromatic hydrocarbons examined.

Case I, S_1 is L_b or L_a and T_2 lies appreciably below S_1.

Case II, S_1 is L_a and T_2 lies at nearly the same energy as S_1 or above S_1.

Case III, S_1 is L_b and T_2 lies at nearly the same energy as S_1 or above S_1.

Benzene and pyrene belong to case I, where the radiationless process from S_1 to T_2 is thought to be very fast because of the extremely favorable Franck-Condon factors, since the S_1-T_2 energy gaps are much smaller than those of S_1-T_1.[15,16] From large $k_{fn}(O_2)$ value comparable to those of benzene and pyrene, perylene seems to belong to case I. Anthracene, its derivatives and tetracene belong to case II, where the radiationless process to T_2 nearly at the same energy as S_1 or above S_1 is thought to be precluded by the presence of fairly large activation energy expected in the process.[21,26] In this case, therefore, the oxygen-enhanced intersystem crossing process from $S_1(L_a)$ to $T_1(L_a)$ is dominant, and we can also applied the expressions (2)-(4) to the radiationless process just as to the case I. Because the symmetry of S_1 is the same as that of T_1 in the case II as seen from Fig.9 and 10, the electronic matrix elements including the totally

symmetric Hamiltonian(H), β, should be larger than those in case III, where the symmetry of $S_1(L_b)$ is different from that of $T_1(L_a)$. It seems reasonable to assume that appreciable difference in the F_{if} values are not expected between case II and case III because of the comparable S_1-T_1 energy gaps important for the oxygen-enhanced radiationless process. So, the remarkably large $k_{fn}(O_2)$ values in case I compared to the other cases can be well interpreted in terms of the dominant role of Franck-Condon factors in the oxygen-enhanced intersystem crossing from S_1 to T_2. Robinson and Frosch[16] have made quantitative calculations of the rates of the intramolecular intersystem crossing $S_1 \rightarrow T_2(\,^1B_{2u} \text{—} ^3E_{1u})$ and $S_1 \rightarrow T_1(\,^1B_{2u} \text{—} ^3B_{1u})$ in free benzene and indicated that $S_1 \rightarrow T_2$ mechanism dominates $S_1 \rightarrow T_1$ mechanism. The T_2 state near S_1 will also play an important role in the oxygen-enhanced intersystem crossing at higher temperatures, as indicated in the temperature dependence of the intramolecular intersystem crossings of free aromatic molecules with appreciable activation energies.[21,26]

Phosphorescence Quenching Efficiencies of Naphthalene and Benzophenone in Liquid Oxygen.——In the previous paper,[8] we detected weak phosphorescence of naphthalene with the extremely short lifetime($<10^{-3}$sec) from naphthalene-porous glass adsorbate immersed in liquid oxygen at 77°K. The natural radiative lifetime of oxygen-perturbed triplet-state naphthalene

was calculated to be 9×10^{-4}sec from the observed $T_1 \leftarrow S_o$ absorption spectrum under the same condition,[8,9] which is very short compared to the unperturbed value, 11 sec.[30] The rate constant of the oxygen-enhanced radiationless transition $k_{pn}(O_2)$ in the phosphorescence quenching of naphthalene can be estimated to be $\sim10^5 sec^{-1}$ from the relative phosphorescence intensities without and with the presence of liquid oxygen, the obtained $k_{fn}(O_2)$ value and the perturbed radiative rate constant in the presence of liquid oxygen, though the phosphorescence lifetime in liquid oxygen could not be measured.

The effect of oxygen on the phosphorescence of benzophenone is very small compared to that of naphthalene. The phosphorescence spectra and decay curves with and without the presence of liquid oxygen are shown in Fig.11 and 12, respectively. $I_p(O_2)/I_p$ is calculated to be 0.22 from the observed phosphorescence intensities. This value agrees with the $\tau_p(O_2)/\tau_p$ value of 0.28 calculated from the decay curves within experimental error [$\tau_p(O_2)$ = 2.8 ms and τ_p = 9.8 ms]. As it is well known that the quantum yield of intersystem crossing in benzophenone is unity even without the presence of oxygen,[31] $I_p(O_2)/I_p$ and $\tau_p(O_2)/\tau_p$ can be expressed by the following equation:

$$I_p(O_2)/I_p = k_p(O_2)\tau_p(O_2)/k_p\tau_p \qquad (5)$$

where k_p and $k_p(O_2)$ indicate the rate constants of the radiative transitions from the unperturbed and perturbed benzophenone, respectively. From the experimental fact that $I_p(O_2)/I_p$

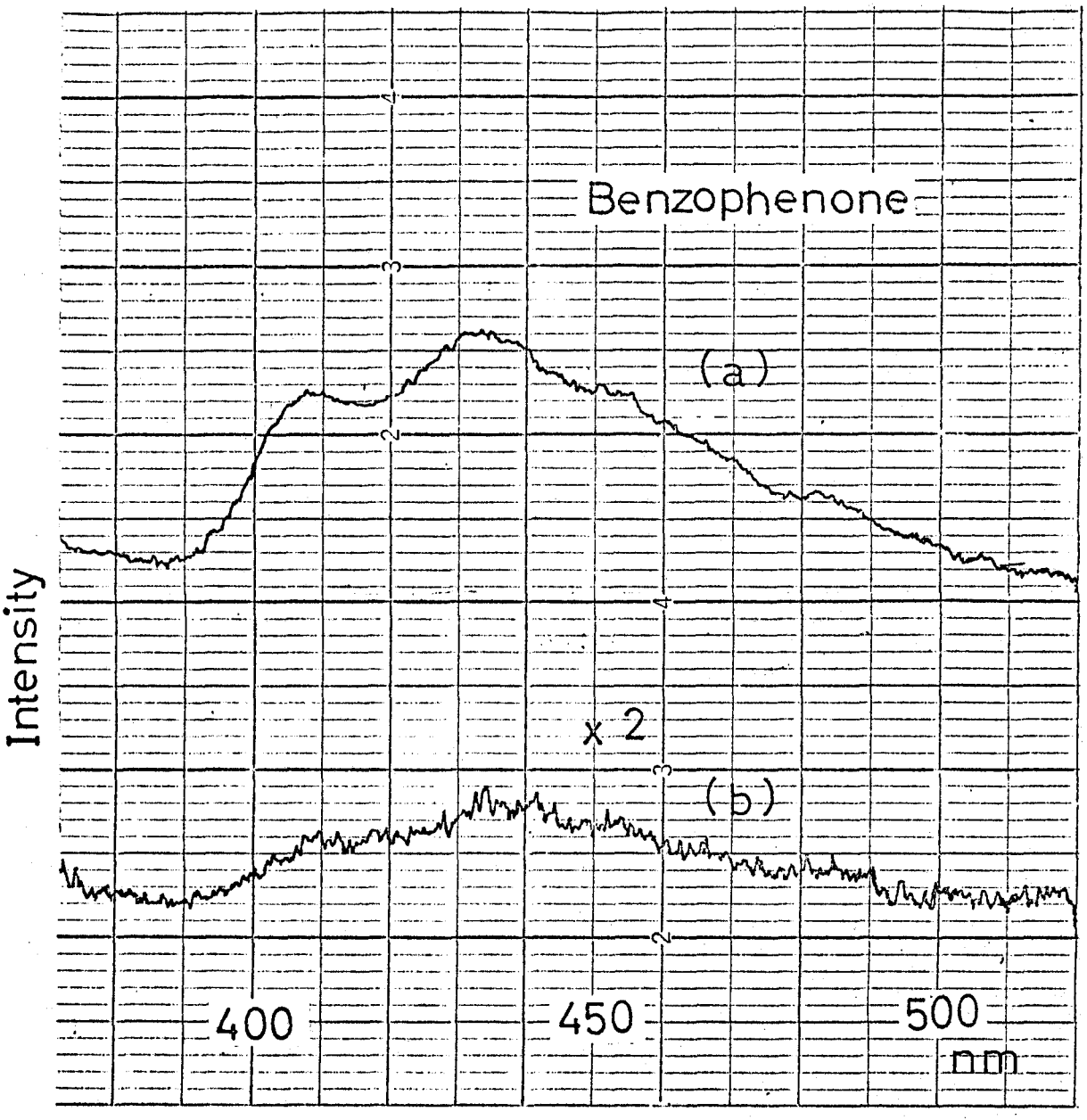

Fig.11. Phosphorescence spectra of benzophenone adsorbed on PVG plate: (a) without and (b) with the presence of liquid oxygen at 77°K.

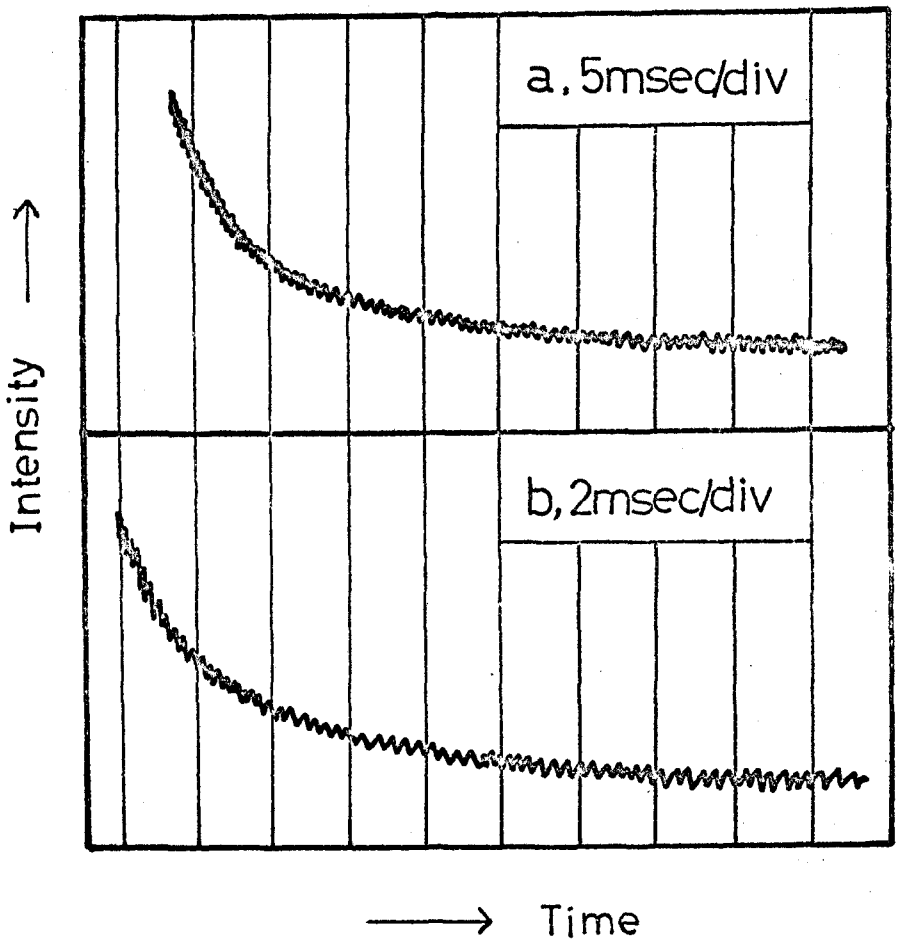

Fig.12. Phosphorescence decay curves of benzophenone adsorbed on PVG plate: (a) without and (b) with the presence of liquid oxygen at 77°K; excited with the light pulse of a Ruby laser(347 nm).

approximately equal to $\tau_p(O_2)/\tau_p$, it can be concluded that the radiative transition is little affected by the presence of oxygen, that is, $k_p \approx k_p(O_2)$. Our conclusion is also consistent with the result by Knada et al.[32], who have showed that the presence of oxygen has no apparent effect on the $T_1 \leftarrow S_o$ absorption of benzophenone in the solution. Consequently, the rate constant of the oxygen-enhanced radiationless transition, $k_{pn}(O_2)$, in liquid oxygen can be obtained by the following equation.

$$I_p(O_2)/I_p = 1/[1 + \tau_p k_{pn}(O_2)] \qquad (6)$$

The calculated $k_{pn}(O_2)$ value, $3.8 \times 10^2 sec^{-1}$, is very small compared to that of naphthalene.

The experimental fact of very weak oxygen effect on the triplet-state benzophenone seems to indicate an important role of the charge-transfer interaction in the oxygen quenching. The charge-transfer state with oxygen will lie at higher energy compared to those of aromatic hydrocarbons due to the large ionization potential(9.45 eV[33]). Consequently, the mixing between the excited phosphorescent n-π^* triplet state and the charge-transfer state will become considerably small. Furthermore, the interaction between the n-π^* state and charge-transfer state, which is important in the oxygen-enhanced radiationless process, is considered to depend on the magnitude of the overlap between the π^* orbital and the electron-accepting orbital $\pi(O_2)$ of oxygen, while the overlap between n orbital of benzophenone and $\pi(O_2)$ orbital is important for the charge-transfer interaction

in the ground state.[13,34] Since the intermolecular geometrical configurations between benzophenone and oxygen at 77°K seems to be determined by the favorable interaction in the ground state, the mixing of the n-π* state with the charge-transfer state will be small due to the unfavorable geometrical configuration for the mixing between them. On the other hand, the geometrical configurations favorable for the interaction between the π-π* excited states of aromatic hydrocarbons and the charge-transfer states with oxygen, π*—π(O_2) interaction, can also contribute to the charge-transfer interaction in the ground state.Recently, it has also been suggested by Brewer[35] based on his experimental results of the oxygen quenching for the fluorescence of benzene derivatives that the lack of observed oxygen quenching of the excited singlet state of many ketones may be due to their high ionization potentials.

CONCLUDING REMARKS

It has been found out that the obtained intrinsic rate constants of oxygen-enhanced radiationless transitions from S_1 in various aromatic hydrocarbons depend to a large extent on the nature of the electronic states inherent in each molecule, and by assuming the oxygen-enhanced intersystem crossing,these new observations are reasonably interpreted in terms of Franck-Condon factors, the location of the second triplet states and the symmetries of the related electronic states(S_1 and T_1).

It is the first case in the field of intermolecular interactions that the important roles of these factors have been pointed out in a quenching process in terms of the general theory of radiationless transitions based on the intrinsic quenching rate constants. Our conclusion that the enhanced intersystem crossing process is a dominant path in the fluorescence quenching by oxygen seems consistent with the recent result by Ottolenghi et al.[7], who examined the fluorescence quenching of aromatic hydrocarbons by oxygen in the solutions by use of a pulsed laser technique and directly observed the first population of T_1 from $T_n \leftarrow T_1$ absorption. In a polar solvent such as acetonitrile, they also found a small drop of T_1 population accompanied by the formation of aromatic cation radical, which is thought to result from the charge-transfer state via $D(S_1)...O_2$.

In our present system, liquid oxygen seems to act as a sort of non-polar solvent on the adsorbed $D^*...O_2$, which seems to be unfavorable for enhancing the internal conversion to the charge-transfer state. In addition, the rigid intermolecular configurations between adsorbed aromatics and oxygen at 77°K might suppress the degree of freedom neccesary for the radiationless relaxation processes of $D^*...O_2$.[37] These factors unfavorable for enhancing the radiationless processes lead to the small $k_{fn}(O_2)$ values

as competing with the fluorescence decays. Consequently, we could directly observe the weakened fluorescence of adsorbed aromatics even under the condition where the fluorescers are surrounded by oxygen molecules. From the energy-level aspect of the aromatic-oxygen pair[$D(S_1)...O_2>$ CT_1 in Fig.7], the fluorescence from S_1 can be regarded as an interesting example of the fluorescence from higher excited electronic states.

As shown in the previous paper,[8] at room temperature, no appreciable difference was observed in the efficiency of fluorescence quenching by oxygen between adsorbed anthracene and naphthalene. Because of the existence of appreciable activation energies in most cases of radiationless processes,[21,26] the $k_{fn}(O_2)$ values are expected to be at least in a few orders of magnitude larger at room temperature than those in the present system($10^7 \sim 10^{11}$ sec^{-1}), in agreement with the above experimental result. Therefore, the oxygen-enhanced radiationless processes in the solutions seems to be so fast as to compete with vibrational or solvent relaxation of the excited molecules at room temperature. This is consistent with the experimental observation that the fluorescence quenchings by oxygen in the solutions are the diffusion-controlled processes.

Recently, Porter et al.[14] and Thomas et al.[38] have revealed using laser phtolysis techniques that the oxygen

quenching of the triplet-state aromatics in the solutions is by a factor of ca. 10 slower than the diffusion-controlled quenching of the fluorescence by oxygen. This observation corresponds to our result that the $k_{pn}(O_2)$ values of naphthalene and benzophenone are extremely small compared to the $k_{fn}(O_2)$ values. These interesting observations can be interpreted reasonably in terms of the Franck-Condon factors for the oxygen-enhanced radiationless transitions, $S_1 \rightarrow T_{1 \text{ or } 2}$ and $T_1 \rightarrow S_o$, which increase with the decrease in the energy gap between the corresponding electronic states. As can be seen from Table 1, the S_1-T_1 or S_1-T_2 energy gaps are fairly small compared to the S_o-T_1 energy gaps. Such a condition is satisfied for the cases of naphthalene and benzophenone even when the well-known energy transfer process involving excited singlet-state oxygen is taken into account.

REFERENCES

1) D.Osborne and G.Porter, Proc.Roy.Soc., 284,9(1965).

2) B.Stevens and B.E.Algar, J.Phys.Chem., 72, 2582(1968).

3) C.S.Parmenter and J.D.Rau, J.Chem.Phys., 51, 2242(1969).

4) K.Kawaoka, A.U.Khan and D.R.Kearns, ibid., 46, 1842(1967); 48, 3272(1968).

5) D.R.Snelling, Chem.Phys.Letters, 2, 346(1968).

6) D.R.Kearns, A.U.Khan. C.K.Duncan and A.H.Maki, J.Am.Chem.Soc., 91, 1039(1969).

7) C.R.Goldschmidt, R.Potashnik and M.Ottolenghi, J.Phys.Chem., 75, 1025(1971); Chem.Phys.Letters, 9,424(1971).

8) H.Ishida, H.Takahashi and H.Tsubomura, Bull.Chem.Soc.Japan, 43, 3130(1970); part II of a series.

9) H.Ishida, H.Takahashi, H.Sato and H.Tsubomura, J.Am.Che.Soc., 92, 275(1970); part I of a series.

10) See Chapter II; H.Iahida and H.Tsubomura, to be published.

11) The authors wish to thank N.Mataga, H.Masuhara and N.Nakashima for the measurement of the fluorescence lifetimes by use of a N_2 laser and a Ruby laser. Detailed instrumental descriptions: see for the N_2 laser, K.Egawa, N.Nakashima, N.Mataga and C.Yamanaka, Bull.Chem.Soc.Japan, 44,3287(1971); for the Ruby laser, H.Masuhara and N.Mataga, Z.Phys.Chem., in press.

12) E.A.Chandross and J.Ferguson, J.Chem.Phys., 43, 4175(1965).

13) H.Tsubomura and R.S.Mulliken, J.Am.Chem.Soc., 82, 5966(1960).

14) L.K.Patterson, G.Porter and M.R.Topp, Chem.Phys.Letters, 7, 612(1970).

15) W.Siebrand, J.Chem.Phys., 44, 4055(1966); 46, 440(1967). For example, Kawaoka et al.[4] derived from the work of Siebrand the following semiempirical expression for Franck-Condon factor,F, and the electronic energy difference between the initial and final states, the amount of electronic energy converted into vibrational energy(ΔE in cm^{-1}):

$F = 0.15 \times 10^{-[(\Delta E-4000)/5000]}$

16) G.W.Robinson and R.P.Frosch, J.Chem.Phys., 37, 1962(1962); 38, 1187(1963). For example, they derived a rough analytic expression, $\log F = -0.1096 \Delta E^{0.4332}$.

17) S.D.Colson and E.R.Bernstein, ibid., 43, 2661(1965); 45, 3873(1966).

18) D.M.Hanson and G.W.Robinson, ibid., 43, 4174(1965).

19) J.Birks, L.G.Christophorou and R.H.Huebner, Nature, 217, 809(1968).

20) R.E.Kellogg, J.Chem.Phys., 44, 4111(1966).

21) R.G.Bennet and P.J.McCartin, ibid., 44, 1969(1966).

22) D.R.Kearns, ibid., 36, 1608(1962).

23) M.W.Windsor and J.R.Novak, in "The Triplet State", Cambridge University Press, 1967, p-229.

24) R.Pariser, J.Chem.Phys., 24, 250(1956).

25) N.S.Ham and K.Ruedenberg, ibid., 25, 13(1956).

26) S.Stevens, M.F.Thomaz and J.Jones, ibid., 46, 405(1967).

27) For example, the intramolecular spin-orbit matrix elements between π-π*excited singlet and triplet states are $\sim 10^{-5}$eV (S.P.McGlynn, T.Azumi and M.Kinoshita, "Molecular Spectroscopy of the Triplet state", Prentice-Hall, 1969, p-229). On the other hand, the indirect mixing via the CT state gives the matrix elements $\beta = \sim 10^{-3}$eV(see ref.4 and 13)

28) J.R.Platt, J.Chem.Phys., 17, 484(1949).

29) M.J.S.Dewar and H.C.Longuet-Higgins, Proc.Phys.Soc., A67, 795(1954).

30) E.H.Gilmore, G.E.Gibson and D.S.McClure, J.Chem.Phys., 23, 399(1955).

31) A.A.Lamola and G.S.Hammond, ibid., 43, 2129(1965).

32) Y.Kanda, H.Kaseda and T.Matsumura, Spectrochim.Acta, 20, 1387(1964).

33) F.I.Vielesov, USP.Fix.Nauk, 81, 669(1963).

34) J.N.Murrell, J.Am.Chem.Soc., 81, 5037(1959).

35) T.Brewer, ibid., 93, 775(1971).

36) A.Morikawa and R.J.Cvetanonic, J.Chem.Phys., 52, 3237(1970).

37) H.Ishida and H.Tsubomura, Chem.Phys.Letters, 9, 296(1971).

38) J.T.Richards, G.West and J.K.Thomas, J.Phys.Chem., 74, 4137(1970).

Chapter IV

Charge-Transfer Complexes in the Adsorbed Phase. Iodine Complexes with Benzene and Diethyl Ether, and Tetracyanoethylene Complex with Naphthalene Adsorbed on Porous Vycor Glass

SUMMARY

The iodine complexes with benzene and diethyl ether, and the tetracyanoethylene complex with naphthalene have been investigated spectrophotometrically in the adsorbed phase using thin porous Vycor glass plates as an adsorbent. In each case, a characteristic charge-transfer absorption spectrum was observed. The band maxima and intensities of the charge-transfer bands and the shifted iodine visible band have been examined at several temperatures. On the basis of the present results and those already obtained in both the gas and liquid phases, the nature of the weak charge-transfer interaction in the liquid phase as well as the characteristic molecular interactions on the surface are discussed by taking into account the possible adsorbent and solvent effects on the complexes.

INTRODUCTION

As described in the previous Chapter,the molecular interactions are somewhat different in the adsorbed phase from those in solutions and gas phase. At higher concentrations of adsorbed aromatic hydrocarbons such as naphthalene and anthracene, excimer-type fluorescence due to the ground-state sandwich dimers formed easily on the surface is observed in addition to the monomer fluorescence.[1,2] For the weak charge-transfer interaction of oxygen with organic molecules(so-called contact charge-transfer interaction), unlike the spectra in the solutions, the charge-transfer absorption bands with clear maxima are observed.[3,4]

For the weak charge-transfer complexes,e.g., the iodine-benzene complex, the question is not settled whether the electrostatic(Coulomb and polarization) or the charge-transfer force is more important for the ground-state stability of the complexes.[5,6] The relative relation between the intensity of the charge-transfer band and the stability is still open to question.[6,7] In the adsorbed phase, the molecular complex is thought not to undergo internal compression effect as exerted by solvent on the dissolved complex[8] and not be surrounded by continuous dielectric medium as in the solution. Furthermore, different from the complex in the gas phase, more fixed geometrical configurations might be expected especially for weak complexes because of the adsorptive

interaction with the surface of adsorbent on one side.

In the present work, we extent our spectrophotometric investigations on the molecular interactions in the adsorbed phase using porous Vycor glass as an adsorbent further to a number of charge-transfer complexes, the spectral and thermodynamic results of which are well known in both the gas and liquid phases and discuss the nature of the molecular interactions in these various media.

EXPERIMENTAL

The preparation of porous Vycor glass(PVG) plates (40x10x0.8mm) and the purifications of benzene, tetracyanoethylene(TCNE) and naphthalene were described in a previous Chapter.[4] Guaranteed reagent iodine from Merck was sublimed in vacuum. Diethyl ether was dried over calcium chloride and fractionally distilled.

The procedure of adsorption was also the same as described in the previous Chapter.[4] For the iodine complex with benzene or ether, the donor was adsorbed on the PVG plate placed in a thin quartz cell(1.5mm) from the vapor phase and the PVG plate was then exposed to iodine vapor through a break-off seal. For the TCNE complex with naphthalene, firstly TCNE and then naphthalene were adsorbed from the vapor phase. In each case, the amounts of adsorbed donor and acceptor were measured. The absorption spectra of the PVG-adsorbates were measured

at various temperatures with a Shimadzu Multi-Purpose recording spectrophotometer, Model 50L. In all cases, the amounts of the adsorbed donors were in large excess compared to those of the acceptors.[4] We can therefore assume that all of the acceptor molecules are in the form of complexes, an assumption, which will be confirmed as described later. Therefore, we have estimated the molar extinction coefficients of the charge-transfer bands based on the concentrations of the acceptor(iodine or TCNE) in the glass as shown in the previous Chapter.[4]

RESULTS

Absorption Spectra of the Iodine Complexes with Benzene and Diethyl Ether.— As shown in Fig.1, the absorption spectrum of adsorbed benzene is almost in good agreement with that in the solutions. When this benzene-PVG plate was exposed to iodine vapor, a new band attributable to the charge-transfer absorption was detected at 280 nm. In the ether-iodine system, a characteristic charge-transfer band was also observed at 250 nm as shown in Fig.2. The well-known visible band of iodine was found to have a maximum at 512 nm in the adsorbed phase at room temperature. The visible spectrum showed only a maximum at 505 nm in the presence of benzene, and at 495 nm in the presence of ether.

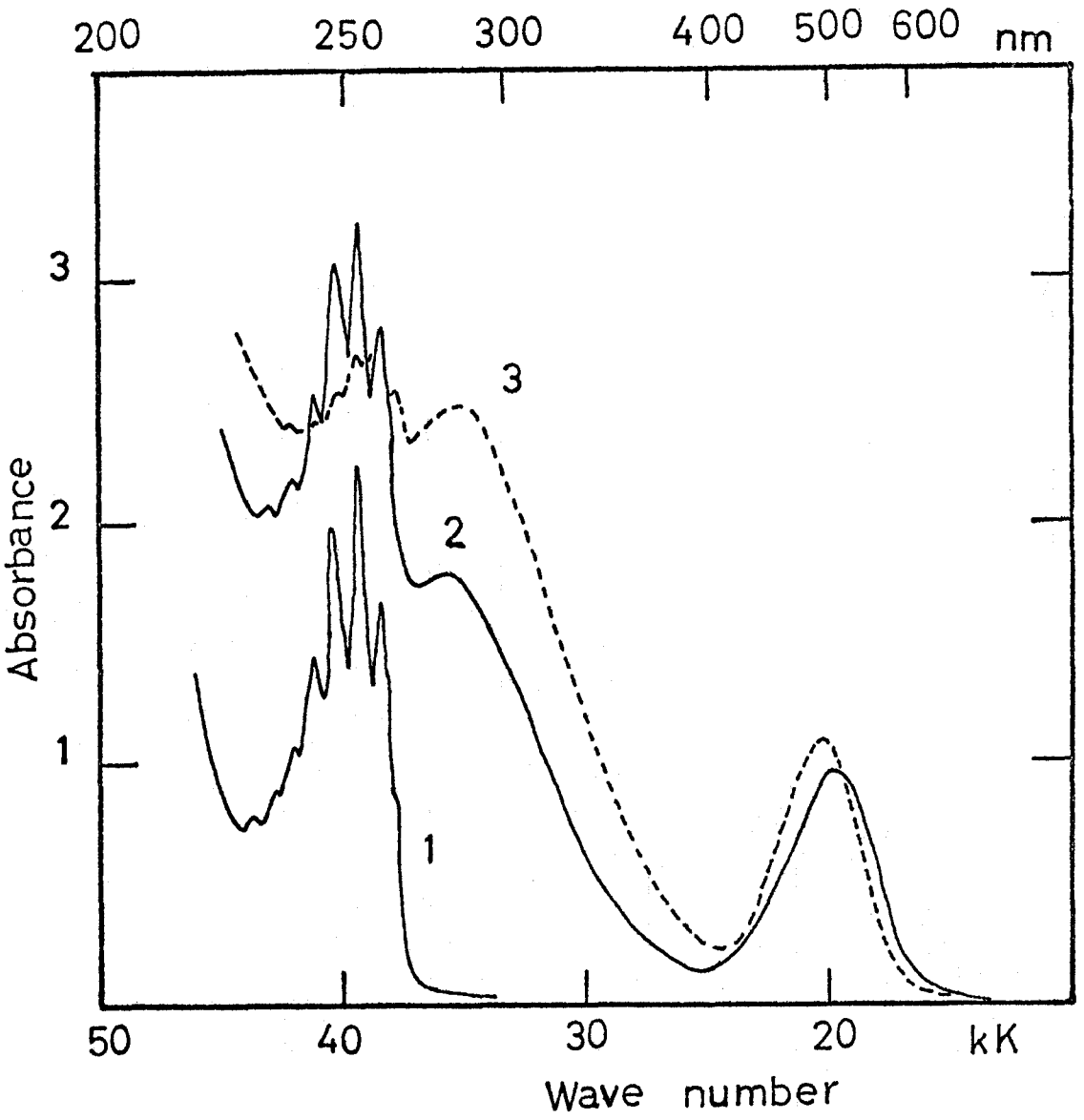

Figure 1. Absorption spectra of the iodine complex with benzene adsorbed on porous Vycor glass(PVG) plate: (1) benzene alone at room temperature, (2) after the adsorption of iodine at room temperature, (3) at -60°C.

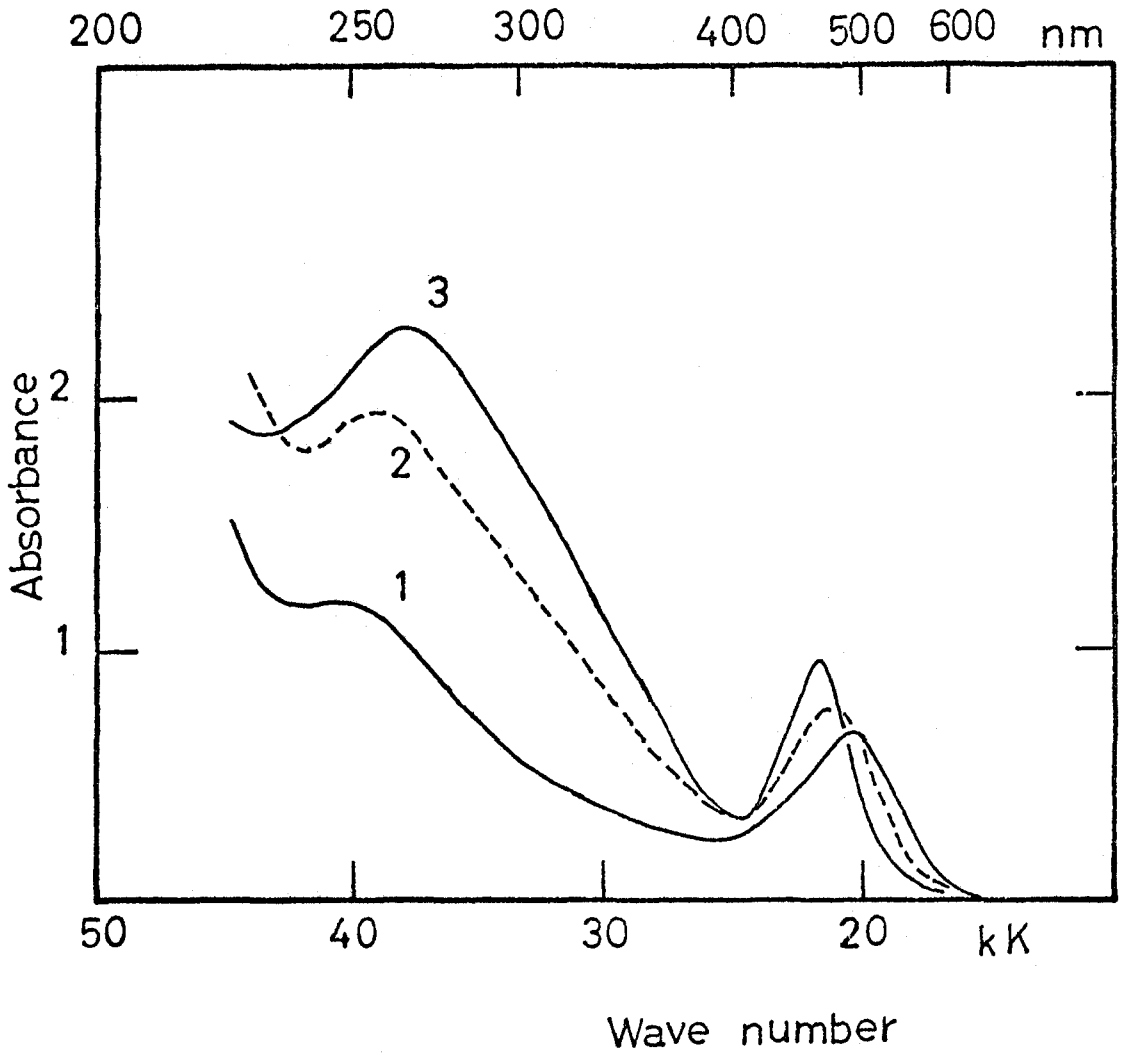

Figure 2. Absorption spectra of the iodine complex with diethyl ether adsorbed on PVG plate: (1) at room temperature, (2) at -60°C, (3) at - 196°C(77°K).

Table 1

Spectral Results of the Iodine Complex with Benzene.

		Charge-transfer band		Shifted iodine visible band[a]		
	ΔH (kcal/mol)	λ_{max} (nm)	ε_{max} ($M^{-1}cm^{-1}$)	λ_{max} (nm)	ε_{max} ($M^{-1}cm^{-1}$)	$\Delta\nu_{1/2}$ (cm^{-1})
Adsorbed phase						
at room temperature		280	1500	505	910	3720
at -60°C		283	1800	495	1000	3600
at -196°C(77°K)		290	2000	482	1150	3350
Gas phase[b]	-2.0±0.1	268	1650±100			
Liquid phase						
at room temperature						
in n-heptane[c,d]	-1.62	288	12000 14000	500		
in CCl_4[e]		292	16400			
at -196°C(77°K)[d]		324	13000	452		

a) For the adsorbed free iodine at room temperature, λ_{max}=512nm and ε=800. For iodine in n-hexane at room temperature, λ_{max}=522 and ε=897: H.Tsubomura and R.P.Lang, J.Am.Chem.Soc., 83, 2085(1961). b) F.T.Lang and L.S.Strong, ibid., 87, 2345(1965). c) Ref.19; T.M.Cromwell and R.L.Scott, ibid., 72, 3825(1950). d) Ref.9. e) L.J.Andrews and R.M.Keefer, ibid., 74, 4500(1952).

Table 2

Spectral Results of the Iodine Complex with Diethyl Ether.

		Charge-transfer band		Shifted iodine visible band		
	ΔH (kcal/mol)	λ_{max} (nm)	ε_{max} ($M^{-1}cm^{-1}$)	λ_{max} (nm)	ε_{max} ($M^{-1}cm^{-1}$)	$\Delta\nu_{1/2}$ (cm^{-1})
Adsorbed phase						
at room temperature		250	1500	495	810	5150
at -60°C		255	2300	475	920	4480
at -196°C(77°K)		262	2900	465	1150	3610
Gas phase[a]	-3.2±o.1	234	2100±400			
Liquid phase						
at room temperature						
in n-heptane[b]	-4.2	252	5650	462	950	4100
in CCl_4[c]	-4.3	249	4700	468	873	4100

a) See footnote b) in Table 1. b) M.Bandon, M.Tamres and S.Searles, J.Am.Chem.Soc., 82, 2129(1960). c) P.A.D.de Maine, J.Chem.Phys., 26, 1192(1957).

In both cases, the band attributable to the adsorbed free iodine could not be detected. It is well known that the visible iodine band shifts to blue upon complexing with various donors[9]. Therefore, the above results indicate that all of the adsorbed iodine is in the form of the complexes with the donor molecules, in support of our assumption in the determination of the molar extinction coefficients(ε_{CT}) of the charge-transfer bands in the adsorbed phase.

The temperature dependence of the absorption spectra of the iodine complexes adsorbed on the PVG plates were also examined as shown in Fig.1 and 2. For the measurement at -60°C, a mixture of 99% ethanol and liquid nitrogen was used as a coolant. Because of the almost negligible amount of the uncomplexed iodine, the concentrations of the complexes can be taken to be constant at different temperatures. So, we can examine the temperature dependence of the charge-transfer interaction itself in the complexes from the spectral results. The obtained spectral results of the iodine complexes are summarized in Table 1 and 2, together with those already obtained in both the gas and liquid phases.

Absorption Spectra of the TCNE Complex with Naphthalene.— The TCNE-naphthalene complex is well known in both the gas and liquid phases to have two charge-transfer absorption bands in the visible region due to the transitions from the

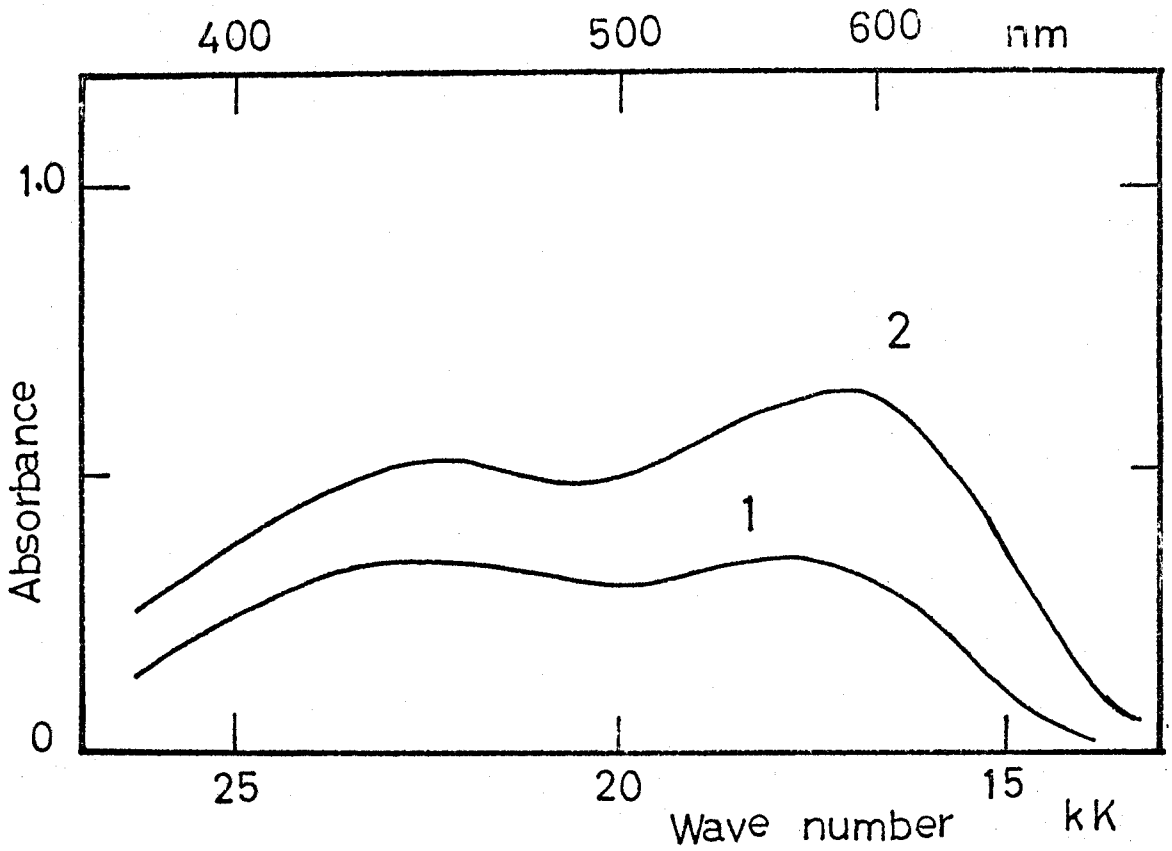

Figure 3. Absorption spectra of the TCNE complex with naphthalene adsorbed on PVG plate: (1) at room temperature, (2) at -196°C(77°K).

Table 3

Spectral Results of the TCNE Complex with Naphthalene.

		First charge-transfer band			Second charge-transfer band		
	ΔH (kcal/mol)	λ_{max} (nm)	ε_{max} ($M^{-1}cm^{-1}$)	$\Delta\nu_{1/2}$ (cm^{-1})	λ_{max} (nm)	ε_{max} ($M^{-1}cm^{-1}$)	$\Delta\nu_{1/2}$ (cm^{-1})
Adsorbed phase							
at room temperature		560	960	4100	440	960	5500
at -196°C (77°K)		585	2000		450	1700	
Gas phase[a]	-7.76	477	575±167	4000	384	610±177	5100
Liquid phase							
at roomtemperature							
in CCL_4[b]	-3.84	550	1640	3950	429	1660	4050
in CH_2CL_2[c]		550	1240		429	1120	

a) I.Hanazaki and R.S.Mulliken, Symposium on Electron-Donor-Acceptor Complexes, at Sendai, 1971, to be published.

b) Ref. 10. c) Ref. 11.

highest and the second highest occupied molecular orbitals of naphthalene to the lowest vacant molecular orbital of TCNE.[10-12] In the crystal of the TCNE-naphthalene complex, the charge-transfer band at the shorter wavelength is negligibly weak compared to other band at the longer wavelength.[13] The intensity ratio of the two charge-transfer bands seems to depend on the surrounding media which might play an important role in determining the ground-state geometries of the complex. It is interesting from this viewpoint to investigate the absorption spectrum of the TCNE-naphthalene complex in the adsorbed phase.

The charge-transfer absorption spectra obtained at room temperature and at 77°K are shown in Fig.3. Similar to those both in the gas and liquid phases, two bands were observed with comparable intensities. Upon cooling the sample to 77°K, the band showed a red shift and increase in the intensity. It is noteworthy that the band at the longer wavelength becomes stronger than the other band at 77°K as shown in Fig.3. The obtained spectral results of the TCNE complex with naphthalene are summarized in Table 3 together with those already obtained in both the gas and liquid phases.

DISCUSSION

Spectral Properties of the Charge-Transfer Complexes in the Adsorbed Phase.—It is well known that, as in the case of dissolved molecules, electronic absorption bands in the adsorbed phase shift generally toward the longer wavelengths in comparison with those in the gas phase.[14,15] It has been found[2] that the absorption spectra of aromatic hydrocarbons adsorbed on the PVG plates are nearly in good agreement with those dissolved in ethanol as seen from Fig.1 in the case of benzene. This is consistent with the expecration[15] based on the refractive index of PVG almost identical with that of silica gel(n=1.420). Therefore, there appears to be no specific interaction of adsorbed molecules with the surface of PVG other than dipol-dipol or van der Waals adsorptive interaction.

It is interesting that the absorption band maximum of the iodine complex with benzene in the adsorbed phase lies between those in the gas phase and solutions. On the other hand, the band maxima for the TCNE complex with naphthalene and the iodine complex with ether, which are relatively strong compared to the iodine-benzene complex as seen from the thermodynamic results in Table 1, 2 and 3, are almost in accord with those in the liquid phase.The presently estimated molar extinction coefficients ε based on the content of iodine seem to be reasonable from the

result that the obtained ε for the iodine visible band are almost in agreement with the values in the solutions within experimental error[16](see also footnote a in Table 1 and 2). Though there appear to be appreciably large experimental errors in the ε_{CT} values for weak complexes such as the iodine-benzene complex in the gas phase and solutions, it can still be found that the ε_{CT} in the adsorbed phase is nearly identical with that in the gas phase and is approximately by a factor of 10 smaller than that in the solutions. It is also of interest that the difference in ε_{CT} for the iodine-ether complex is considerably small compared with that for the iodine-benzene complex and the ε_{CT} value for the TCNE-naphthalene complex in the adsorbed phase is almost identical with that in the solution.

Orgel and Mulliken[17] explained the apparent anomaly of decreasing ε_{CT} with the increasing stability of the complex for weak complexes in terms of the contact charge-transfer absorption. Such a effect is considered to be negligible for strong complexes such as the TCNE complex and is expected to be less significant in the gas and adsorbed phases where the cage effect exerted by solvent is negligible. Trotter[8] has shown that the internal compression exerted by solvent on the solute molecules shows significant effects on the weak and compressible charge-transfer complexes such as the iodine-benzene complex, which lead to the large vapor-

liquid shift and the increase in the intensity of the charge-transfer band. One suggestion is possible that the solvent cage around the contact pair in solution might confine it under some pressure and make it stable in solution. On the other hand, in the adsorbed phase, the characteristic attractive interaction of adsorbed molecules with the adsorbent might be favorable for fixing the geometrical configurations of the weak complexes. We have shown from the spectral results that adsorbed organic molecules and oxygen have more fixed geometrical configurations than those in the solutions.[3,4] Therefore, it seems highly probable that the extremely small ε_{CT} for the adsorbed iodine-benzene complex compared to those in the solutions is mostly due to the large decrease of the contribution from the contact charge-transfer interaction. Furthermore, from the anomalous blue shift of the charge-transfer band of the iodine-benzene complex in the adsorbed phase even compared with those in the non-polar solvents, the internal compression effect of the solvent on the intermolecular distance of the weak and compressible complex and the resulting increased interaction[18] should also be taken into account in the explanation for the differences in the molecular interaction between the adsorbed and liquid phases.

As seen clearly from Table 2, the shift of the visible iodine band upon the complexing is smaller than those in

the solutions at room temperature even though the charge-transfer bands lie almost at the same wavelength. This can also be attributable to the interaction of the iodine in the complex with solvent molecules on other sides, which is unexpected in the adsorbed phase. Recently, Bhowmik[19] has also shown from the thermodynamic properties that the iodine-solvent interaction plays an important role in the iodine-benzene complex in the solutions.

Temperature Dependence of the Charge-Transfer Absorption Bands and Iodine Visible Band.— As evident from Fig.1 and 2, the charge-transfer bands shift toward longer wavelengths and the iodine visible band toward shorter wavelengths with decreasing the sample temperature. These shifts can be explained by the increased charge-transfer interaction at low temperature arising from the closer contact between the donor and acceptor molecules and the resulting higher overlap. Consequently, the blue shift of the iodine visible band is due mainly to the exchange repulsion between the suddenly swollen iodine molecule in the excited state and the the closer donor molecule.[20] As can be seen from Fig.1, the absorption of benzene itself becomes broader and lower in intensity at low temperature compared with that at room temperature, probably due to the increased interaction at low temperature.

It is worth noting that the iodine visible band is sharpened at low temperatures. This band is due to the transition from a somewhat antibonding orbital(π_g) to a lowest-vacant strongly antibonding σ-type orbital(σ_u).[21] As the dative(ionic) structure, $D^+I_2^-$, increases in the ground state of the complex with increasing charge-transfer interaction at low temperatures, the I-I bond distance of iodine(I_2) in the complex increases because of the increased anionic character of the iodine molecule in the ground state. The equilibrium bond distance of iodine in the $\sigma_u \leftarrow \pi_g$ excited state will be fairly larger than that in the ground state because of the strong antibonding σ_u orbital. Therefore, the differnce in the equilibrium bond distance between the ground and the excited states of iodine will decrease with the increasing charge-transfer interaction, which results in the less steep slope of the corresponding potential curve of the I-I bond in the excited state and leads to the sharper visible band of iodine together with the blue shift of the band.

In the case of the relatively strong π-π type complex of TCNE-naphthalene, the spectral properties in the adsorbed phase are in good agreement with those in the solutions. The red shift of the charge-transfer bands upon cooling are also due to the increased interaction at low temperature. It is interesting that the intensity of

the band at the longer wavelength becomes higher at 77°K than other charge-transfer band. A similar behavior has been observed for the solution of the TCNE-naphthalene complex under high external pressures.[22] These can be explained by assuming the corresponding two possible ground-state geometrical configurations of the complex as expected from the symmetrical consideration of the corresponding molecular orbitals of naphthalene and TCNE.[13] Under high pressures in the solution or at low temperature in the adsorbed phase, the relatively more stable geometrical configuration corresponding to the charge-transfer band at the longer wavelength is considered to become dominant.

REFERENCES

1) H.Ishida, H.Takahashi and H.Tsubomura, Bull.Chem.Soc.Japan, 43, 3130(1970).

2) See Chapter III.

3) H.Ishida, H.Takahashi, H.Sato and H.Tsubomura, J.Am.Chem.Soc., 92, 275(1970).

4) See Chapter II.

5) M.W.Hanna, J.Am.Chem.Soc., 90, 285(1968).

6) R.S.Mulliken, ibid., 91, 3409(1969).

7) J.N.Murrell, ibid., 81, 5037(1959).

8) P.J.Trotter, ibid., 88, 572(1966).

9) J.Ham, ibid., 76, 3875(1954).

10) G.Briegleb, J.Czekalla and G.Reuss, Z.Physik.Chem.N.F., 30, 316;333(1961).

11) R.E.Merrifield and W.D.Phillips, J.Am.Chem.Soc., 80, 2778(1958).

12) J.Aihara, M.Tsuda and H.Inokuchi, Bull.Chem.Soc.Japan, 42, 1824(1969).

13) H.Kuroda, T.Amano, I.Ikemoto and H.Akamatsu, J.Am.Chem.Soc., 89, 6056(1967).

14) W.West and A.L.Geddes, J.Phys.Chem., 68, 837(1964).

15) P.A.Leermakers, H.T.Thomas, L.D.Weiss and F.C.James, J.Am.Chem.Soc., 88, 5075(1966); M.Okuda, J.Chem.Soc. Japan, Pure Chem.Sec.(Nippon Kagaku Zasshi), 82, 1151;1121(1961).

16) J.Ham, J.Am.Chem.Soc., 76, 3886(1954).

17) L.E.Orgel and R.S.Mulliken, ibid., 79, 4839(1957).

18) M.Kroll, ibid., 90, 1097(1968).

19) B.B.Bhowmik, Spectrochimica Acta, 27A, 321(1971).

20) R.S.Mulliken, Rec.Trav.Chim., 75, 845(1956).

21) R.S.Mulliken, "Molecular Complexes", Wiley-Interscience, 1969, p-158;439.

22) J.R.Gott and W.G.Maisch, J.Chem.Phys., 39, 2229(1963).

Chapter V

Experimental Determination of the Charge-Transfer States between Acetone and Electron-Donating and Electron-Accepting Olefins

It was proposed by Turro and co-workers that the stereospecifical oxetane formation of aliphatic ketones in the n-π* singlet state with trans-dicyanoethylene(DCE) proceeds via a singlet complex as an intermediate[1] and that the ketone fluorescence is strongly quenched by both electron-donating and electron-accepting olefins possibly because of the nucleophilic and electrophilic properties of the n-π* excited state.[2]

We wish here to show experimentally that acetone acts both as an n-donor and as a π-acceptor by detecting the charge-transfer absorption bands with tetramethylethylene (TME) and DCE.

We have recently shown that the adsorption technique allows us to detect the charge-transfer absorption bands of very weak complexes even in the absorption region of component molecules[3,4](see also Chapter II). The porous Vycor glass(PVG) plate of Corning Glass Works, which is transparent down to 210 nm, was used as an adsorbent.[5] The PVG plate(40x10x0.8mm) placed in a thin quartz cell

was exposed to acetone vapor through a break-off seal, then cooled to 77°K and exposed to TME or DCE vapor through the other break-off seal. The absorption spectra of the plates were measured before and after the adsorption of olefins as shown in Fig.1.

Weak absorption bands characteristic of neither component alone were observed in the region of acetone absorption by the adsorption of DCE and TME. The intensities of the new bands increase with decreasing the temperature and vice versa. This fact seems to indicate that the new bands arise from weak charge-transfer type interactions between adsorbed acetone and olefins. From the viewpoint of acetone molecular orbitals, it can be expected that acetone acts as both an n-donor and π-acceptor.

The position of the charge-transfer state can be estimated in a similar way as for an ordinary complex. The ionization potential of TME(I_p) is 8.30 eV[6] and the electron affinity of acetone(E_A) is considered to be negative, leading to a charge-transfer complex with the absorption in a region of fairly short wavelengths. The Coulomb attraction energy(C) between acetone anion and TME cation is calculated to be 3.5∿4.0 eV by point charge approximation for the probable geometrical configurations. Hence, the charge-transfer state can be calculated by use of the equation, $E_{CT} = I_p - E_A - C$, to be approximately at 5 eV(40kK)

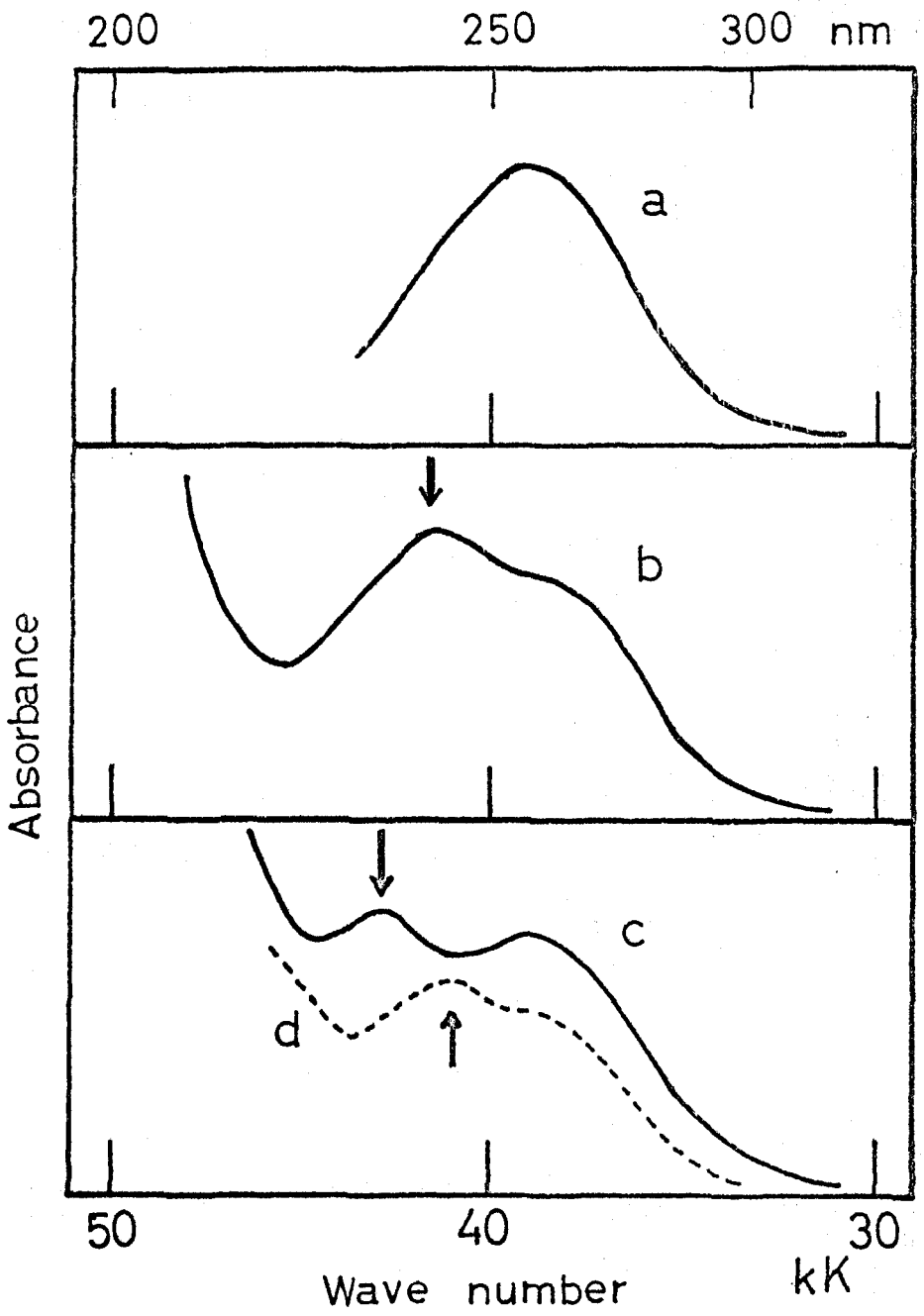

Fig.1. Absorption spectra of acetone and olefins adsorbed on PVG Plates at 77°K: (a) acetone, (b) acetone and tetramethylethylene, (c) acetone and trans-dicyanoethylene, (d) acetone and iodine.

above the ground state, in good agreement with the observed new band(Fig.1 b).

In the case of acetone and DCE, the observed new band can also be reasonably assigned to the charge-transfer absorption band between acetone as a donor(I_p=9.7 eV[6]) and DCE as an acceptor. When the acetone-PVG adsorbate was exposed to iodine vapor instead of DCE, a new band ascribable to the charge-transfer band with acetone as a donor was detected also in the region of acetone absorption. It was also found that the absorption band of iodine in the visible region is shifted from 512 nm to 455 nm upon complexing with acetone. These results seem to indicate that DCE has almost the same electron affinity as iodine, the vertical electron affinity of which is known to be 1.7 ± 0.5 eV[7].

On account of the weak charge-transfer interaction of acetone with the olefins in the ground state, a fairly large concentration of acetone is required to detect the charge-transfer band in the solutions. So, in the spectral studies so far carried out for the acetone complexes in the solutions, the measurement of the absorption spectra in the region of acetone absorption has been obscured by the strong absorption of acetone itself.

We have recently observed charge-transfer absorption bands sufficiently above the fluorescent equilibrium

charge-transfer states for the system of weak charge-transfer interaction such as aromatic hydrocarbons-aliphatic amines (exciplex) system.[4] Taking into account the similar behavior expected for the present system, the singlet complex proposed by Turro as an intermediate of the oxetane formation between n-π* exited acetone and DCE is supposed to correspond to the equilibrium charge-transfer state largely stabilized below the n-π* excited singlet state of acetone by the solvent reorientation and the structural change of the complex in the excited state. Furthermore, the nucleophilic (electron-donating) and electrophilic(electron-accepting) properties of the n-π* excited state of carbonyl compounds proposed in the fluorescence quenching by olefins can be well interpreted in terms of the charge-transfer interaction of carbonyl compounds in the n-π* excited state with the corresponding charge-transfer states with olefins, leading to the nonfluorescent reactive charge-transfer states such as the singlet complex mentioned above.

REFERENCES

1) N.J.Turro, P.Wriede, and J.D.Dalton, J.Am.Chem.Soc., 90, 3274(1968).

2) N.J.Turro, J.C.Dalton, G.Farrington, N.Niemczyk, D.M.Pond, ibid., 92, 6979(1970).

3) H.Ishida, H.Takahashi, H.Sato, and H.Tsubomura, ibid., 92, 275(1970).

4) H.Ishida and H.Tsubomura, Chem.Phys.Letters, 9, 296(1971).

5) See Chapter II.

6) F.I.Vilesov, USP.Fiz.Nauk, 81, 669(1963).

7) W.B.Person, J.Chem.Phys., 38, 109(1963).

ACKNOWLEDGMENTS

I wish to express my sincere thanks to Professor Hiroshi Tsubomura for his helpful advices and kind encouragement throughout the work. My greatful thanks are also expressed to Professor Noboru Mataga for his useful discussions. Finally, I wish to thank Assistant Professor N.Yamamoto, Mr.Y.Torihashi, Mr.T.Okada, Dr.H.Masuhara, Mr.N.Nakashima, and my colleagues for their technical assistants and their useful and active discussions.

PUBLICATION LIST

1) " The Interaction of Oxygen with Organic Molecules. I. Absorption Spectra Caused by Adsorbed Organic Molecules and Oxygen ", H.Ishida, H.Takahashi, H.Sato, and H.Tsubomura, J.Am.Chem.Soc., 92, 275(1970).

2) " The Interaction of Oxygen with Organic Molecules. II. Oxygen Quenching of the Excited States of Adsorbed Aromatic Hydrocarbons ", H.Ishida, H.Takahashi, and H.Tsubomura, Bull.Chem.Soc.Japan, 43, 3130(1970).

3) " Absorption Spectra Arising from the Interaction between Aromatic Hydrocarbons and Aliphatic Amines", H.Ishida and H.Tsubomura, Chem.Phys.Letters, 9, 296(1971).

4) " Experimental Determination of the Electronic Absorption Spectrum Ascribable to the O_2^- Ion Adsorbed on Porous Glass ", H.Tsubomura, N.Yamamoto, H.Sato, K.Yoshinaga, H.Ishida, and K.Sugishima, J.Phys.Chem., 72, 367(1968).

[Reprinted from the Journal of the American Chemical Society, 92, 275 (1970).]

The Interaction of Oxygen with Organic Molecules. I. Absorption Spectra Caused by Adsorbed Organic Molecules and Oxygen

H. Ishida, H. Takahashi, H. Sato, and H. Tsubomura

Contribution from Department of Chemistry, Faculty of Engineering Science, Osaka University, Toyonaka, Osaka, Japan. *Received June 30, 1969*

Abstract: Electronic absorption spectra, arising from interactions between oxygen and aromatic compounds adsorbed on porous glass or silica gel, were measured. Unlike the spectra induced by oxygen in organic solvents, absorption spectra with a certain number of clear maxima have been observed in most cases. These maxima have been interpreted to represent separate charge-transfer excited states, of which the theoretical aspects are discussed. The effect on the spectra of lowering the temperature has been studied. Strong adsorption spectra caused by the singlet → triplet transitions have been obtained for naphthalene adsorbed on porous glass immersed in liquid oxygen. Charge-transfer absorption spectra arising from the interaction between iodine and aniline derivatives adsorbed on silica gel have also been measured, and the results are discussed in relation to the oxygen–aniline systems.

Evans found that oxygen dissolved in aromatic solvents gives rise to extra absorption bands at wavelengths longer than the absorption edges of the aromatics.[1a] Many experiments related to this problem have been done, and now it seems to be quite reasonable that the extra absorption bands are caused by the charge-transfer interaction between oxygen, as an electron acceptor, and organic molecules, as electron donors, although no stable complexes are formed between them.[1c,2-6] Therefore, these absorption bands can be considered to be quite similar to the contact charge-transfer bands found in iodine solutions.[6,7] Evans[1b] also found additional small peaks at the long-wavelength tail of the extra absorption bands when oxygen is dissolved under high pressure in the solutions of aromatic compounds, or when it is mixed with aromatic vapor. He concluded that these weak bands are singlet–triplet absorption bands enhanced by oxygen. Theoretical investigations of these phenomena were also undertaken by many authors.[3,8,9] The contribution of the charge-transfer state in which an electron is removed from the donor molecule to the oxygen molecule has been pointed out. However, the relative importance of the charge-transfer or the exchange mechanism in perturbing the singlet–triplet transition is still open to question, though it would depend on the system, as well as on the orientation of one molecule to another. No detailed information on the electronic energy levels of the charge-transfer states has been obtained, since the extra absorption bands found so far in solutions show no absorption maxima but increase monotonically toward shorter wavelength.

It was expected that the technique of adsorption would afford new means for understanding the nature of intermolecular interaction.[10-12] In the present work, the measurement and interpretation of the absorption spectra caused by the interaction between oxygen and organic molecules adsorbed on the solid surface are carried out. Moreover, the characteristics of intermolecular interaction in the adsorbed state, as well

(1) (a) D. F. Evans, *J. Chem. Soc.*, 345 (1953); (b) *ibid.*, 1351, 3885 (1957); 2753 (1959); 1735 (1960); (c) *ibid.*, 1987 (1961).
(2) A. U. Munck and J. R. Scott, *Nature*, 177, 587 (1956).
(3) H. Tsubomura and R. S. Mulliken, *J. Am. Chem. Soc.*, 82, 5966 (1960).
(4) J. Jortner and U. Sokolov, *J. Phys. Chem.*, 65, 1633 (1961); L. Paoloni and M. Cignitti, *Sci. Rept. Ist. Super. Sanita*, 2, 45 (1962).
(5) E. C. Lim and V. L. Kowalski, *J. Chem. Phys.*, 36, 1729 (1962); H. Bradley and A. D. King, *ibid.*, 47, 1189 (1967).
(6) L. E. Orgel and R. S. Mulliken, *J. Am. Chem. Soc.*, 79, 4839 (1957).
(7) D. F. Evans, *J. Chem. Phys.*, 23, 1426 (1955).
(8) G. J. Hoijtink, *Mol. Phys.*, 3, 67 (1906).
(9) J. N. Murrel, *ibid.*, 3, 319 (1960).
(10) A. D. McLachlan, *ibid.*, 7, 381 (1964).
(11) H. Sato, K. Hirota, and S. Nagakura, *Bull. Chem. Soc. Jap.*, 38, 962 (1965).
(12) N. Okuda, *J. Chem. Soc. Jap., Pure Chem. Sect.*, 82, 1118 (1961).

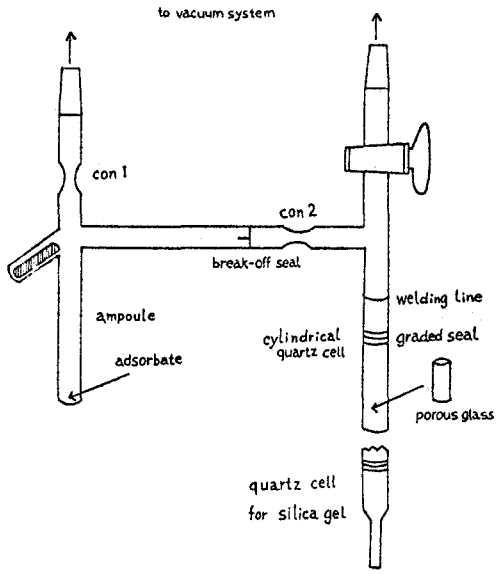

Figure 1. Adsorption apparatus.

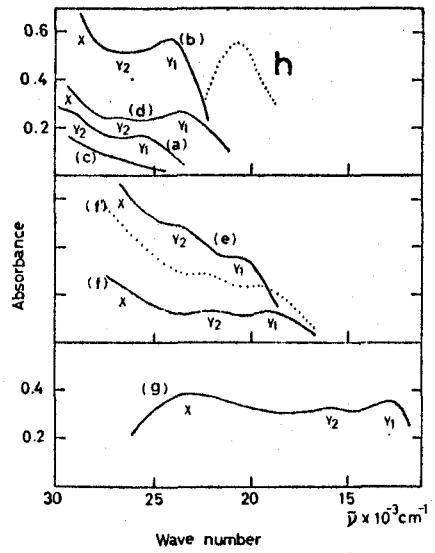

Figure 2. Electronic absorption spectra caused by oxygen and aromatic amines adsorbed on porous glass. The glass was exposed to an oxygen atmosphere of 200 mm at room temperature: (a) N-methylaniline, (b) N,N-dimethylaniline, (c) N,N-dimethyl-*o*-toluidine, (d) N,N-dimethyl-*m*-toluidine, (e) N,N-dimethyl-*p*-toluidine, (f) N,N-diethylaniline, (f') the same as (f), cooled to 77°K, (g) N,N-dimethyl-*p*-phenylenediamine, (h) fluorescence spectrum for N,N-dimethylaniline.

as the extra absorption spectra obtained so far in solutions, are discussed.

Experimental Section

Materials. The commercial high-purity oxygen was led into a vacuum line and purified by several distillations using liquid nitrogen as a coolant, and the vapor of liquid oxygen at liquid nitrogen temperature was used. The silica gel used was from Nakarai Chemical Corp. (30-42 mesh). Porous glass was donated by Central Research Laboratory of Mitsubishi Electric Corp., Amagasaki, Japan. The glass was supplied in the form of a tube with an outer diameter of 11 mm, from which many short tubes were cut for use. The surface area was measured to be about 271 m^2/g. It is transparent up to near-ultraviolet region.

N-Methylaniline, N,N-diethylaniline, N,N-dimethylaniline, and its *o*-, *m*-, and *p*-methyl derivatives were obtained commercially, dried with sodium hydroxide, and distilled under reduced pressure. Commercially available N,N-dimethyl-*p*-phenylenediamine was purified by distillation followed by sublimation in vacuum. N,N,N',N'-Tetramethyl-*p*-phenylenediamine was purified in the same way as described elsewhere.[13] Naphthalene was purified by column chromatography over silica gel, followed by recrystallization. Iodine was purified by sublimation in vacuum.

Procedure. The adsorbent, porous glass or silica gel, was heated in the air at 500° for about 20 hr. Then it was placed in the quartz cell, which is welded onto the apparatus as shown in Figure 1. After evacuation and heating the adsorbent at 500° for 6–8 hr in the cell, the apparatus was sealed off at the constriction (con 1) and removed from the vacuum line at the conical joint. The adsorbent was then exposed to the vapor of organic material, which was previously degassed in the ampoule, *via* a breakoff seal, at room temperature. The vapor which was not adsorbed in the system was taken back into the ampoule cooled by liquid nitrogen, after which the ampoule was sealed off at con 2.

Absorption spectra were measured before and after the introduction of oxygen into the cell. The absorption spectra of the porous glass adsorbates were measured with a Cary Model 15 spectrophotometer, with the measuring light passing through the cell and sample. For the case of silica gel, a quartz cell having two planar windows separated from each other by 2 mm was used. The absorption spectra of the silica gel adsorbates were measured by the reflection method with a Shimadzu Multi-Purpose recording spectrophotometer, Model 50L. The monochromatized sample beam of the spectrophotometer hits upon the planar surface of the quartz cell, which is placed just before the photomultiplier. The specularly reflected light is led into a specially designed absorber, and only the intensity of the randomly reflected light is measured by the photomultiplier. That the scanning of the ratio of the light intensity to the intensity of the reference beam agrees fairly well with the absorption spectra measured by usual methods is well established for powder materials, adsorbed species, opaque materials, etc.

The emission spectra were measured with an Aminco-Bowman spectrophotofluorimeter, using powdered porous glass put in an apparatus similar to that shown in Figure 1, with the quartz cell having a diameter of only 4 mm. The decay of the emission was followed by use of a high-speed flash apparatus constructed by N. Mataga and others.

Results

Absorption Spectra Caused by Oxygen. The absorption spectra caused by oxygen and aromatic amines adsorbed on the porous glass are shown in Figure 2, where the absorption before introducing oxygen is subtracted. The intensity of the absorption bands increased with the pressure of oxygen introduced, and gradually decreased with evacuation. When the sample was cooled down to liquid nitrogen temperature, the intensity of the absorption bands increased as shown in Figure 2 in the case of N,N-diethylaniline, and the bands showed a slight blue shift. The change of the spectra with temperature was found to be reversible. We could also obtain almost the same absorption spectra in the case of oxygen and aromatic amines adsorbed on silica gel, as shown in Figure 3, where the ordinate, "reflex attenuance," corresponds to absorbance. It is attributable to the reflection method that the intensity of the absorption bands of silica gel adsorbates is weak in the shorter wavelength region, as compared with that of porous glass adsorbates. This was confirmed by measuring the well-known absorption spectrum of Würster's blue iodide adsorbed on silica gel, by both reflection and transmission methods with the Multi-Purpose spectrophotometer.

Distinct absorption maxima and shoulders were found for adsorbed oxygen and aromatic amines except for N,N-dimethyl-*o*-toluidine. Each of the absorption spectra seems to consist of a strong band, hereafter

(13) N. Yamamoto, Y. Nakato, and H. Tsubomura, *Bull. Chem. Soc. Jap.*, 39, 2903 (1966).

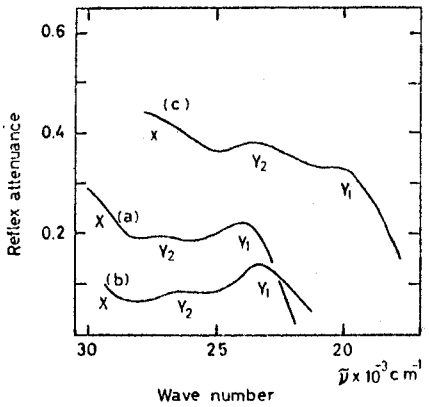

Figure 3. Electronic absorption spectra caused by oxygen and N,N-dimethylaniline derivatives adsorbed on silica gel. The silica gel was exposed to an oxygen atmosphere of 200 mm at room temperature: (a) N,N-dimethylaniline, (b) N,N-dimethyl-*m*-toluidine, (c) N,N-dimethyl-*p*-toluidine.

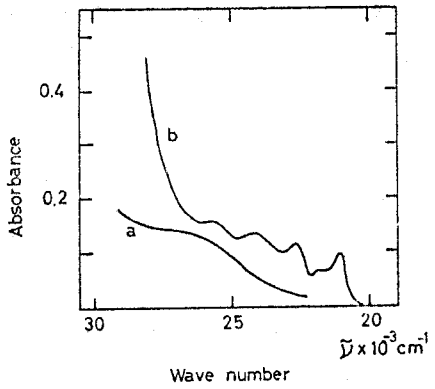

Figure 4. Electronic absorption spectra caused by oxygen and naphthalene adsorbed on porous glass: (a) in an oxygen atmosphere of 200 mm at room temperature, (b) in liquid oxygen at liquid nitrogen temperature.

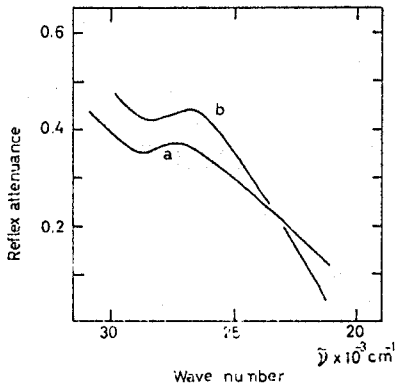

Figure 5. Electronic absorption spectra caused by iodine and N,N-dimethylaniline derivatives adsorbed on silica gel. The silica gel was exposed to iodine vapor at room temperature: (a) N,N-dimethylaniline, (b) N,N-dimethyl-*p*-toluidine.

called X band, in the shorter wavelength region, and two weak bands, Y_1 and Y_2, in the longer wavelength region. The maximum of the X band is found clearly only in the case of N,N-dimethyl-*p*-phenylenediamine (DMPD). In other cases the whole shape of the X band cannot be observed, because it overlaps with the strong absorption band of the organic molecule itself.

In the case of DMPD, which has an ionization potential lower than the alkyl derivatives of anilines, the specimen giving the absorption spectrum shown in Figure 2 was found to be unstable. Under humid conditions, for example, when the sample was exposed to air, DMPD$^+$ [14] formed rapidly. In the case of N,N,N′,N′-tetramethyl-*p*-phenylenediamine (TMPD), which has an ionization potential lower than DMPD, TMPD$^+$ [13] formed instantaneously on introducing oxygen at 200 mm pressure, possibly because of very slight moisture contained in the oxygen, and by virtue of the effect of the polar adsorbent. The absorption spectrum caused by oxygen could not be detected on account of the strong absorption of TMPD$^+$ formed.

We also tried to measure emission spectra of the porous glass adsorbates, by exciting them at the absorption bands caused by oxygen and aromatic amines. Although no emission was detected at room temperature, broad and weak emission bands were detected distinctly in the cases of N,N-dimethylaniline, N,N-dimethyl-*m*-toluidine, N,N-dimethyl-*p*-toluidine, and N-methylaniline, at liquid nitrogen temperature. These emission bands form approximate mirror images of the Y_1 bands, which are the extra absorption bands at the longest wavelengths. As an example, the emission spectrum for the case of N,N-dimethylaniline is shown in Figure 2. The decay of this emission was found to be exponential, the lifetime being 110 nanosec.

Absorption Spectra Caused by Liquid Oxygen. In order to see the effect of liquid oxygen on the spectra of adsorbates, we have carried out some experiments. A piece of porous glass was placed in an apparatus such as shown in Figure 1. Naphthalene was adsorbed on it, and the cell was cooled with liquid nitrogen. Then, dry oxygen was introduced into the cell until the porous glass was immersed in liquid oxygen. The absorption spectra caused by liquid oxygen and by an oxygen atmosphere of 200 mm are shown in Figure 4. As Figure 4 shows, a pronounced shoulder was present at *ca.* 26 kK for the spectrum obtained in the latter case, while in the former case, there is no such shoulder at the same region. It was confirmed that the weak absorption bands observed in liquid oxygen at the long wavelength tail agree very well with the singlet–triplet absorption bands of naphthalene, measured with oxygen dissolved in the solutions under high pressure.[1b,15] The molar extinction coefficient of the singlet–triplet absorption band at the longest wavelength was calculated to be 0.4, based on the content of naphthalene in the glass. The same experiment was done also for N,N-dimethylaniline. The sample turned a deep yellow in liquid oxygen. The absorption spectrum is much stronger than that shown by the curve of Figure 2(b), and rises monotonically toward shorter wavelength. However, the absorption spectrum obtained after the removal of liquid oxygen from the glass was the same as that shown in Figure 2.

Absorption Spectra Caused by Iodine. We also tried to measure absorption spectra by exposing the silica gel adsorbates of aniline derivatives to iodine vapor instead of oxygen. The absorption spectra caused are shown in Figure 5. Studies on the molecular complexes

(14) K. Kimura, K. Yoshinaga, and H. Tsubomura, *J. Phys. Chem.*, 71, 4485 (1967).

(15) G. J. Hoijtink, *Mol. Phys.*, 5, 643 (1962).

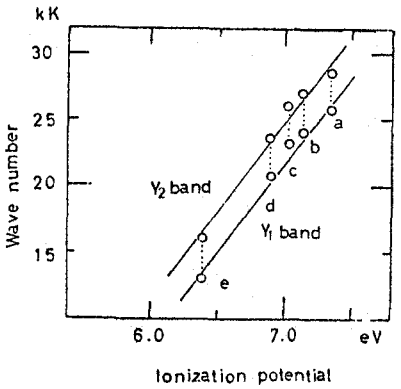

Figure 6. Relationship between the wave numbers of the Y_1 and Y_2 bands and the ionization potentials of organic molecules: (a) N-methylaniline, (b) N,N-dimethylaniline, (c) N,N-dimethyl-*m*-toluidine, (d) N,N-dimethyl-*p*-toluidine, (e) N,N-dimethyl-*p*-phenylenediamine.

of various anilines with iodine, in solution, have been previously made by Chandra and Mukherjee,[16] and by Tsubomura.[17] Chandra and Mukherjee have observed a characteristic charge-transfer absorption band in the near-ultraviolet region as well as another charge-transfer band present in the shorter wavelength region. The absorption spectra obtained on silica gel in this laboratory agree closely with those reported,[16] although they show a slight red shift and have more distinct absorption bands in the near-ultraviolet region.

Discussion

As described in the Experimental Section, the intensities of the extra absorption bands of several organic molecules adsorbed on the solid surfaces together with oxygen decrease with evacuation and increase reversibly with temperature decrease. This indicates that the observed bands are due to weak interactions between organic molecules and oxygen, and not to the oxidation products. This result also shows that the interaction between oxygen and organic molecules is strengthened at lower temperature. This increased interaction may be due to the closer contact between the adsorbed organic molecules and oxygen at low temperature.[18]

It has been confirmed from studies of solutions that the smaller the ionization potential of the organic molecule, the longer the wavelength of the spectra caused by oxygen.[3] It may also be found from Table I that the smaller the ionization potential, the smaller the wave numbers of the Y_1 and Y_2 bands. Moreover, Figure 6 shows two parallel linear relationships between wave numbers and ionization potentials (see also Table I). It seems, therefore, very reasonable to postulate that the absorption bands caused by oxygen and aromatic amines adsorbed on a solid surface are also due to transitions to charge-transfer states, with oxygen as an electron acceptor and an organic molecule as an electron donor. In the case of N,N-dimethyl-*o*-toluidine, the absorption maximum and shoulder are not found distinctly in the longer wavelength region, and the intensity of the absorption band is very weak. This result may be explained by the steric effect of the *o*-methyl group, which prohibits the approach of the lone-pair

(16) A. K. Chandra and D. C. Mukherjee, *Trans. Faraday Soc.*, 60, 62 (1964).
(17) H. Tsubomura, *J. Am. Chem. Soc.*, 82, 40 (1960).
(18) H. Tsubomura and R. P. Lang, *J. Chem. Phys.*, 36, 2155 (1962).

Table I. The Wave Numbers of the Y_1 and Y_2 Bands and the Ionization Potentials of Organic Molecules

Organic molecule	Y_1 band, ν_1, kK	Y_2 band, ν_2, kK	$\Delta E = \nu_2 - \nu_1$, kK	Ionization potential, eV
N-Methylaniline	25.6	(28.6)[a]	(3.0)	7.35[c]
N,N-Dimethylaniline	24.2	27.1	2.9	7.14[c]
N,N-Dimethyl-*o*-toluidine[b]				
N,N-Dimethyl-*m*-toluidine	23.8	26.7	2.9	(7.0)[d]
N,N-Dimethyl-*p*-toluidine	20.5	23.6	3.1	(6.9)[d]
N,N-Diethylaniline	19.2	22.1	2.9	
N,N-Dimethyl-*p*-phenylenediamine	13.0	16.0	3.0	(6.4)[d]
N,N,N′,N′-Tetramethyl-*p*-phenylenediamine				6.25[e]

[a] A weak shoulder. [b] No distinct band maximum has been obtained. [c] F. I. Vilesov, *Zh. Fiz. Khim.*, 35, 2010 (1961). [d] These values were tentatively estimated from the ionization potentials of aniline, *p*-toluidine, *p*-phenylenediamine (G. Briegleb and J. Czekalla, *Z. Elektrochem.*, 63, 6 (1959)), and N,N-dimethylaniline (ref *c* given above). [e] M. Batley, Ph.D. Thesis, University of Sydney, 1966.

electrons of the nitrogen atom, because of the twisting of the dimethylamino group.[17,19] In the case of DMPD and TMPD, having ionization potentials lower than alkyl derivatives of anilines, the complexes with oxygen were found to be very unstable and to form cation radicals of the donors easily. This finding seems to indicate that these complexes have an appreciable ionic character, even in the ground state, because of the stronger charge-transfer interaction between oxygen and donors.

It is worth noting that the separation between the Y_1 and Y_2 bands is roughly constant, irrespective of the donor molecules, as shown in Table I. This strongly suggests that each of the two bands (Y_1 and Y_2) corresponds to the transition of an electron from the highest filled orbital of the organic molecule to each of the two electron-accepting orbitals of oxygen which is occupied by an unpaired electron. A simple theoretical treatment will be made later in this paper, based on this assumption.

In the case of DMPD, the separation between the Y_1 band and the X band is found to be 10.3 kK. This can be compared with the separation between the two charge-transfer bands found for the TMPD–TCNE (tetracyanoethylene) complex, 13.0 kK.[20] It is generally accepted that the two charge-transfer bands observed in the TCNE complexes with some aromatic molecules are due to the transition of an electron from, respectively, the highest occupied and the second highest occupied orbital of the donor to the lowest vacant orbital of TCNE.[21,22] Taking account of the difference between TMPD and DMPD, our results on the Y_1 and X bands may be interpreted as arising from the transitions from the highest and the second highest occupied levels of DMPD.

(19) E. C. McRae and L. Goodman, *J. Mol. Spectrosc.*, 2, 464 (1958).
(20) W. Liptay, G. Briegleb, and K. Schindler, *Z. Elektrochem.*, 66, 331 (1962).
(21) R. E. Merrifield and W. D. Phillips, *J. Am. Chem. Soc.*, 80, 2778 (1958).
(22) T. Matsuo and H. Aiga, *Bull. Chem. Soc. Jap.*, 41, 271 (1968).

It is also well known that benzene derivatives having strong electron-donating substituents show two distinct charge-transfer bands in their complexes with iodine, such as N,N-dimethylaniline–I_2[16] or anisole–I_2,[23] and these are attributed to the two donor orbitals[24] such as were described in the case of TMPD–TCNE complex. The absorption spectra found for substituted anilines and iodine adsorbed on silica gel show distinct maxima, as seen in Figure 5. The maximum and the stronger absorption in the shorter wavelength region are interpreted to be caused, respectively, by the transition from the highest and the second highest filled orbital of the donor. Similarly, the absorption spectra due to oxygen and aniline derivatives adsorbed on porous glass seem to have Y_1 and Y_2 bands and stronger absorption in the shorter wavelength region. The latter may be interpreted to be the X band, arising from the charge transfer from the second highest occupied orbitals of the donor molecules.

The emission spectra found for the adsorbed oxygen–aromatics form approximate mirror images with the Y_1 bands, as stated in the Results of this paper. This indicates that these emission bands are most probably the charge-transfer fluorescence, *i.e.*, due to the transition from the lowest charge-transfer state (corresponding to the Y_1 band) to the ground state. If this interpretation is true, these bands are the first example of charge-transfer fluorescence involving oxygen as the electron acceptor. The lifetime measured, 110 nanosec, is rather long compared with other charge-transfer fluorescence previously measured. This result is consistent with the theoretical interpretation, in that the transition for the present case is geometrically nearly forbidden.

Simple Theoretical Investigation of the Absorption Spectra Caused by Oxygen. Let us discuss the validity of the assignment for the Y_1 and Y_2 bands described in the preceding section. Although a donor molecule might interact with many surrounding oxygen molecules simultaneously, we assume for simplicity that the oxygen and donor moleule form a 1:1 pair. The appearance of the definite peaks in each of the absorption spectra of the oxygen–aromatic systems strongly indicates the formation of complexes having fairly strong binding and rather fixed geometries. This statement is in contrast to our previous opinion that there is no complex formed between oxygen and organic molecules in solutions.[3] It seems highly probable that in the adsorbed state, the attractive force between adsorbent and adsorbate may cause the oxygen and aromatic molecules to bind each other at a fixed configuration or fixed configurations.

The energy of the charge-transfer states E_{ct} may generally be approximated by the equation

$$E_{ct} = I_D - E_A - Q \qquad (1)$$

where I_D and E_A are, respectively, the ionization potential of the donor and the electron affinity of the acceptor, in this case, oxygen. Q is the electrostatic interaction energy between D^+ and A^-. According to our theory, the Y_1 and Y_2 bands correspond to the charge-transfer transition from the highest occupied MO, Ψ_D, of the donor to the two lowest vacant MO's of an oxygen molecule, Ψ_x and Ψ_y. These can be given as follows by the use of real $2p\pi$ atomic wave functions, π_x and π_y for one oxygen atom and π_x' and π_y' for another oxygen atom.

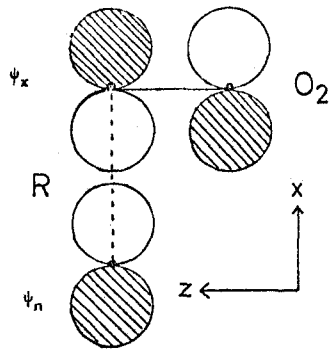

Figure 7. Schematic diagram indicating a particular arrangement for the donor orbital ψ_n and the oxygen acceptor orbital ψ_x. Shaded and unshaded volumes in the orbitals indicate positive and negative regions, respectively.

$$\psi_x = 2^{-1/2}(\pi_x - \pi_x') \qquad (2)$$
$$\psi_y = 2^{-1/2}(\pi_y - \pi_y')$$

In eq 2, π_x and π_y are directed, respectively, along the x and y axes, both perpendicular to the molecular axis. For simplicity, the overlap integrals between π_x and π_x' and π_y and π_y' are neglected.

The separation between bands Y_1 and Y_2 should then correspond to the difference between the energies of the two charge-transfer states E_{ctx} and E_{cty} as given by eq 1. In the present case, both I_D and E_A for the Y_1 and Y_2 bands may be taken as equal, and, therefore, neglecting exchange or other minor interactions, the energy difference between Y_1 and Y_2 may be set equal to the difference between the electrostatic energy Q for the two charge-transfer states.

To calculate the electrostatic energy, the wave function for the highest filled MO of the donor and the shape of the D···A pair must be known. For the methyl-substituted anilines, it has been pointed out that the nitrogen $2p\pi$ AO plays an overwhelmingly large part in the highest filled MO.[17] Hence, for a simple treatment, the highest filled MO of these molecules may be approximated simply by the $2p\pi$ AO of nitrogen. Taking into account the theoretical result that the nitrogen $2p\pi$ AO, ψ_n, plays the largest part in the charge transfer, it may be reasonable to assume that the structure of the complex is such that the axis of ψ_n is perpendicular to the molecular axis of oxygen. Tentatively, the structure is assumed to be as shown in Figure 7, where ψ_n lies in an end-on position with the oxygen π_x AO. This assumption of the structure is still very artificial in the choice of the position of the nitrogen atom with respect to that of oxygen, but a minor change in that will not produce a large difference in the results.

The electrostatic energy has been calculated as intermolecular two-center Coulomb integrals[25] by use of the multipole expansion method proposed by Parr.[26] Figure 8 shows the energy difference ΔE between E_{cty} and E_{ctz} plotted *vs.* the distance between the oxygen and nitrogen atoms. At a distance of 3 Å, a reasonable value for

(23) P. A. D. de Maine, *J. Chem. Phys.*, 26, 1189 (1957).
(24) L. E. Orgel, *ibid.*, 23, 1352 (1955).
(25) K. Kimura and H. Tsubomura, *Mol. Phys.*, 11, 349 (1966).
(26) R. G. Paar, *J. Chem. Phys.*, 33, 1184 (1960).

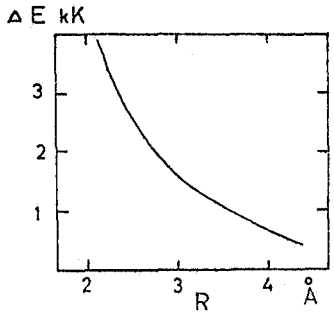

Figure 8. The energy difference ΔE calculated as a function of the distance R between oxygen and nitrogen atoms.

the nitrogen–oxygen distance in complexes, ΔE becomes 1.5 kK, with E_{ct_y} higher than E_{ct_x}. This is approximately half of the observed separation between the Y_1 and Y_2 bands, which is about 3 kK in most cases (Table I). Taking into account the neglect of exchange interactions between donor and acceptor orbitals which seems to contribute to the separation between E_{ct_y} and E_{ct_x}, and the interaction of the charge-transfer states with various other excited states, the agreement between experimental and observed values may be taken to be fairly good. It can also be concluded from these calculations that the Y_1 band and the fluorescence band mentioned before correspond to CT_x, and the Y_2 band, weaker than the former, to CT_y.

Further Discussion on the Absorption Spectra of N,N-Dimethylaniline and Naphthalene Caused by Oxygen. Evans measured the absorption spectrum caused by bubbling oxygen into pure N,N-dimethylaniline and found a shoulder near 380 mμ, which he regarded as one of the two charge-transfer bands corresponding to the two ionization potentials predicted for substituted benzenes.[1c] Recently, this result of Evans has been reconfirmed in this laboratory for the *n*-hexane solution of N,N-dimethylaniline.

It seems most likely that the above-mentioned shoulder corresponds to our Y_1 and Y_2 bands amalgamated together, though the Y_1 band lies at longer wavelength than the shoulder. The difference between the absorption spectrum obtained for the adsorbate and that obtained in solution may be caused by the change of environment. In the adsorbed state, we can expect the more restricted orientation and closer contact between anilines and oxygen, the red shift being attributable to the effect of the electric field of the polar adsorbent, while in solution an oxygen molecule is considered to interact weakly with surrounding organic molecules having random orientations. Similar explanation can be given for the complexes with iodine.

Dijkgraaf, *et al.*,[27] found a pronounced shoulder near 350 mμ (29 kK) in addition to the singlet–triplet absorption bands of naphthalene, when oxygen under high pressure was dissolved in the chloroform solution of naphthalene, and assigned it to a simultaneous transition involving naphthalene and oxygen.[8] This result has recently been confirmed in this laboratory. However, in the present results for liquid oxygen (Figure 4(b)), the shoulder is apparently missing, while the curve for gaseous oxygen (Figure 4a) has a distinct shoulder at about 27 kK.

It has already been seen that the shoulder appearing for N,N-dimethylaniline–oxygen in solution (26 kK) is split to Y_1 (24 kK) and Y_2 (27 kK) bands when adsorbed on porous glass or silica gel. Therefore, it is rather likely that the shoulder reported by Dijkgraaf, *et al.*, may be due to a transition essentially identical with that for the shoulder found here for the adsorbed specimens. If this interpretation is true, the shoulder is due more probably to a charge-transfer-type transition than to the simultaneous transition, although the two relevant excited states may mix together to a certain extent. The reason that no strong shoulder is found in the case of liquid oxygen (Figure 4b) is not clear at present.

In closing, it may be suggested that further study on the interaction between adsorbed molecules and oxygen would provide valuable information on the nature of the interaction between these molecules, which may be important in connection with biological problems, for example, those related to hemoglobin or cytochrome.

Acknowledgment. The authors wish to express their thanks to Professor S. Teranishi for his suggestions on the use of porous glass, and to Professor N. Mataga and H. Ohari for helping us to measure the decay of emission spectra.

(27) C. Dijkgraaf, R. Sitters, and G. J. Hoijtink, *Mol. Phys.*, 5, 643 (1962).

[Reprinted from the Bulletin of the Chemical Society of Japan, Vol. 43, No. 10, pp. 3130-3136 (1970)]

BULLETIN OF THE CHEMICAL SOCIETY OF JAPAN VOL. 43 3130—3136 (1970)

The Interaction of Oxygen with Organic Molecules. II.[1] Oxygen Quenching of the Excited States of Adsorbed Aromatic Hydrocarbons

Hideyuki ISHIDA, Hiroshi TAKAHASHI and Hiroshi TSUBOMURA

Department of Chemistry, Faculty of Engineering Science, Osaka University, Toyonaka, Osaka

(Received June 16, 1970)

Quenching of phosphorescence and fluorescence of aromatic hydrocarbons adsorbed on powdered porous glass or silica gel have been examined as a function of oxygen pressure. It has been found that the phosphorescence quenching at low temperature can be explained mostly by assuming that only those aromatic molecules having an oxygen molecule or molecules within an effective interaction radius are nonphosphorescent (static quenching model). The fluorescence quenching occurs only at much higher oxygen pressures and it has been proposed that contact pairs between aromatic and oxygen molecules, which have shorter intermolecular distances compared to the distances effective for the phosphorescence quenching and give rise to the charge-transfer absorption bands, are relevant. It has been observed that the excimer fluorescence of naphthalene appearing at a higher sample concentration is more strongly affected by oxygen than the monomer fluorescence. The emission spectra from naphthalene-porous glass adsorbate immersed in liquid oxygen and nitrogen have also been examined. The formation of the singlet oxygen ($^1\Delta_g$ or $^1\sum_g^+$) through the interaction of oxygen with triplet molecules has been confirmed by use of the peroxidation reaction of adsorbed anthracene.

The interaction of oxygen with electronically excited organic molecules is associated with a number of interesting phenomena.[2] For example, it is well known that molecular oxygen quenches both the excited singlet and triplet states of organic molecules. Theoretical investigation of the quenching of organic triplet states by oxygen indicated that singlet-state oxygen are formed by the intermolecular energy transfer.[3] This mechanism has now been supported by the results of recent experiments.[4-6] The oxygen quenching has been studied mainly in fluid media where the bimolecular quenching is controlled by the diffusion of oxygen and organic

1) Part I of this series; H. Ishida, H. Takahashi, H. Sato and H. Tsubomura, *J. Amer. Chem. Soc.*, **92**, 275 (1970).

2) P. Pringsheim, "Phosphorescence and Fluorescence," Interscience Publisher, Inc., New York (1965).

3) K. Kawaoka, A. U. Khan and D. R. Kearns, *J. Chem. Phys.*, **47**, 1842 (1967); **48**, 3272 (1968).

4) D. R. Snelling, *Chem. Phys. Lett.*, **2**, 346 (1968).

5) D. R. Kearns, A. U. Khan, C. K. Duncan and A. H. Maki, *J. Amer. Chem. Soc.*, **91**, 1039 (1969).

6) E. Wasserman, V. J. Kuck, W. M. Delavan and W. A. Yager, *ibid.*, **91**, 1041 (1969).

molecules.[7-10] It has not been possible to estimate intrinsic quenching efficiencies from such diffusion-controlled reactions. Siegel and Judeikis have recently determined the relative interaction radius for the oxygen quenching of naphthalene triplet-state in rigid matrices where material diffusion is minimized.[11] Oxygen quenching of phosphorescence of aromatic molecules has been used to measure the diffusion rates of oxygen in polymer matrices.[12,13]

It is well known that molecules adsorbed on solid surface have relatively long lifetimes in their triplet states even at room temperature. The luminescent properties of adsorbed molecules have been extensively investigated in the presence of oxygen.[14-17] Previous investigations of oxygen quenching have almost extensively dealt with dye molecules adsorbed on silica gel. In the preceding paper, we have reported the extra charge-transfer absorption spectra caused by the interaction between adsorbed oxygen and organic molecules.[1] The present paper is mainly concerned with the effective quenching interaction between oxygen and electronically excited aromatic hydrocarbons adsorbed on porous glass or silica gel.

Experimental

Materials. Oxygen and naphthalene were purified in the same way as described in the preceding paper. Commercially available α-chloronaphthalene was distilled under reduced pressure. Anthracene and biphenyl were purified by recrystallization from benzene and ethanol, respectively, and by sublimation in vacuum. The particle sizes of silica gel and powdered porous glass[1] used here were 30—42 mesh, and were treated in the same way as described in the preceding paper. It was confirmed that no luminescence was detectable from porous glass itself by excitation in the near ultraviolet region even at liquid nitrogen temperature (77°K). The phosphorescence of silica gel itself at 77°K was negligible in comparison with that of adsorbed molecules.

Procedure. Naphthalene, α-chloronaphthalene and biphenyl were adsorbed from the vapor phase in the same way as described before.[1] Anthracene was adsorbed from the chloroform solution and the adsorbate was dried and thoroughly evacuated at 100—150°C. Sample concentrations ranged from 1×10^{-7}—5×10^{-6} mol/g of the adsorbent for the study of the fluorescence and phosphorescence quenching by oxygen. In this range we detected no luminescence characteristic of the aggregates or microcrystals of adsorbed molecules. However, when sample concentrations were increased (above 5×10^{-5} mol/g), a new band ascribable to excimer fluorescence was detected besides monomer fluorescence in the case of naphthalene or α-chloronaphthalene.

After adsorption, the sample in the ampoule was distributed into several cylindrical quartz cells, 4 mm in diameter, previously attached to the ampoule. Then oxygen was introduced into the vacuum system at room temperature and the quartz cells were sealed off carefully from the ampoule at desired oxygen pressure. Pressures below 5 Torr were read with a McLeod gauge. An ordinary mercury manometer was used for reading higher pressures.

The emission spectra were measured with an Amineo-Bowmann Spectrophotofluorometer. The lifetimes of the phosphorescence were determined from the decay curves traced on an osciloscope. Fluorescence decay curves were measured by exciting the samples with a device for producing nanosecond flash light.[18] The absorption spectra of adsorbed molecules was measured by the reflection method with a Shimadzu MPS-50L Recording Spectrometer as described in the preceding paper.

Results

Phosphorescence and Fluorescence of Adsorbed Aromatic Hydrocarbons. Phosphorescence spectra of the adsorbed molecules at 77°K were found to be nearly in agreement with those

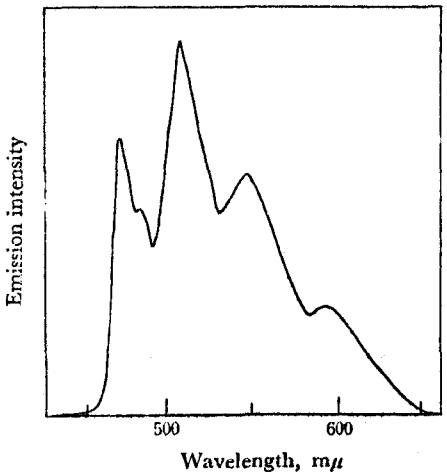

Fig. 1. Phosphorescence spectrum of naphthalene adsorbed on porous glass at 77°K.
Sample concentration: 1×10^{-6} mol per gram of porous glass.

7) W. R. Ware, *J. Phys. Chem.*, **66**, 455 (1962).
8) B. Stevens and B. E. Algar, *ibid.*, **72**, 2582 (1968).
9) A. D. Osborne and G. Porter, *Proc. Roy. Soc.*, **A284**, 9 (1965).
10) C. S. Parmenter and J. D. Rau, *J. Chem. Phys.*, **51**, 2242 (1969).
11) S. Siegel and H. S. Judeikis, *ibid.*, **48**, 1613 (1968).
12) G. Shaw, *Trans. Faraday Soc.*, **63**, 2181 (1967).
13) B. A. Baldwin and H. W. Offen, *J. Chem. Phys.*, **49**, 2933 (1968).
14) H. Kautsky, *Trans. Faraday Soc.*, **35**, 216 (1939).
15) S. Kato, This Bulletin, **30**, 34 (1957).
16) R. F. Weiner and H. H. Seliger, *Photochem. Photobiol.*, **4**, 1207 (1965).
17) J. L. Rosenberg and F. S. Humphries, *J. Phys. Chem.*, **71**, 330 (1967).
18) N. Mataga, M. Tomura and H. Nishimura, *Mol. Phys.*, **9**, 367 (1965).

measured for the same molecules dissolved in rigid matrices, although the spectra showed slight broadening of their vibrational structures in the adsorbed state. As an example, phosphorescence spectrum of naphthalene adsorbed on porous glass is shown in Fig. 1. The similar broadening was found also for fluorescence spectra. This broadening can be interpreted to be due to the wide energy distribution of the adsorbed molecules in the variety of the field of the polar adsorbent.

No difference in the luminescent properties of aromatic molecules have been found between silica gel and porous glass adsorbates. The phosphorescence lifetimes (τ_p) of adsorbed biphenyl, naphthalene and α-chloronaphthalene at 77°K were 4.0, 2.3 and 0.2 sec, respectively, at negligible oxygen pressures. These values also agree very closely with those in rigid matrices at 77°K.[19]

The band maxima of fluorescence show a slight blue shift when cooled down to 77°K. The fluorescence lifetime of naphthalene adsorbed on porous glass was 100 ns at room temperature, in good agreement with the values in the solutions.[19] Increase of the concentrations of naphthalene and α-chloronaphthalene resulted in the appearance of new broad bands almost identical with the corresponding excimer fluorescence in solutions.[20] The intensity ratio of this new band to the monomer fluorescence band depends on the wavelength of the exciting light as shown in Fig. 2 for the case of naphthalene. This ratio increases with increasing the sample concentration. The lifetimes of the new fluorescence band of naphthalene were found to

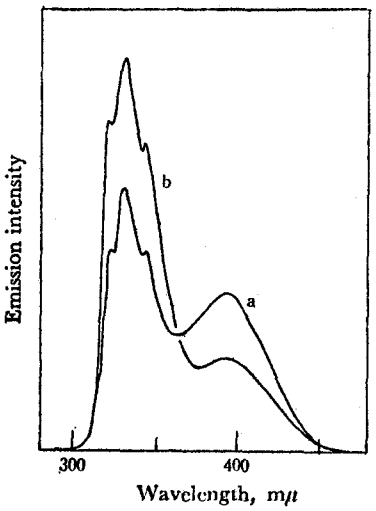

Fig. 2. Fluorescence spectra of naphthalene adsorbed on porous glass at 77°K.
Sample concentration: 5×10^{-5} mol per gram of porous glass; excitation wavelength: (a) 275 mμ and (b) 300 mμ.

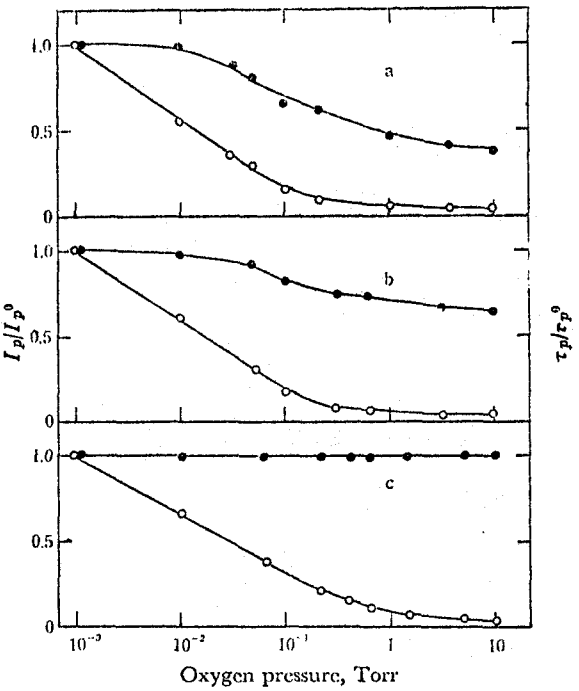

Fig. 3. The relative phosphorescence intensities I_p/I_p^0 (○) and lifetimes τ_p/τ_p^0 (◉) of aromatic-porous glass adsorbates as a function of oxygen pressure at 77°K. (a), for biphenyl; (b), for naphthalene; (c), for α-chloronaphthalene. I_p^0 and τ_p^0 are, respectively, the phosphorescence intensity and lifetime at negligible oxygen pressures. The value of I_p/I_p^0 was normalized to be 1 at 10^{-3} Torr oxygen pressure. τ_p^0 at 77°K is 4.0 sec for biphenyl, 2.3 sec for naphthalene and 0.2 sec for α-chloronaphthalene.

be 65 and 100 ns at 300°K and 77°K, respectively, in good agreement with the long lifetimes characteristic of excimer fluorescence.[21] It is therefore concluded that, with increasing the sample concentration, adsorbed naphthalene molecules are forced to form loosely bound dimers on the surface and when this dimer is excited as well as monomer, the dimer is led to the configuration favorable to excimer formation.[22] The effect of oxygen on excimer fluorescence as well as monomer fluorescence is of considerable interest.

Quenching of Phosphorescence by Oxygen. The phosphorescence of the samples prepared in the way described in the experimental section was too weak at room temperature to examine the effect of oxygen quantitatively. Therefore, most of the studies were made at low temperature. The quenching effect of oxygen at 77°K is shown by the curves in Fig. 3, in which the values of the

19) D. S. McClure, *J. Chem. Phys.*, **17**, 905 (1949).
20) C. A. Parker, *Spectrochemica Acta*, **19**, 989 (1963).
21) N. Mataga, Y. Torihashi and Y. Ota, *Chem. Phys. Lett.*, **1**, 335 (1967).
22) E. A. Chandross, J. Ferguson and E. G. McRae, *J. Chem. Phys.*, **45**, 3546 (1966); **45**, 3554 (1966).

relative phosphorescence intensities I_p/I_p^0 and the relative phosphorescence lifetimes τ_p/τ_p^0 are plotted as a function of oxygen pressure. I_p^0 and τ_p^0 are, respectively, the phsophorescence intensity and lifetime of the sample containing negligible amounts of oxygen. The phosphorescence decays at various oxygen pressures were found to obey the first order kinetics. The dependence of the phosphorescence lifetime on oxygen pressure was also examined at 203°K (−70°C) in the case of biphenyl. The temperature was obtained by dropping liquid nitrogen into the Dewar containing 99% ethanol. This curve, being different from that at 77°K, showed a rapid decrease in the lifetime with increasing the oxygen pressure. Although the absolute amount of adsorbed oxygen at each oxygen pressure is unknown, qualitative discussion on the interaction of oxygen with excited molecules can be made from these quenching curves.

Although oxygen pressure above 10 Torr is sufficient to quench phosphorescence totally, weak emission was detected from the naphthalene-porous glass adsorbate immersed in liquid oxygen at 77°K. This emission was observed to lie in almost the same region as the phosphorescence of naphthalene and could not be detected using a sector presumably because of the extremely short lifetime ($<10^{-3}$ sec). The phosphorescence of naphthalene from the naphthalene-porous glass adsorbate immersed in liquid nitrogen was strong and the lifetime was 1.4 sec. This short lifetime in liquid nitrogen compared to the original value (τ_p^0, 2.3 sec) may be due to impurities, such as oxygen, possibly contained in liquid nitrogen.

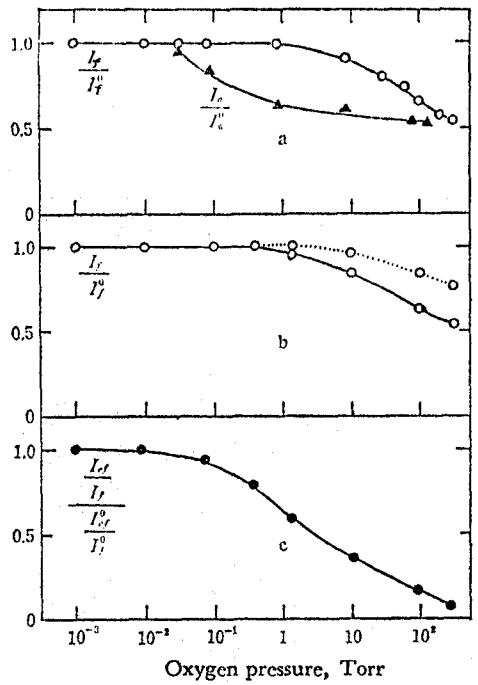

Fig. 4. The relative fluorescence intensities I_p/I_p^0 (○) and the relative ratios of the intensity of excimer fluorescence versus monomer fluorescence $(I_{ef}/I_f)/(I_{ef}^0/I_f^0)$ (●) of aromatic-porous glass adsorbates as a function of oxygen pressure at room temperature (———) and 77°K (- - - - -). (a), for anthracene; (b) and (c), for naphthalene. I_f^0 and I_{ef}^0 are, respectively, the fluorescence intensities of monomer and excimer at negligible oxygen pressures. The relative absorption intensities I_a/I_a^0 (△) of adsorbed anthracene are shown in (a) as a function of oxygen pressure, when the sample containing a known pressure of oxygen is irradiated. I_a^0 is the absorption intensity of adsorbed anthracene before irradiation.

Quenching of Fluorescence by Oxygen. The quenching effect of oxygen was examined mainly at room temperature. The quenching effect of oxygen on monomer fluorescence is shown in Fig. 4 (a) and (b) in cases of naphthalene and anthracene. The values of the relative fluorescence intensities I_f/I_f^0 are plotted as a function of oxygen pressure. It is found from the curves in Fig. 4 that the quenching curve of naphthalene is almost the same as that of anthracene in spite of the large difference between the fluorescence lifetimes (4.2 ns for anthracene[23] and 100 ns for naphthalene), and the quenching by oxygen is less effective at 77°K than at room temperature. No fluorescence quenching is found at oxygen pressures below 1 Torr where phosphorescence is quenched to some extent. Fluorescence quenching occurs gradually at oxygen pressures above 1 Torr where phosphorescence is quenched to a great extent. No difference was found between the quenching curves of anthracene for both porous glass and silica gel adsorbates.

The quenching effect of oxygen on excimer fluorescence is shown in Fig. 4 (c) in the case of naphthalene (5×10^{-5} mol naphthalene per gram of porous glass). The wavelength of the excitation was fixed at 275 mμ. The relative ratio of the intensity of excimer fluorescence versus monomer fluorescence is plotted as a function of oxygen pressure. It is found from this curve that excimer fluorescence is more strongly affected by oxygen than monomer fluorescence, though the lifetime of excimer fluorescence (65 ns) is rather short compared to monomer fluorescence (100 ns). The flourescence of monomer and excimer was little quenched by nitrogen gas admitted to the sample instead of oxygen.

Liquid oxygen also showed a remarkable effect on the fluorescence of naphthalene. The fluorescence intensity of the naphthalene-porous glass adsorbate immersed in liquid oxygen condensed at 77°K was roughly 1/7 of the original intensity (I_p^0). Liquid nitrogen showed no effect on the fluorescence of adsorbed naphthalene.

23) W. R. Ware and B. A. Baldwin, *ibid.*, **40**, 1703 (1946).

Discussion

Quenching of Phosphorescence by Oxygen. As shown in Fig. 3 the dependence of I_p/I_p^0 on oxygen pressure is obviously different from that of τ_p/τ_p^0 and the curves of I_p/I_p^0 for the three compounds show almost common behavior. I_p/I_p^0 decreases rapidly with increasing the oxygen pressure and approaches to zero at oxygen pressures above 10 Torr. The lifetimes of biphenyl and naphthalene are affected a little by oxygen, but do not decrease indefinitely with increasing the oxygen pressure in such a way as the intensities do, and the values approach approximately to 1.6 and 1.4 sec, respectively, so far as we could detect the phosphorescence. On the other hand, the lifetime of α-chloronaphthalene, naturally having a short lifetime (0.2 sec), is almost constant irrespective of oxygen presure.

In the case where the quenching of phosphorescence of adsorbed organic molecules is assumed to take place by the collision of these organic molecules with oxygen (dynamic quenching model), the lifetime of phosphorescence should be shortened in the presence of oxygen. Under such a condition, the curve of the relative phosphorescence intensity, I_p/I_p^0, should be almost in accord with that of the relative phosphorescence lifetime, τ_p/τ_p^0. On the other hand, in the absence of such collisional processes, the lifetime of the observed phosphorescence should be independent of oxygen pressure. In that case, it should be assumed that only those molecules that have oxygen molecules within an effective interaction radius before excitation are nonphosphorescent (static quenching model). Our results indicate that in the case of α-chloronaphthalene, the phosphorescence quenching is due to static quenching alone and in the cases of naphthalene and biphenyl, having naturally longer lifetimes compared to the former, there exists a slight contribution from the dynamic quenching as well as the static quenching. From these results, it is suggested that the dynamic quenching process is considerably slow at 77°K in the adsorbed state, although the quantitative interpretation of the curves of τ_p/τ_p^0 is impossible because of the inhomogeneity of the surface condition. As the dynamic process is controlled by the diffusion of oxygen, the observed behaviors of τ_p/τ_p^0 should be explained by the slow surface diffusion of oxygen at 77°K. This conclusion is supported by the result of the lifetimes of biphenyl phosphorescence measured at 230°K where the diffusion of oxygen must be faster than at 77°K.

As described in the preceding paper, we have found the existence of the contact pairs between the adsorbed oxygen and organic molecules at high oxygen pressures, which give rise to the charge-transfer absorption spectra. From the absence of any observed effect of oxygen on the absorption spectra at low oxygen pressures where phosphorescence quenching occurs to a large extent, it should be concluded that no contact pairs are formed at such oxygen pressures. It may be worthwhile to add that the effect of oxygen on the phosphorescence quenching is easily removed by evacuation. As it is reported that the binding energy between oxygen and aromatics is negligible in the ground state,[3,24] it is expected that oxygen is physically adsorbed at random on the aromatic-porous glass adsorbate at low oxygen pressures and the aromatic molecules form pairs with some of the adsorbed oxygen which can have an effective interaction for the phosphorescence quenching. The amount of these pairs is considered to increase with increasing the oxygen pressure, in agreement with the observed monotonous decrease of I_p/I_p^0 at low oxygen pressures. The relative situations between the adsorbed aromatic and oxygen molecules are illustrated schematically in Fig. 5.

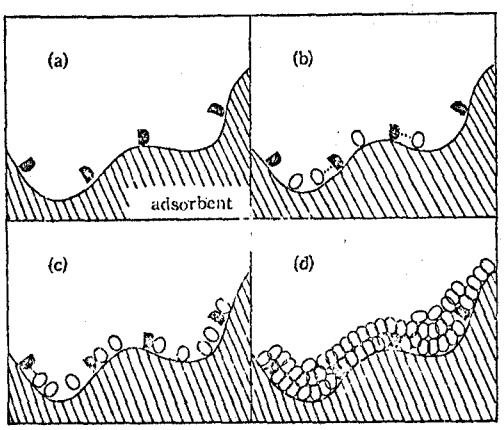

Fig. 5. Schematic illustrations indicating the relative situation between aromatic (◗) and oxygen (○) molecules in the adsorbed state. (a), before admitting oxygen; (b), at low oxygen pressures where phosphorescence quenching occurs; (c), at high oxygen pressures where contact pairs responsible for fluorescence quenching are formed between them; (d), when immersed in liquid oxygen.

Figure 6 shows the schematic potential curves for the states caused between aromatic and oxygen molecules versus the distance between them. Kearns *et al.*,[3] have suggested theoretically that a significant binding energy is expected through the interaction of triplet-state organic molecules with oxygen (curve b in Fig. 6). At a low oxygen pressure where effective phosphorescence quenching, but not the fluorescence quenching, occurs, we assume that most of the oxygen molecules are at distance r_2, or

24) H. Tsubomura and R. S. Mulliken, *J. Amer. Chem. Soc.*, 82, 5966 (1960).

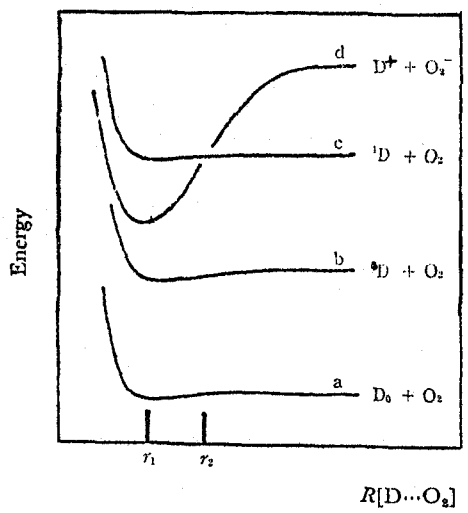

Fig. 6. Schematic potential curves for the states caused between aromatic (D) and oxygen (O_2) molecules versus the distance (R) between D and O_2. D_0 indicates the ground state of aromatic molecule. ^1D and ^3D indicate, respectively, the excited singlet and triplet states. In the adsorbed state, the intermolecular distance R is throught to decrease with increasing oxygen pressure.

larger, from the aromatic molecule D_0. When the aromatic molecule is excited to a ^3D level at such a distance, the interaction between ^3D and oxygen at that distance is thought to be sufficiently strong to cause a radiationless decay process which competes with the slow natural radiative decay process of the phosphorescent state, leading to the quenching of the phosphorescence.

Rosenberg and Humphries[17] have studied the phosphorescence quenching of acriflavine adsorbed on silica gel and suggested the existence of relatively nonphosphorescent complex between the dye and oxygen. Recently, Siegel and Judeikis[11] have investigated the oxygen quenching of naphthalene triplet state in 3-methylpentane glass at 77°K and found a slight contribution from the dynamic quenching process in addition to the static quenching process. They have also determined the effective interaction distance for the quenching to be 10.5 Å. These results seem to be consistent with our conclusion.

We have reported in the preceding paper that the S→T absorption spectrum of naphthalene is enhanced to a great extent when the naphthalene-porous glass adsorbate is immersed in liquid oxygen. The weak emission observed under such an environment may be assigned to the phosphorescence of naphthalene having a shortened lifetime, one possible explanation for this being that the T→S radiative decay process as well as the radiationless decay process is enhanced remarkably by the strong perturbation due to liquid oxygen (see Fig. 5d). The natural radiative lifetime of naphthalene triplet state, which can be calculated in the same way as described by McGlynn and Azumi[25] using the observed S→T absorption, was 9×10^{-4} sec. This value is very short compared to the unperturbed one, 11 sec,[26] in agreement with the observed shortlived emission.

Quenching of Fluorescence by Oxygen. Our results of fluorescence quenching show no difference in the characteristics between the two curves for naphthalene and anthracene despite of the large difference in their fluorescence lifetimes. This indicates that the decreases in I_f/I_f^0 are due to the static quenching alone at room temperature (21°C), and seems to indicate the surface diffusion of oxygen to be much slow compared to the decay of fluorescence. As described in the preceding paper, the extra charge-transfer absorption spectra caused through the interaction between adsorbed oxygen and organic molecules have been detected at high oxygen pressures where fluorescence quenching is observable. It can therefore be concluded that the fluorescence quenching occurs between oxygen and organic molecules in such a close contact as giving rise to the charge-transfer absorption bands, because of the fast decay of fluorescence (for example, at a distance r_1 in Fig. 6). The amount of contact pairs formed on the surface is thought to increase with increasing the oxygen pressure as Fig. 5 shows. From the results obtained for naphthalene fluorescence in liquid oxygen and at 77°K, it seems to be reasonable to assume that the radiationless decay process in contact pair becomes slow when cooled down to the low temperature and becomes comparable to the decay processes of fluorescence.

We have also found that the excimer fluorescence of naphthalene is affected more strongly by oxygen than the monomer fluorescence. This result is consistent with the earlier qualitative report on oxygen quenching of aromatic-hydrocarbon excimers in liquid solutions.[27] Chandross and Ferguson[28] found a very marked heavy-atom effect on the excimer fluorescence which can be explained by the increase in the intersystem crossing to the nearby triplet state of the excimer. Recently, the excimer phosphorescence of naphthalene has been observed in liquid solutions at low temperature.[29,30]

25) S. P. McGlynn and T. Azumi, *J. Chem. Phys.*, **40**, 507 (1964).
26) E. H. Gilmore, G. E. Gibson and D. S. McClure, *J. Chem. Phys.*, **23**, 399 (1955).
27) N. S. Bazilevskaya and A. S. Cherkason, *Opt. Spectry.*, **18**, 77 (1965).
28) E. A. Chandross and J. Ferguson, *J. Chem. Phys.*, **45**, 397 (1966).
29) J. Langelaar, R. P. H. Rettschnick, A. M. F. Lambooy and G. J. Hoytink, *Chem. Phys. Lett.*, **1**, 609 (1968).
30) G. Briegleb, H. Shuster and W. Here, *ibid.*, **4**, 53 (1969).

One possible explanation for the remarkable quenching of excimer fluorescence by oxygen is to take account of the smaller energy difference of excimer between the lowest singlet and triplet states compared to that of monomer.

The Relationship between the Oxygen Quenching and Peroxidation Reaction of Adsorbed Anthracene. Here we present the evidence for the formation of singlet oxygen ($^1\Delta_g$ or $^1\Sigma^+_g$) during the course of oxygen quenching by use of the well-established peroxidation reaction of anthracene with the singlet oxygen.[31] Anthracene adsorbed on silica gel was exposed to a known pressure of oxygen and irradiated with a 250 W high pressure Hg-lamp for five minutes at the wavelength of the first absorption band. The decrease in the first absorption band of anthracene due to the formation of anthracene peroxide was measured by use of the reflection method[1] as a function of oxygen pressure. The result is shown in Fig. 4 (a). The decrease of the anthracene absorption is seen to occur at low oxygen pressures where no fluorescence quenching is observed, although no decrease was observed by the irradiation of the sample without oxygen. This result has thus provided a rigorous experimental proof for the formation of singlet oxygen through the interaction between oxygen and triplet-state anthracene. The rate of peroxidation reaction showed a tendency to become independent of oxygen pressure in the region of high oxygen pressures where the fluorescence quenching begins to be observed and, no characteristic relationship was obtained between the rate of the peroxidation and the fluorescence quenching by oxygen. This seems to indicate that the singlet oxygen is not formed through the interaction with anthracene in the singlet excited state. However, further detailed experimental and theoretical investigations are necessary in order to establish the mechanism of fluorescence quenching by oxygen.

The authors are indebted to Professor N. Mataga and Mr. H. Ohari for the measurement of fluorescence lifetimes by use of a nanosecond flash apparatus.

31) B. Stevens and B. E. Algar, *J. Phys. Chem.*, **72**, 3468 (1968).

ABSORPTION SPECTRA ARISING FROM THE INTERACTION BETWEEN AROMATIC HYDROCARBONS AND ALIPHATIC AMINES

H. ISHIDA and H. TSUBOMURA
Department of Chemistry, Faculty of Engineering Science, Osaka University, Toyonaka, Japan

Received 29 March 1971

Absorption spectra arising from the interaction between various aromatic hydrocarbons and aliphatic amines have been newly observed in the ultraviolet region by the technique of adsorption, and interpreted as being due to transitions to the charge-transfer Franck-Condon states which may correspond electronically to the fluorescent charge-transfer states observed recently in solutions. No charge-transfer fluorescence was observed in the present system. The formation of the fluorescent charge-transfer states seems to be prevented because of the rigid spatial configurations between adsorbed molecules.

1. INTRODUCTION

It has been established recently that the unusual large Stokes shifts observed for the weak charge-transfer (CT) complexes in solutions are due to the difference in the electronic and geometrical structures between the excited CT Franck-Condon state and the fluorescent equilibrium CT state [1]. Recently, Nakajima [2] and Kuzmin and Guseva [3] have found new fluorescence bands between aromatic hydrocarbons and aliphatic amines and interpreted them to be CT fluorescence bands. In these systems, though characteristic CT absorption bands corresponding to the CT fluorescence bands have not been detected (i.e., the so-called exciplex system), it may be expected that CT absorption bands arising from intermolecular configurations different from those in the fluorescent state lie in the region of sufficiently short wavelengths. It has been impossible, however, to measure the absorption spectra of these systems in solutions in such a region because of the strong absorption of amines used as solvents.

We have shown recently that the CT absorption bands between oxygen and aromatic amines lying in the region of amine absorption can be measured by use of the technique of adsorption [4]. In the present paper, the absorption spectra of some systems composed of aromatic hydrocarbons and aliphatic amines were measured down to the ultraviolet region by the technique of adsorption.

2. EXPERIMENTAL

Aromatic hydrocarbons were adsorbed from *n*-hexane solutions on ordinarily treated silica gel(30-42 mesh) [5,6], and the adsorbate, after drying and evacuation, was exposed to the vapour of the aliphatic amine through a break-off seal. The absorption spectrum of the adsorbate placed in a thin quartz cell (4 cm × 2 cm × 1.3 mm) was measured with a Shimadzu Multi-Purpose Spectrophotometer, model 50L [4].

3. RESULTS AND DISCUSSION

Absorption spectra of adsorbed anthracene and aliphatic amines are shown in fig. 1. The absorption of the amine itself adsorbed on silica gel is negligible above 240 mμ as shown by curve b for the case of triethylamine. The concentration of adsorbed aromatic hydrocarbon was set within the range from 1×10^{-7} to 1×10^{-6} mole per gram of silica gel, where neither fluorescence nor absorption, characteristic of the sandwich dimers appearing at higher concentration [5], are detected. The absorption spectra of adsorbed aromatic hydrocarbons show a broadening of the vibrational structure and a slight red shift compared to those in solutions.

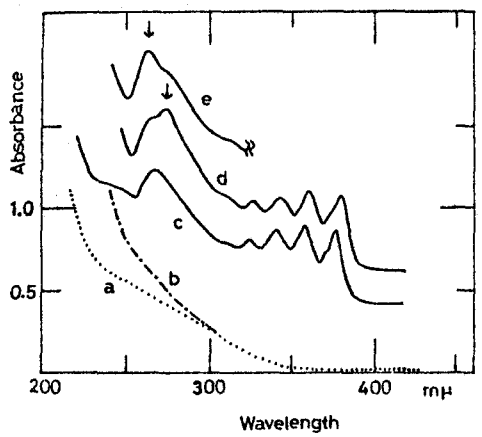

Fig. 1. Absorption spectra of anthracene and aliphatic amines adsorbed on silica gel (30-42 mesh) at 77°K (a), silica gel only; (b), triethylamine; (c), anthracene; (d), anthracene-tri-*n*-propylamine; (e), anthracene-triethylamine. The concentration of adsorbed anthracene is 3×10^{-7} mole/g.

New absorption bands were observed by the adsorption of amine in the vicinity of the broadened ^1B_b band of anthracene at shorter wavelength as shown in fig. 1, while the ^1L_a band showed a slight red shift. Similar new bands were found also for pairs of various other amines and aromatic hydrocarbons as summarized in tables 1 and 2. From these tables, it can be seen that the relationships between the band maxima and the ionization potentials of amines or the half-wave reduction potentials of hydrocarbons are those characteristic of CT absorption bands. It was confirmed that these new peaks are removed reversibly by desorption of amines under vacuum. It seems reasonable from these results that the observed new absorption bands are due to transitions to the excited CT states arising from the interaction between amines as donors and hydrocarbons as acceptors.

No essential change of the fluorescence of hydrocarbons was observed by the presence of amines at room or liquid nitrogen temperature and the broad characteristic fluorescence spectra, which were observed for these systems in solutions at longer wavelengths than the fluorescence of hydrocarbons [2,3], could not be observed. In the case of pyrene which has a long-lived fluorescent state (^1L_b), the vibrational structure changed slightly and the fluorescence lifetime was decreased from 280 nsec to 60-90 nsec by the presence of amines. The excitation spectra for the fluorescence of hydrocarbons

Table 1
The maximum wave numbers of the absorption bands arising between anthracene and various aliphatic amines and the ionization potentials of the amines

Amine	10^3 cm^{-1} (mμ)	ionization potential (eV)
triethylamine	38.3 (261)	7.50 [11]
tri-*n*-propylamine	36.6 (273)	7.23 [11]
tri-*n*-butylamine	36.8 (272)	
tri-*n*-amylamine	37.7 (265)	7.3 a)
tri-*n*-hexylamine	38.0 (263)	
tri-*n*-octylamine	38.2 (262)	
triethylenediamine	38.3 (261)	
N,N,-dimethyl-cyclohexylamine	36.0 (278)	

a) Measured by the photoionization method in our laboratory by M. Ozaki and Y. Nakato.

Table 2
The maximum wave numbers of the absorption bands arising between various aromatic hydrocarbons and tri-*n*-propylamine and the half-wave reduction potentials ($-E_{1/2}$) of the aromatic hydrocarbons

Aromatic hydrocarbon	10^3cm^{-1}(mμ)	$-E_{1/2}$(V) [12]
perylene	33.3 (300)	1.67
anthracene	36.6 (273)	1.96
1,2-benzanthracene	37.0 (270)	2.00
pyrene	40.0 (250) a)	2.11

a) The absorption band was not observed distinctly because of the strong continuous absorption bands of pyrene in the ultraviolet region.

corresponded qualitatively to the observed absorption spectra including the new CT bands. These results indicate that when excited to the CT state or the locally excited states of hydrocarbon, the internal conversion to the weakly interacting, lowest locally excited state of the hydrocarbon is much faster than to the fluorescent equilibrium CT state having an intermolecular configuration different from that in the Franck-Condon state, because of the rigid spatial configurations between adsorbed molecules.

It seems reasonable to assume that the observed CT absorption band is the first (lowest) CT band, because of the following arguments. The energy difference between the first and second CT bands, as estimated from the lowest and second lowest vacant molecular orbitals, is 1.6 eV according to an SCF MO calculation of anthracene [7]. Hence, if the observed CT band were due to the transition to the second CT state, then the first CT state should be lower than the

lowest locally excited state (^1L_a) of anthracene, leading to remarkable quenching of the fluorescence of anthracene by amine.

It seems, therefore, highly probable that the observed CT absorption bands are due to transitions to the lowest CT Franck-Condon states which correspond electronically to the fluorescent equilibrium CT states found in solutions. For the anthracene-tri-*n*-butylamine system, a large Stokes shift of 16000 cm^{-1} has been obtained between the observed new CT absorption band (272 mμ) and the CT fluorescence (483 mμ) observed in solution. This value is rather large compared to those of weak CT complexes ($\approx$12000 cm^{-1} [1]).

It is worthwhile noting that the absorption intensities of CT bands for large-size hydrocarbons are weaker than that for anthracene. This can be explained by the difference in the degree of overlap between the interacting localized orbitals of amine and the molecular orbitals spread over the whole ring of the hydrocarbon. Similar behavior is observed for the CT complexes of iodine with hydrocarbons [8]. In our system, the interaction between hydrocarbons and amines in the ground state is expected to be stronger [4] than in solutions where binding between them is considered to be negligible. As indicated by Hanna and co-workers for weak complexes [9], electrostatic interactions may play an important role in determining the stable intermolecular configurations in the ground state which may give rise to a rather intense contact-CT type absorption band [8]. The contributions of the locally excited states of the hydrocarbon and amine to the CT Franck-Condon state are now being investigated theoretically. The excited state of amine (Rydberg state [10]) interacts with the CT state to a considerable extent, since the overlap between the lowest vacant molecular orbital of hydrocarbon and the Rydberg orbital (3p orbital of nitrogen atom) is much larger, due to the large size of the Rydberg orbital, than those between the molecular orbitals of hydrocarbon and the lone-pair orbital of amine. Absorption spectra have also been measured in the well-known exciplex system (aromatic amines-aromatic hydrocarbons) down to the ultraviolet region. The details of these experimental and theoretical results will be reported elsewhere.

ACKNOWLEDGMENT

The authors are greatly indebted to Professor N. Mataga and Mr. T. Okada of Osaka University for their helpful discussions.

REFERENCES

[1] N. Mataga and Y. Murata, J. Am. Chem. Soc. 91 (1969) 3144;
H. Masuhara and N. Mataga, Chem. Phys. Letters 6 (1970) 608.
[2] A. Nakajima, Bull. Chem. Soc. Japan 42 (1969) 3409.
[3] M. G. Kuzmin and L. N. Guseva, Chem. Phys. Letters 3 (1969) 71.
[4] H. Ishida, H. Takahashi, H. Sato and H. Tsubomura, J. Am. Chem. Soc. 92 (1970) 275.
[5] H. Ishida, H. Takahashi and H. Tsubomura, Bull. Chem. Soc. Japan 43 (1970) 3130.
[6] J. L. Rosenberg and D. J. Shombert, J. Phys. Chem. 82 (1960) 3252.
[7] N. Mataga, private communication.
[8] J. N. Murrel, J. Am. Chem. Soc. 81 (1959) 5037.
[9] J. L. Lippert, M. W. Hanna and P. J. Trotter, J. Am. Chem. Soc. 91 (1969) 4035.
[10] A. M. Halpern, J. L. Roebber and K. Weiss, J. Chem. Phys. 49 (1968) 1348.
[11] K. Watanabe and J. R. Mottle, J. Chem. Phys. 26 (1957) 1773.
[12] A. Streitwieser, Molecular orbital theory for organic chemists (Wiley, New York, 1961) p. 178.

[Reprinted from the Journal of Physical Chemistry, 72, 367 (1968).]

Experimental Determination of the Electronic Absorption Spectrum Ascribable to the O_2^- Ion Adsorbed on Porous Glass

by Hiroshi Tsubomura, Naoto Yamamoto, Hiroyasu Sato, Kunio Yoshinaga, Hideyuki Ishida, and Kiyoshi Sugishima

Department of Chemistry, Faculty of Engineering Science, Osaka University, Toyonaka, Osaka, Japan
(Received August 5, 1967)

A tube of porous glass[1] 3–4 cm long and with an outer diameter of 11 mm was placed in a vacuum line. N,N,N′,N′-tetramethyl-*p*-phenylenediamine (TMPD) was adsorbed onto it, and the absorption spectrum of the glass was measured with light incident across the tube. The absorption spectrum obtained was essentially that of the TMPD molecule itself. The sample was then irradiated with a high-pressure mercury lamp. The absorption spectrum arising from the irradiation is shown in Figure 1. In the visible region, it has three characteristic bands readily identified with those of $TMPD^+$ and another band with a maximum at 4200 A (hereafter called the Y band). The intensity of the Y band produced under various conditions is proportional to the intensity of the $TMPD^+$ band. The specimen also gives an esr pattern shown in Figure 2 (curve a), which is regarded to be the sum of the symmetric esr

(1) Made and kindly donated by Central Research Laboratories, Mitsubishi Electric Corp., Amagasaki, Japan. It is prepared by treating alkali borosilicate glass with strong acid, and said to have pores with fairly uniform diameter, 30–100 A. The surface area is measured to be about 271 m^2/g. The glass is slightly opaque.

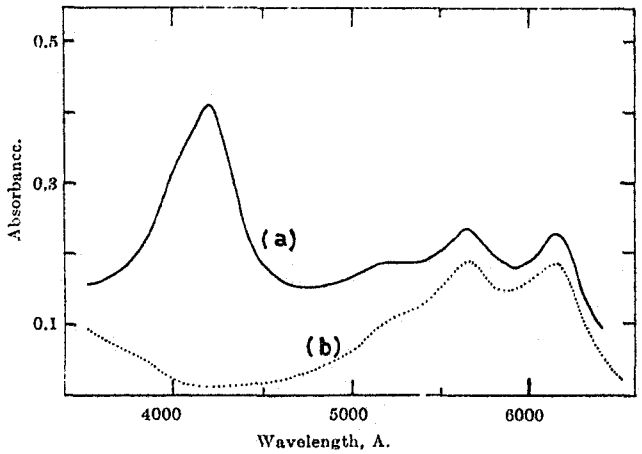

Figure 1. Curve 1: the electronic absorption spectrum of TMPD adsorbed on porous glass and irradiated by ultraviolet light. Curve b: that of TMPD$^+$ (Br^-) in an ethanol solution.

spectrum centered at $g = 2.003$ for TMPD$^+$ and another spectrum with considerably large anisotropic g factors (curve b). The latter seems to be in accordance with the spectrum assigned to the O_2^- ion formed on the surface of zinc oxide.[2,3]

It has been confirmed that the irradiation of porous glass itself causes neither a special electronic spectrum nor an esr spectrum.

The intensity of the Y band depends much on the treatment of the porous glass before adsorption. The results in Figure 1 are for the glass activated at about 500° for several hours under vacuum. With higher temperature and longer time of activation, the intensity of the band decreases. By a similar experiment using the glass treated with hydrogen gas at 500°, both the TMPD$^+$ band and the Y band appear only faintly. To the contrary, the introduction of pure, dry oxygen (10 mm pressure) into the vacuum line for about 1 min increases to a large extent the intensities of both absorption bands produced by irradiation.[4]

In the case where an aromatic hydrocarbon (A) as well as TMPD is adsorbed on the porous glass, there is a marked effect on the intensity of the photochemically formed Y band. For the case of anthracene, terphenyl, or naphthalene used as (A), the Y band disappears and, instead, the spectrum corresponding to the A^- anion appears. For the case of fluorene, both the Y band and the band of fluorene$^-$ appear. For the case of diphenyl, no spectrum of diphenyl$^-$ appears but the Y band does appear. These results are in good accord with the sequence of the electron affinities of the aromatic hydrocarbons. The species related to the Y band, therefore, may be roughly regarded to have an electron affinity nearly the same as that of fluorene.

Similar photoionization experiments using N,N-dimethyl-*p*-phenylenediamine instead of TMPD resulted in the appearance of the Y band as well as those for the phenylenediamine cation.

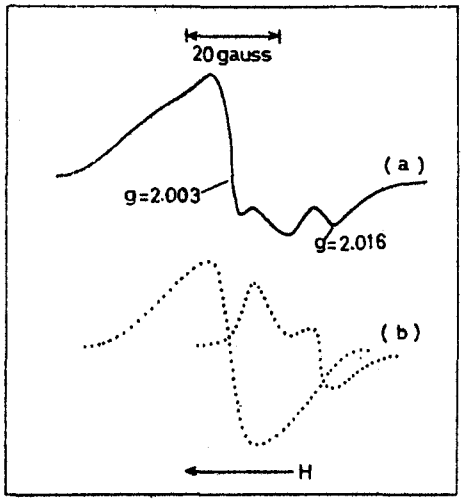

Figure 2. Curve a: the esr spectrum of irradiated TMPD adsorbed on porous glass. Curve b: the spectrum is tentatively divided into two components in such a way that their sum agrees with curve a.

All the above results seem to suggest fairly strongly that the carrier for the Y band is O_2^-.

The photoionization of TMPD in low temperature matrices has been extensively studied.[5,6] It is concluded that photoionization under near-ultraviolet light is caused by a two-step mechanism *via* the lowest triplet state. For the present case, therefore, it is reasonable to suppose that electrons are ejected from TMPD by a two-step excitation. Our present results suggest that the electrons thus ejected return quickly to TMPD$^+$ unless an acceptor, O_2 or an aromatic, traps it.

Thompson and Kleinberg[7] reported many years ago that alkali superoxides formed in liquid ammonia showed a band at about 3800 A, which they assigned to O_2^-. We prepared potassium superoxide and measured the absorption spectrum of its solution in liquid ammonia. No absorption peak has been found, but an absorption arising monotonically to 3000 A has been obtained.

(2) For example, R. J. Kokes, *Proc. 3rd Intern. Congr. Catalysis, Amsterdam, 1964*, 1, 484 (1965); J. H. Lunsford and J. P. Jayne, *J. Chem. Phys.*, 44, 1487 (1966).

(3) According to McLachlan, *et al.*, the O_3^- ion in an aqueous solution shows an ultraviolet absorption spectrum at about the same region of wavelength as the Y band, but its esr spectrum is quite different from that obtained in the present paper: A. D. McLachlan, M. C. R. Symons, and M. G. Townsend, *J. Chem. Soc.*, 952 (1959).

(4) Under humid conditions, TMPD$^+$ is instantaneously formed by the introduction of oxygen. Under strictly dry conditions, no TMPD$^+$ is formed with the introduction of oxygen until the specimen is irradiated.

(5) N. Yamamoto, Y. Nakato, and H. Tsubomura, *Bull. Chem. Soc. Japan*, 40, 451 (1967), and papers cited therein.

(6) K. D. Cadogan and A. C. Albrecht, *J. Chem. Phys.*, 43, 2550 (1965); G. E. Johnson, W. M. McClain, and A. C. Albrecht, *ibid.*, 43, 2911 (1965); W. M. McClain and A. C. Albrecht, *ibid.*, 43, 465 (1965).

(7) J. K. Thompson and J. Kleinberg, *J. Am. Chem. Soc.*, 73, 1243 (1951). We are indebted to Professor Kleinberg for detailed information on his work published a long time ago.

Rolfe, *et al.*,[8] recently reported a broad absorption spectrum at 2500 A, together with a fluorescence spectrum which they assign to O_2^- in the crystal of alkali halides fused in an oxygen atmosphere. Also, Czapski and Dorfman[9] assigned the absorption band at about 2400 A obtained by the pulse radiolysis of the H_2O–O_2 system to O_2^-. These two results seem to offer reliable data for the spectrum of the O_2^- ion. Our spectrum, though at a different wavelength, may also be valid, because the position of the spectrum may be susceptible to the environment. Another alternative is that our Y band might be the first band of O_2^-, which is much weaker than the second band, which may be the spectra found by the above authors. (In our experiment, no absorption band below 3500 A can be measured.)

(8) J. Rolfe, F. R. Lipsett, and W. J. King, *Phys. Rev.*, 123, 447 (1961).

(9) G. Czapski and L. M. Dorfman, *J. Phys. Chem.*, 68, 1169 (1964).

Appendix of the Reprint [The Interaction of Oxygen with Organic Molecules.II].

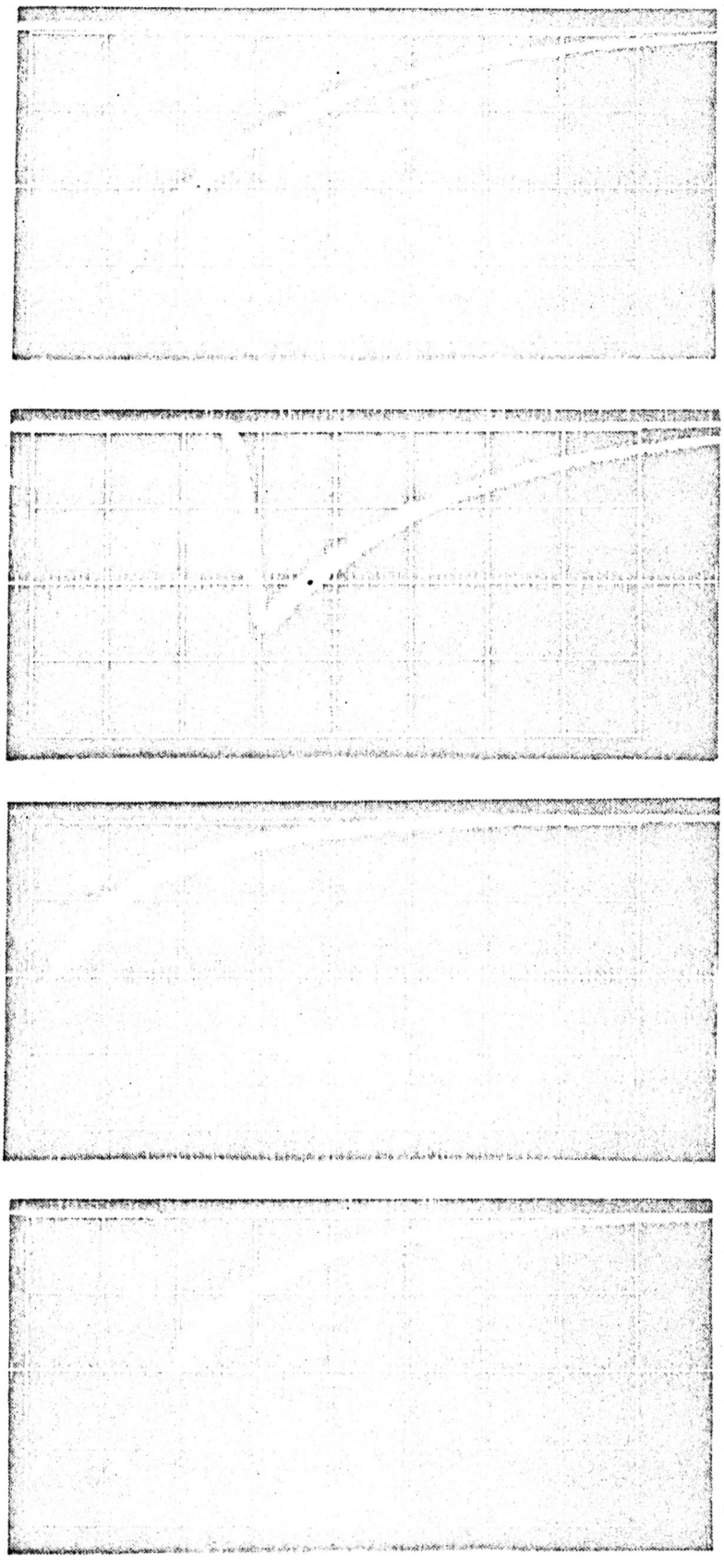

A-1 Phosphorescence decay curves of adsorbed α-Cl-naphthalene at various oxygen pressures at 77°K.

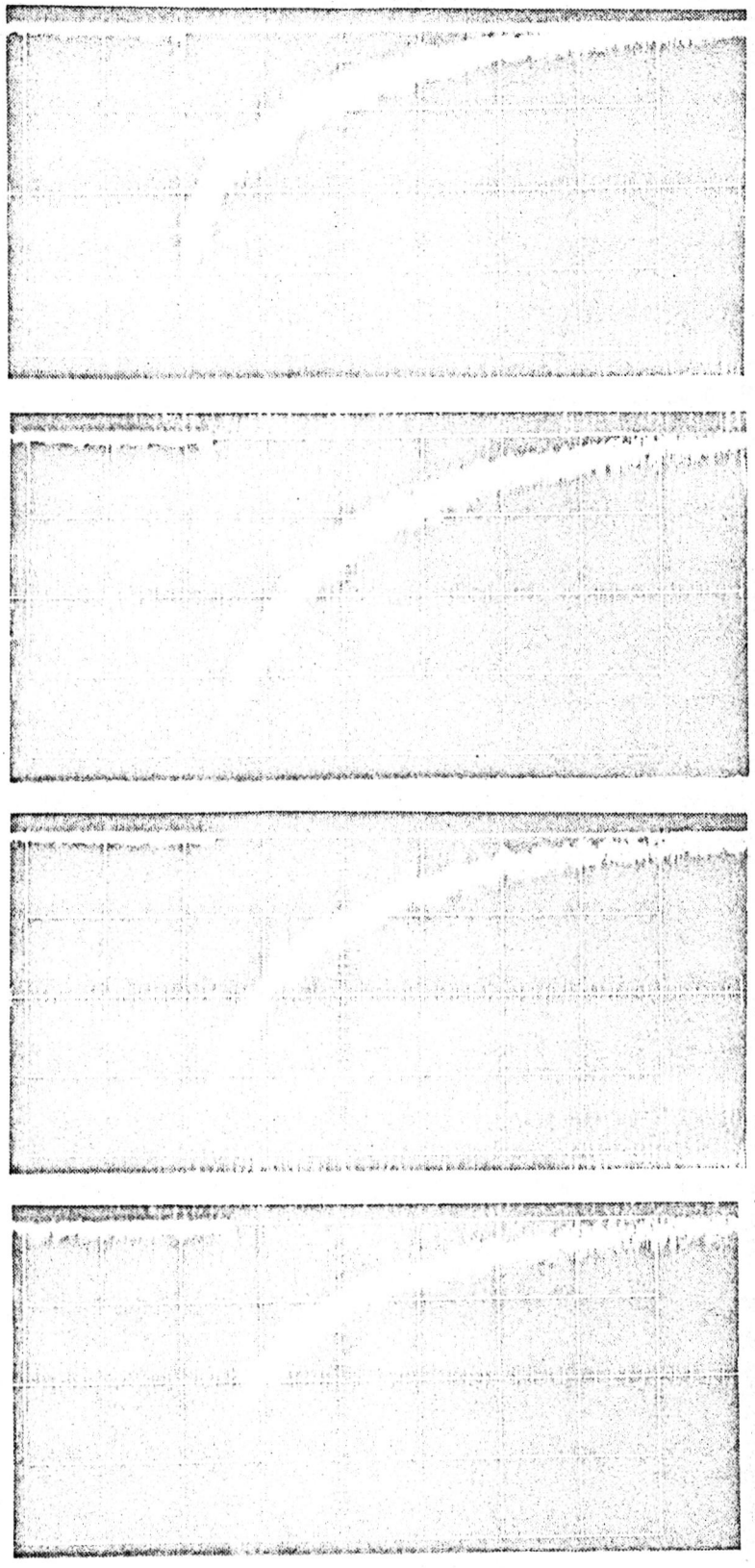
O_2
6×10^{-1} Torr
1.5
5
20
0.1 sec/div

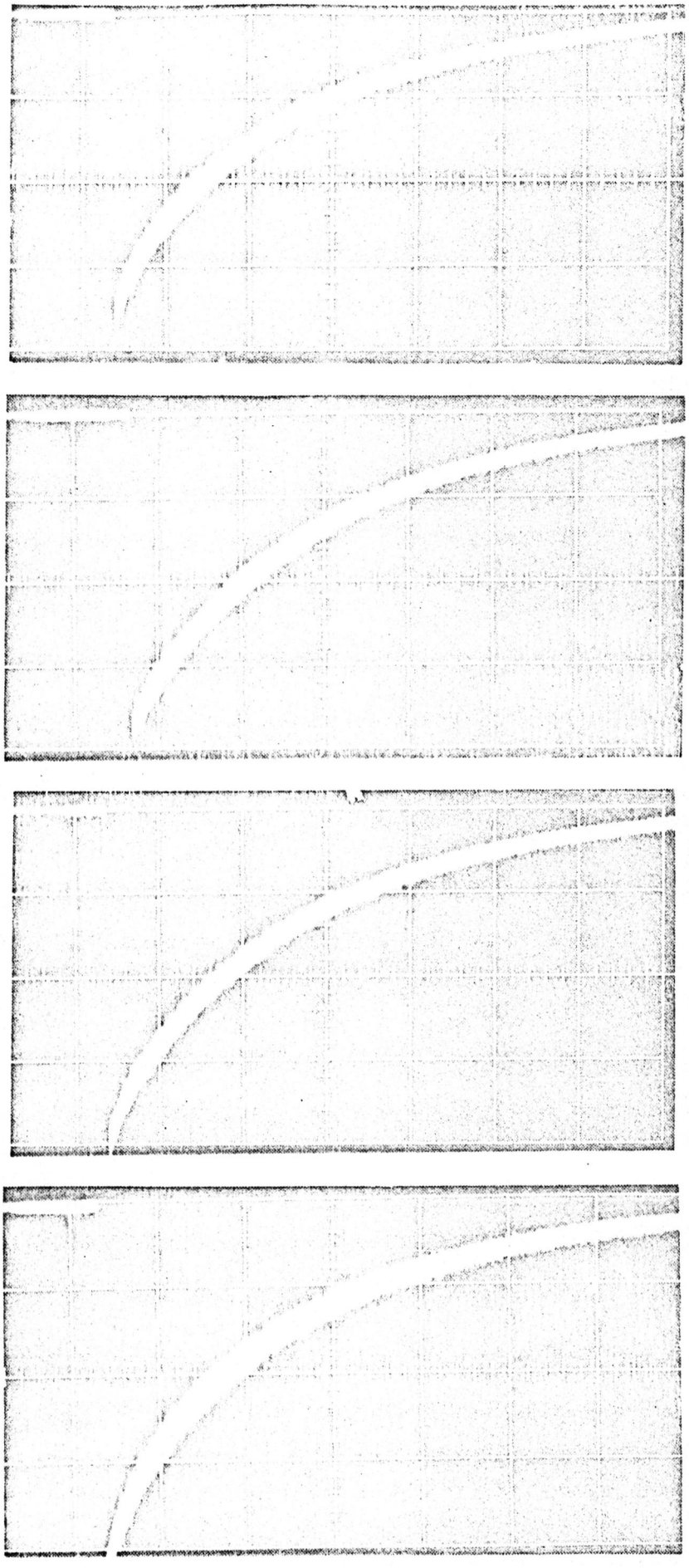

A-2 Phosphorescence decay curves of adsorbed naphthalene at various oxygen pressures at 77°K.

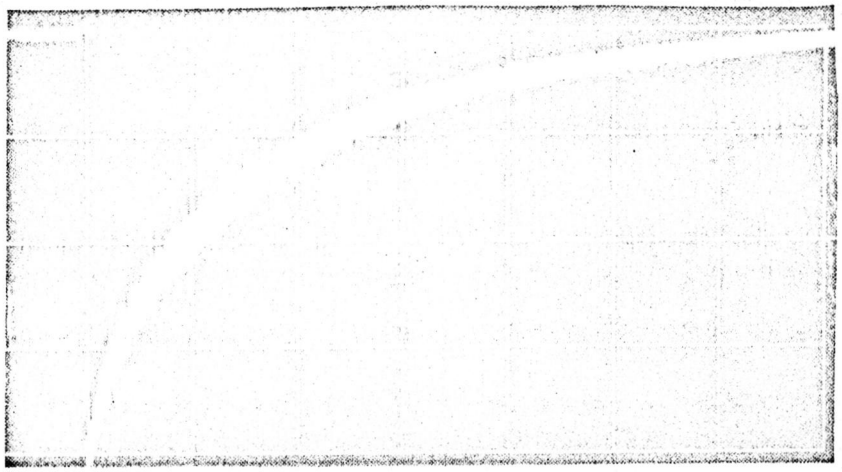

O_2

10^{-1} Torr

1.0 sec/div

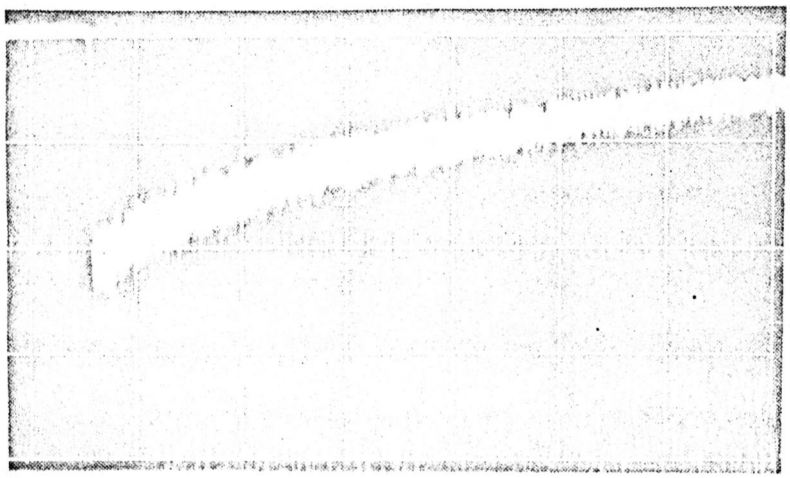

4×10^{-1}

0.4 sec/div

↓

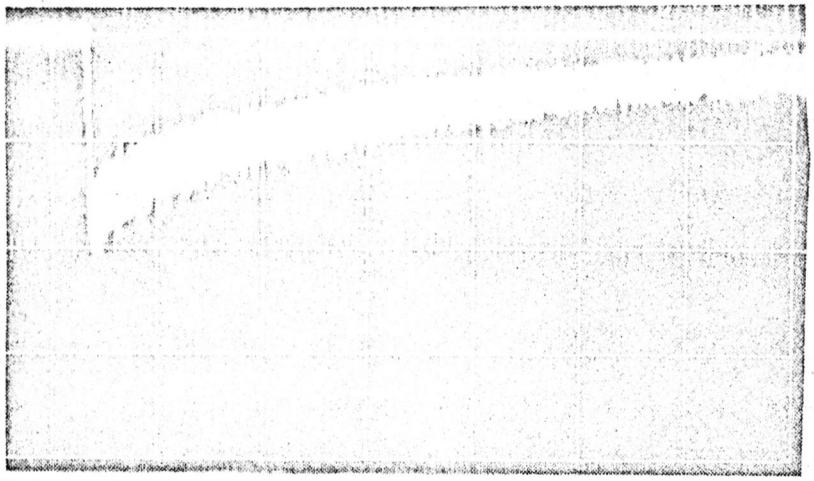

1.5

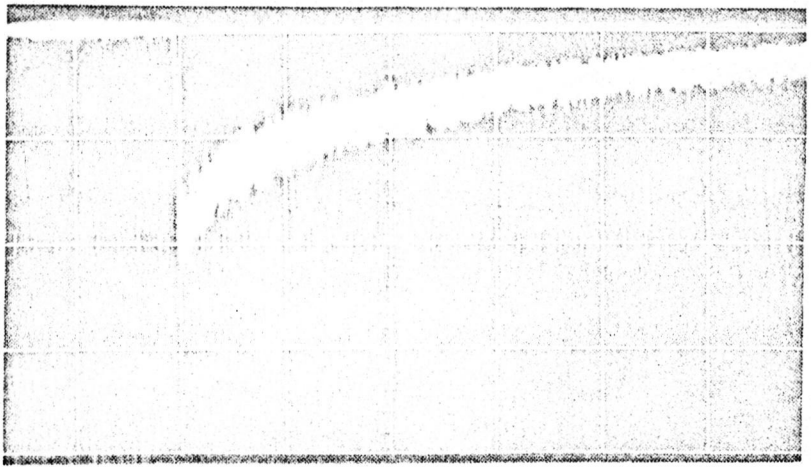

5.0

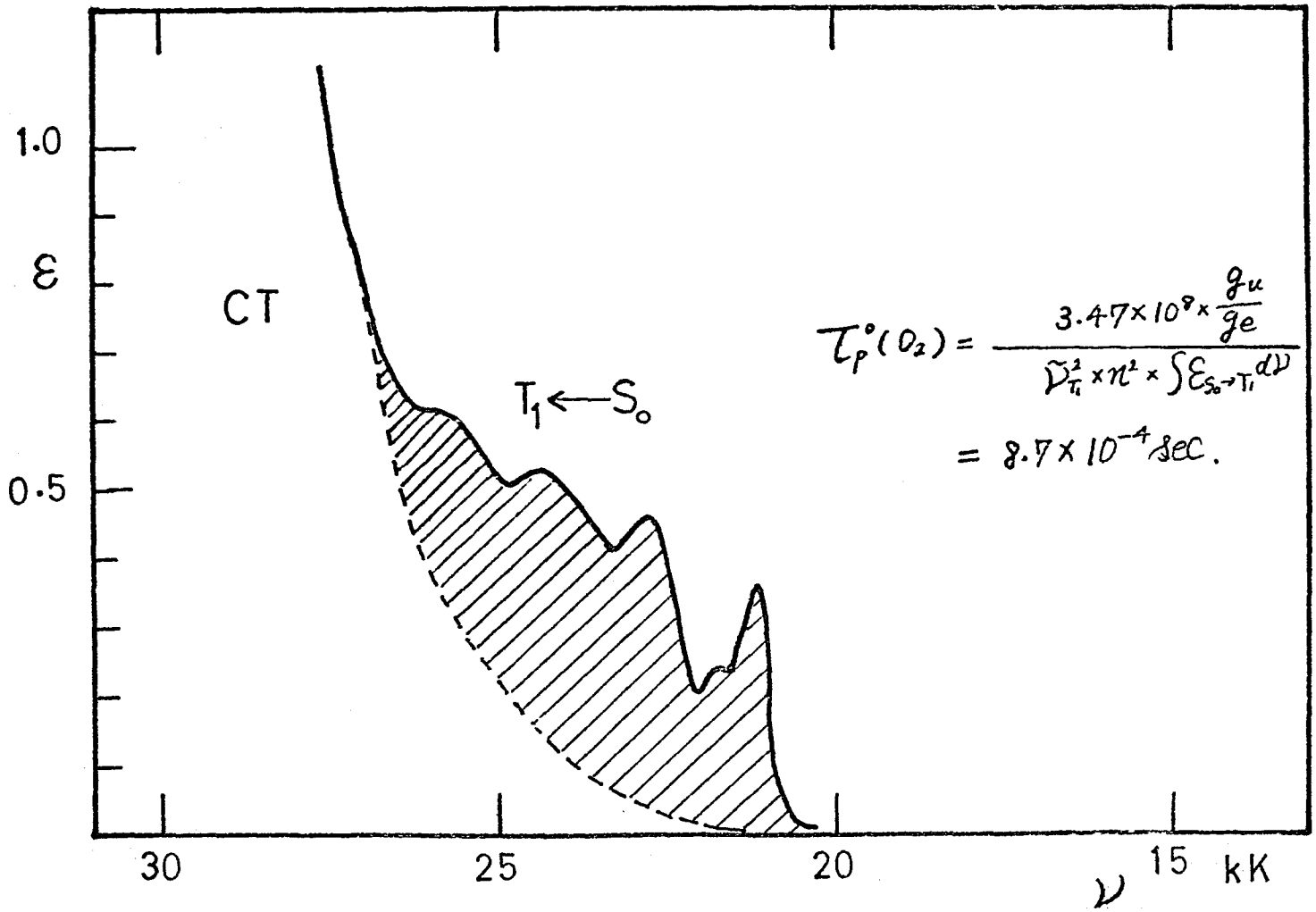

A–3 Calculation of the natural radiative lifetime of triplet-state naphthalene from the observed triplet—singlet absorption spectrum of naphthalene-porous glass adsorbate immersed in liquid oxygen at 77°K.

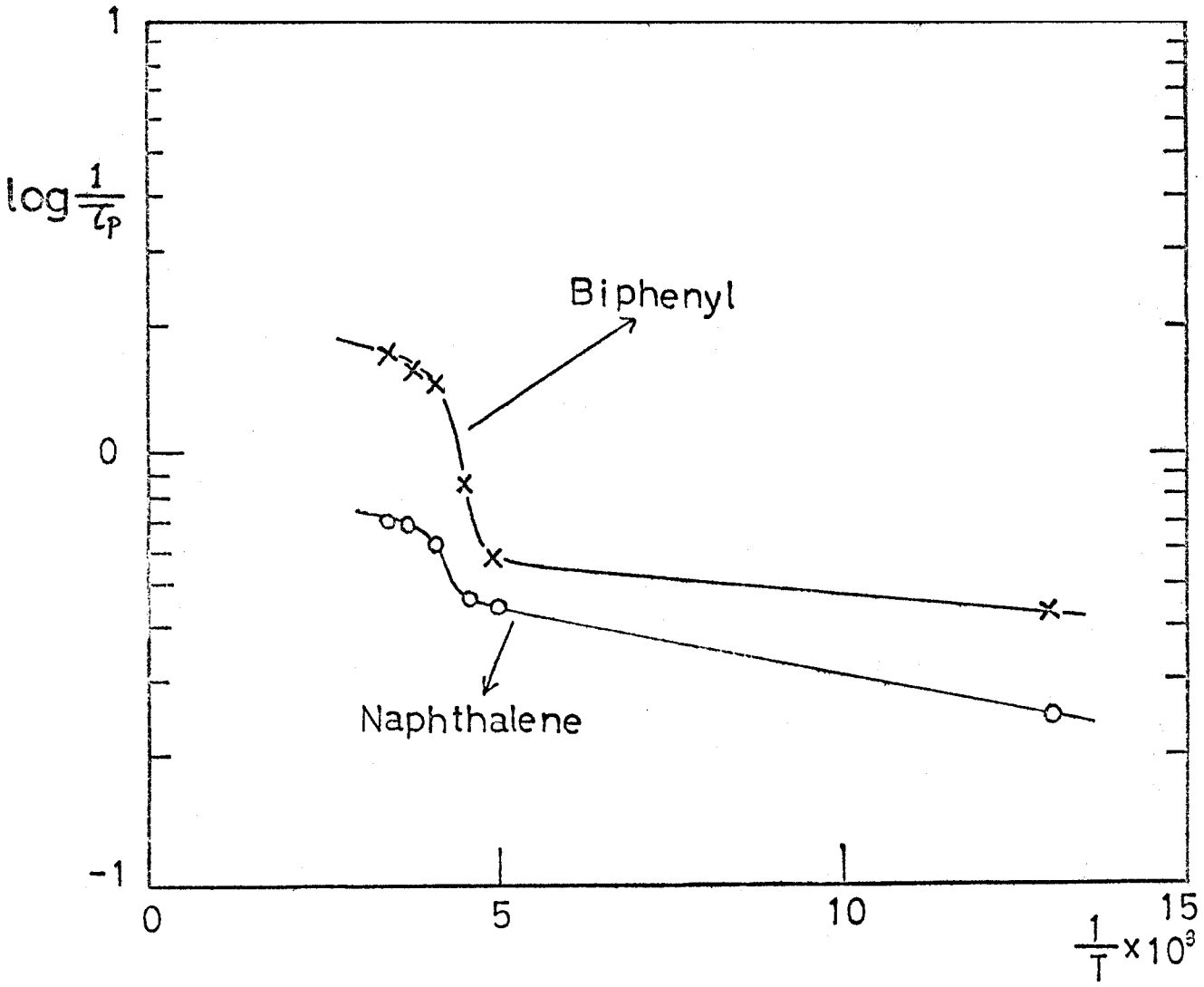

A—4

Temperature dependences of the phosphorescence lifetimes of adsorbed biphenyl and naphthalene at negligible oxygen pressure.

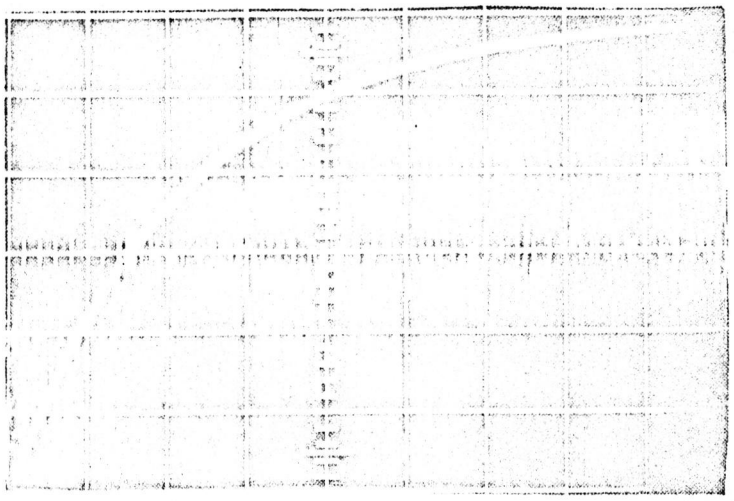

-70°C

1.0 sec/div

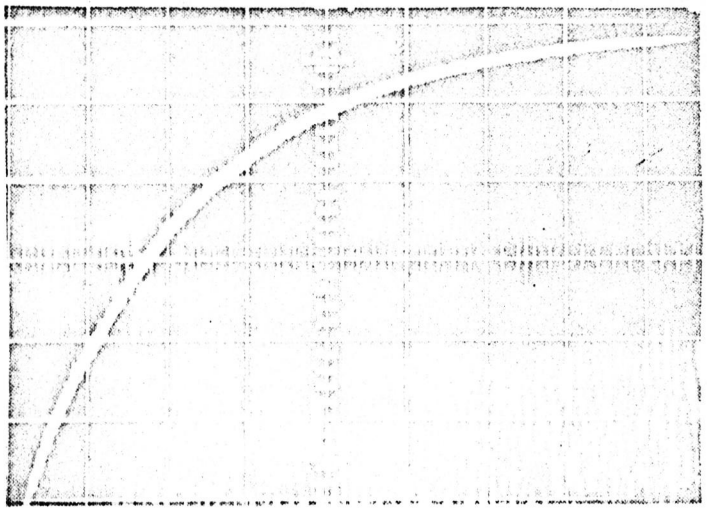

-50°C

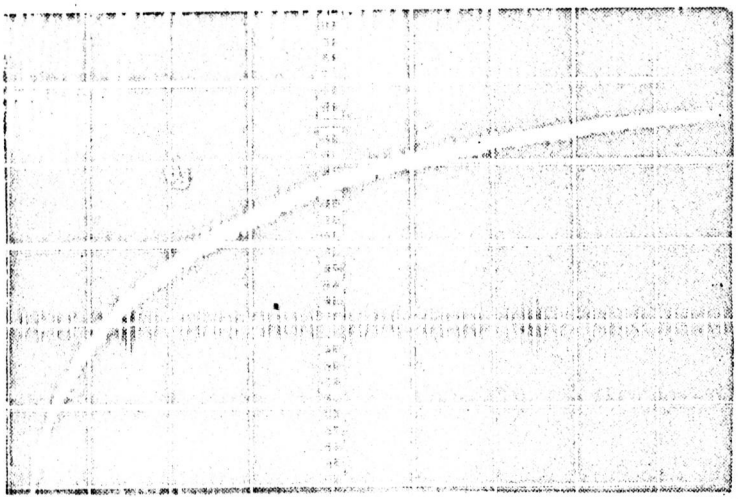

-30°C
0.5 sec/div

A—5

Phosphorescence decay curves of adsorbed biphenyl at various temperatures. Oxygen pressure; 10^{-3} Torr.

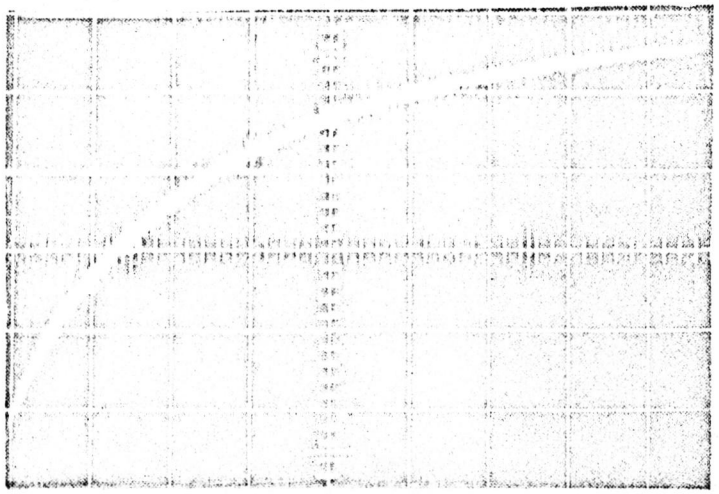

-15°C

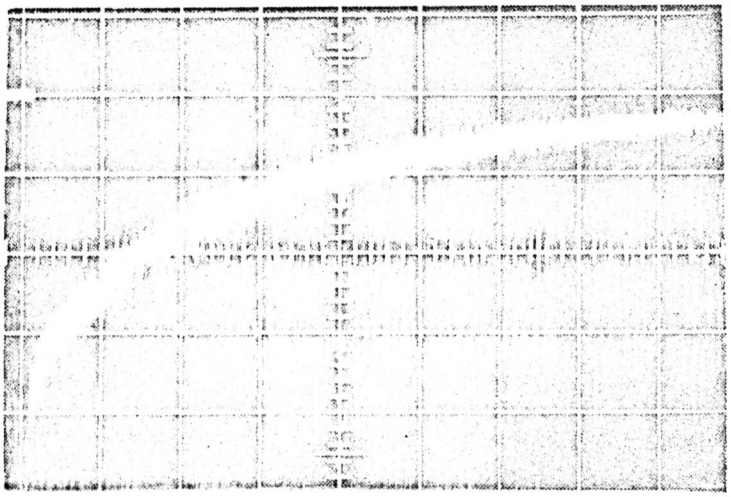

0°C

15°C

0.5 sec / div